STARS

University of Central Florida
STARS

Electronic Theses and Dissertations, 2004-2019

2016

An Integrated Hydrodynamic-Marsh Model with Applications in Fluvial, Marine, and Mixed Estuarine Systems

Karim Alizad
University of Central Florida

 Part of the Civil Engineering Commons
Find similar works at: https://stars.library.ucf.edu/etd
University of Central Florida Libraries http://library.ucf.edu

This Doctoral Dissertation (Open Access) is brought to you for free and open access by STARS. It has been accepted for inclusion in Electronic Theses and Dissertations, 2004-2019 by an authorized administrator of STARS. For more information, please contact STARS@ucf.edu.

STARS Citation

Alizad, Karim, "An Integrated Hydrodynamic-Marsh Model with Applications in Fluvial, Marine, and Mixed Estuarine Systems" (2016). *Electronic Theses and Dissertations, 2004-2019*. 5287.
https://stars.library.ucf.edu/etd/5287

AN INTEGRATED HYDRODYNAMIC-MARSH MODEL WITH APPLICATIONS IN FLUVIAL, MARINE, AND MIXED ESTUARINE SYSTEMS

by

KARIM ALIZAD
B.S. Semnan University, 2005
M.S. University of Tehran, 2008
M.S. University of California, Riverside, 2011

A thesis submitted in partial fulfillment of the requirements
for the degree of Doctor of Philosophy
in the Department of Civil, Environmental, and Construction Engineering
in the College of Engineering and Computer Science
at the University of Central Florida
Orlando, Florida

Spring Term
2016

Major Professors: Scott C. Hagen and Stephen C. Medeiros

© 2016 Karim Alizad

ABSTRACT

Coastal wetlands experience fluctuating productivity when subjected to various stressors. One of the most impactful stressors is sea level rise (SLR) associated with global warming. Research has shown that under SLR, salt marshes may not have time to establish an equilibrium with sea level and may migrate landward or become open water. Salt marsh systems play an important role in the coastal ecosystem by providing intertidal habitats and food for birds, fish, crabs, mussels, and other animals. They also protect shorelines by dissipating flow and damping wave energy through an increase in drag forces. Due to the serious consequences of losing coastal wetlands, evaluating the potential future changes in their structure and distribution is necessary in order for coastal resource managers to make informed decisions. The objective of this study was to develop a spatially-explicit model by connecting a hydrodynamic model and a parametric marsh model and using it to assess the dynamic effects of SLR on salt marsh systems within three National Estuarine Research Reserves (NERRs) in the Northern Gulf of Mexico.

Coastal salt marsh systems are an excellent example of complex interrelations between physics and biology, and the resulting benefits to humanity. In order to investigate salt marsh productivity under projected SLR scenarios, a depth integrated hydrodynamic model was coupled to a parametric marsh model to capture the dynamic feedback loop between physics and biology. The hydrodynamic model calculates mean high water (MHW) and mean low water (MLW) within the river and tidal creeks by harmonic analysis of computed tidal constituents. The responses of MHW and MLW to SLR are nonlinear due to localized changes in the salt marsh platform elevation and biomass productivity (which influences bottom friction). Spatially-varying MHW and MLW are

utilized in a two-dimensional application of the parametric Marsh Equilibrium Model to capture the effects of the hydrodynamics on biomass productivity and salt marsh accretion, where accretion rates are dependent on the spatial distribution of sediment deposition in the marsh. This model accounts both organic (decomposition of in-situ biomass) and inorganic (allochthonous) marsh platform accretion and the effects of spatial and temporal biomass density changes on tidal flows. The coupled hydro-marsh model, herein referred to as HYDRO-MEM, leverages an optimized coupling time step at which the two models exchange information and update the solution to capture the system's response to projected linear and non-linear SLR rates.

Including accurate marsh table elevations into the model is crucial to obtain meaningful biomass productivity projections. A lidar-derived Digital Elevation Model (DEM) was corrected by incorporating Real Time Kinematic (RTK) surveying elevation data. Additionally, salt marshes continually adapt in an effort to reach an equilibrium within the ideal range of relative SLR and depth of inundation. The inputs to the model, specifically topography and bottom roughness coefficient, are updated using the biomass productivity results at each coupling time step to capture the interaction between the marsh and hydrodynamic models.

The coupled model was tested and validated in the Timucuan marsh system, located in northeastern Florida by computing projected biomass productivity and marsh platform elevation under two SLR scenarios. The HYDRO-MEM model coupling protocol was assessed using a sensitivity study of the influence of coupling time step on the biomass productivity results with a comparison to results generated using the MEM approach only. Subsequently, the dynamic effects of SLR were investigated on salt marsh productivity within the three National Estuarine Research Reserves

(NERRs) (Apalachicola, FL, Grand Bay, MS, and Weeks Bay, AL) in the Northern Gulf of Mexico (NGOM). These three NERRS are fluvial, marine and mixed estuarine systems, respectively. Each NERR has its own unique characteristics that influence the salt marsh ecosystems.

The HYDRO-MEM model was used to assess the effects of four projections of low (0.2 m), intermediate-low (0.5 m), intermediate-high (1.2 m) and high (2.0 m) SLR on salt marsh productivity for the year 2100 for the fluvial dominated Apalachicola estuary, the marine dominated Grand Bay estuary, and the mixed Weeks Bay estuary. The results showed increased productivity under the low SLR scenario and decreased productivity under the intermediate-low, intermediate-high, and high SLR. In the intermediate-high and high SLR scenarios, most of the salt marshes drowned (converted to open water) or migrated to higher topography.

These research presented herein advanced the spatial modeling and understanding of dynamic SLR effects on coastal wetland vulnerability. This tool can be used in any estuarine system to project salt marsh productivity and accretion under sea level change scenarios to better predict possible responses to projected SLR scenarios. The findings are not only beneficial to the scientific community, but also are useful to restoration, planning, and monitoring activities in the NERRs. Finally, the research outcomes can help policy makers and coastal managers to choose suitable approaches to meet the specific needs and address the vulnerabilities of these three estuaries, as well as other wetland systems in the NGOM and marsh systems anywhere in the world.

ACKNOWLEDGMENTS

This research is funded in part by Award No. NA10NOS4780146 from the National Oceanic and Atmospheric Administration (NOAA) Center for Sponsored Coastal Ocean Research (CSCOR) and the Louisiana Sea Grant Laborde Chair endowment. The computations for the hydrodynamic model simulations were performed using the STOKES Advanced Research Computing Center (ARCC) at University of Central Florida, Center for Computation and Technology at Louisiana State University (LSU), the Louisiana Optical Network Initiative (LONI), and Extreme Science and Engineering Discovery Environment (XSEDE). I would like to extend my appreciation to Apalachicola National Estuarine Research Reserve (ANERR), Grand Bay National Estuarine Research Reserve (GBNERR), and Weeks Bay National Estuarine Research Reserve (WBNERR) staffs, especially Mrs. Jenna Harper, Mr. Will Underwood, and Dr. Scott Phipps for their continuous help and support. The statements and conclusions do not necessarily reflect the views of NOAA-CSCOR, Louisiana Sea Grant, STOKES ARCC, LSU, LONI, XSEDE, ANERR or their affiliates.

I would like to express my gratitude to all those people who have made this dissertation possible, specifically Dr. Scott Hagen and Dr. Stephen Medeiros for their support, patience, and guidance that helped me conquer many critical situations and accomplish this dissertation. They provided me with the opportunity to be a part of the CHAMPS Lab and develop outstanding scientific knowledge as well as enriching my skills in teamwork, leadership, presentation, and field study. Their continuous support in building these skills with small steps and providing me with the opportunities such as participating in international conferences, tutoring students, and working

with knowledgeable scientists, coastal researchers and managers have prepared me with the strongest tools to be able to help the environment, nature, and human beings. Their mentorship exemplifies the famous quote from Nelson Mandela that "Education is the most powerful weapon which you can use to change the world."

I would also like to thank Dr. Dingbao Wang, and Dr. John Weishampel for their guidance and collaboration in this research and developing Hydro-MEM model as well as for serving on my committee. I am really grateful to Dr. James Morris at University of South Carolina and Dr. Peter Bacopoulos at University of North Florida for their outstanding contribution, guidance, and support on developing the model. I look forward to more collaboration in the future.

I would like to thank Dr. Scott Hagen again for equipping me with my second home CHAMPS Lab that built friendships and memories in a scientific community. I want to specifically thank Dr. Davina Passeri and Matthew Bilskie, who not only taught me invaluable scientific skills, but informed me with techniques in writing. They have been wonderful friends who have supplied five years of fun and great chats about football and other American culture. You are the colleagues who are lifelong friends. I also would like to thank Daina Smar who was my first instructor in the field study and equipped me with swimming skills. Special thanks to Aaron Thomas and Paige Hovenga for all of their help and support during field works as well as memorable days in birding and camping. Thank you to former CHAMPS Lab member Dr. Ammarin Daranpob for his guidance in my first days at UCF and special thanks to Milad Hooshyar, Amanda Tritinger, Erin Ward, and Megan Leslie for all of their supports in the CHAMPS lab. Thank you to the other CHAMPS lab

members Yin Tang, Daljit Sandhu, Marwan Kheimi, Subrina Tahsin, Han Xiao, and Cigdem Ozkan.

I also wish to thank Dave Kidwell (EESLR-NGOM Project Manager). In addition, I would like to thank K. Schenter at the U.S. Army Corps of Engineers Mobile District for his help in accessing the surveyed bathymetry data of the Apalachicola River.

I am really grateful to have supportive parents, Azar Golshani and Mohammad Ali Alizad who were my first teachers and encouraged me with their unconditional love. They nourished me with a lifelong passion for education, science, and nature. They inspired me with love, and perseverance. Thank you to my brother Amir Alizad, who was my first teammate in discovering aspects of life. Most importantly, I would like to specifically thank my wife, Sona Gholizadeh, the most wonderful woman in the world. She inspired me with the strongest love, support, and happiness during the past five years and made this dissertation possible.

TABLE OF CONTENTS

LIST OF FIGURES

LIST OF TABLES

CHAPTER 1. INTRODUCTION

Coastal wetlands can experience diminished productivity under various stressors. One of the most important is sea level rise (SLR) associated with global warming. Research has shown that under extreme conditions of SLR, salt marshes may not have time to establish an equilibrium with sea level and may migrate upland or convert to open water (Warren and Niering, 1993; Gabet, 1998; Donnelly and Bertness, 2001; Hughes, 2001; Castillo et al., 2002). Salt marsh systems play an important role in the coastal ecosystem by providing intertidal habitats, nurseries and food sources for birds, fish, shellfish, and other animals such as raccoons (Bertness, 1984; Halpin, 2000; Pennings and Bertness, 2001; Hughes, 2004). They also protect shorelines by dissipating flow and damping wave energy and increasing friction (Knutson, 1987; King and Lester, 1995; Leonard and Luther, 1995; Möller and Spencer, 2002; Costanza et al., 2008; Shepard et al., 2011). Due to the serious consequences of losing coastal wetlands, resource managers play an active role in the protection of estuaries and environmental systems by planning for future changes caused by global climate change, especially SLR (Nicholls et al., 1995). In fact, various restoration plans have been proposed and implemented in different parts of the world (Broome et al., 1988; Warren et al., 2002; Hughes and Paramor, 2004; Wolters et al., 2005).

In addition to improving restoration and planning, predictive ecological models provide a tool for assessing the systems' response to stressors. Coastal salt marsh systems are an excellent example of complex interrelations between physics, biology, and benefits to humanity (Townend et al., 2011). These ecosystems need to be studied with a dynamic model that is able to capture feedback mechanisms (Reed, 1990; Jørgensen and Fath, 2011). Specifically, integrated models allow

researchers to investigate the response of a system to projected natural or anthropogenic changes in environmental conditions. Data from long-term tide gauges show that global mean sea level has increased 1.7 mm-yr^{-1} over the last century (Church and White, 2006). Additionally, data from satellite altimetry shows that mean sea level from 1993-2009 increased 3.4 ± 0.4 mm.yr^{-1} (Nerem et al., 2010). As a result, many studies have focused on developing integrated models to simulate salt marsh response to SLR (Reed, 1995; Allen, 1997; Morris et al., 2002; Temmerman et al., 2003; Mudd et al., 2004; Kirwan and Murray, 2007; Mariotti and Fagherazzi, 2010; Stralberg et al., 2011; Tambroni and Seminara, 2012; Hagen et al., 2013; Marani et al., 2013; Schile et al., 2014). However, models that do not account for the spatial variability of salt marsh platform accretion may not be able to correctly project the changes in the system (Thorne et al., 2014). Therefore, there is a demonstrated need for a spatially-explicit model that includes the interaction between physical and biological processes in salt marshes.

The future of the Northern Gulf of Mexico (NGOM) coastal environment relies on timely, accurate information regarding risks such as SLR to make informed decisions for managing human and natural communities. NERRs are designated by NOAA as protected regions with the mission of allowing for long-term research and monitoring, education, and resource management that provide a basis for more informed coastal management decisions (Edmiston et al., 2008a). The three NERRs selected for this study, namely Apalachicola, FL, Grand Bay, MS, and Weeks Bay, AL represent a variety of estuary types and contain an array of plant and animal species that support commercial fisheries. In addition, the coast attracts millions of residents, visitors and businesses. Due to the unique morphology and hydrodynamics in each NERR, it is likely that they will respond differently to SLR, with unique impacts to the coastal wetlands.

1.1 Hypothesis and Research Objective

This study aims to assess the dynamic effects of SLR on fluvial, marine, and mixed estuary systems by developing a coupled physical-biological model. This dissertation intends to test the following hypothesis:

Capturing more processes into an integrated physical-ecological model will better demonstrate the response of biomass productivity to SLR and its nonlinear dependence on tidal hydrodynamics, salt marsh platform topography, estuarine system characteristics and geometry, and climate change.

Assessing the hypothesis introduces research questions that this study seeks to answer:

At what SLR rates ($mm.yr^{-1}$) will the salt marsh: increase/decrease productivity; migrate upland; or convert to open water?

How does the estuary type (fluvial, marine, and mixed) affect salt marsh productivity under different SLR scenarios?

What are the major factors that influence the vulnerability of a salt marsh system to SLR?

Finally, this interdisciplinary project provides researchers with an integrated model to make reasonable predictions salt marsh productivity under different conditions. This research also enhances the understanding of the three different NGOM wetland systems and will aid restoration and planning efforts. Lastly, this research will also benefit coastal managers and NERR staff in monitoring and management planning.

1.2 Review of the Salt Marsh Evolution Models for Assessing Sea Level Rise Effects on Wetlands

Salt marsh systems are complex regions within estuary ecosystems. They are habitats for many species and protect shorelines by increasing flow resistance and damping wave energy. These systems are an environment where physics and biology are interconnected. SLR significantly affects these systems and have been studied by researchers using hydrodynamic and biological models along with applying coupled models. Understanding SLR, in addition to implementing it in hydrodynamic and marsh models to study the effects of SLR on the estuarine systems is critical. A variety of hydrodynamic and salt marsh models have been used and developed to study SLR effects on coastal systems. Both low and high resolution models have been used for variety of purposes by researchers and coastal managers. These models have various levels of accuracy and specific limitations that need to be considered when used for developing a coupled model.

1.3 Methods and Validation of the Model

A spatially-explicit model (HYDRO-MEM) that couples astronomic tides and salt marsh dynamics was developed to investigate the effects of SLR on salt marsh productivity. The hydrodynamic component of the model simulates the hydroperiod of the marsh surface driven by astronomic tides and the marsh platform topography, and demonstrates biophysical feedback that non-uniformly modifies marsh platform accretion, plant biomass, and water levels across the estuarine landscape, forming a complex geometry. The marsh platform accretes organic and inorganic matter depending on the sediment load and biomass density which are simulated by the ecological-marsh component (MEM) of the model and are, in turn, functions of the hydroperiod. In order to validate the model

in the Timucuan marsh system in northeast Florida, two sea-level rise projections for the year 2050 were simulated: 11 cm (low) and 48 cm (high). The biomass-driven topographic and bottom friction parameter updates were assessed by demonstrating numerical convergence (the state where the difference between biomass densities for two different coupling time steps approaches a small number). The maximum effective coupling time steps for low and high sea-level rise cases were determined to be 10 and 5 years, respectively. A comparison of the HYDRO-MEM model with a stand-alone parametric marsh equilibrium model (MEM) showed improvement in terms of spatial pattern of biomass distribution due to the coupling and dynamic sea-level rise approaches. This integrated HYDRO-MEM model provides an innovative method by which to assess the complex spatial dynamics of salt marsh grasses and predict the impacts of possible future sea level conditions.

1.4 Application of the Model in a Fluvial Estuarine System

The HYDRO-MEM model was applied to assess Apalachicola fluvial estuarine salt marsh system under four projected SLR scenarios. The HYDRO-MEM model incorporates the dynamics of sea-level rise and captures the effect of SLR rate in the simulations. Additionally, the model uses the parameters derived from a two year bio-assay in the Apalachicola marsh system. In order to increase accuracy, the marsh platform topography lidar DEM was adjusted using Real Time Kinematic topographic surveying data and a river inflow (flux) boundary condition was imposed. The biomass density results generated by the HYDRO-MEM model were validated using remotely sensed biomass densities.

The SLR scenario simulations showed higher water levels (as expected) but also more water level variability under the low and intermediate-low SLR scenarios. The intermediate-high and high scenarios displayed lower variability with a greatly extended bay. In terms of biomass density patterns, the model results showed more uniform biomass density with higher productivity in some areas and lower productivity in others under the low SLR scenario. Under the intermediate-low SLR scenario, more areas in the no productivity regions of the islands between the Apalachicola River and East Bay were flooded. However, lower productivity, marsh loss, and movement to higher lands for other marsh lands were projected. The higher sea-level rise scenarios (intermediate-high and high) demonstrated massive inundation of marsh areas (effectively extending bay) and showed the generation of a thin band of new wetland in the higher lands. Overall, the study results showed that HYDRO-MEM is capable of making reasonable projections in a large estuarine system and that it can be extended to other estuarine systems for assessing possible SLR impacts to guiding restoration and management planning.

1.5 Salt Marsh System Response to Sea Level Rise in Marine and Mixed Estuarine Systems

In order to assess the response of different salt marsh systems to SLR, specifically marine and mixed estuarine systems in Grand Bay, MS, and Weeks Bay, AL, were compared and contrasted using the HYDRO-MEM model. The Grand Bay estuary is a marine dominant estuary located along the border of Alabama and Mississippi with dominant salt marsh species including *Juncus roemerianus* and *Spartina alterniflora* (Eleuterius and Criss, 1991). Sediment transport in this estuary is driven by wave forces from the Gulf of Mexico and SLR that cause salt marshes to migrate landward (Schmid, 2000). Therefore, with no fluvial sediment source, Grand Bay is

particularly vulnerable to SLR under extreme scenarios. The Weeks Bay estuary, located along the southeastern shore of Mobile Bay in Baldwin County, AL is categorized as a tributary estuary. This estuary is driven by the fresh water inflow from the Magnolia and Fish Rivers, as well as Mobile Bay, which is the estuary's coastal ocean salt source. Weeks Bay has a fluvial source like Apalachicola, but is also significantly influenced by Mobile Bay. The estuary is getting shallower due to sedimentation from the river, Mobile Bay, and coastline erosion (Miller-Way et al., 1996). In fact, it has already lost marsh land because of both SLR and forest encroachment into the marsh (Shirley and Battaglia, 2006).

Under future SLR scenarios, Weeks Bay benefitted from more protection from SLR provided by its unique topography to allow marsh migration and creation of new marsh systems, whereas Grand Bay is more vulnerable to SLR demonstrated by the conversion of its marsh lands to open water.

1.6 References

Allen, J. R. L. (1997). "Simulation models of salt-marsh morphodynamics: some implications for high-intertidal sediment couplets related to sea-level change." *Sedimentary Geology* 113(3–4): 211-223.

Bertness, M. D. (1984). "Ribbed Mussels and Spartina Alterniflora Production in a New England Salt Marsh." *Ecology* 65(6): 1794-1807.

Broome, S. W., Seneca, E. D. and Woodhouse Jr, W. W. (1988). "Tidal salt marsh restoration." *Aquatic Botany* 32(1–2): 1-22.

Castillo, J., Rubio-Casal, A., Luque, C., Nieva, F. and Figueroa, M. (2002). "Wetland loss by erosion in Odiel Marshes (SW Spain)." *Journal of Coastal Research* 36: 134-138.

Church, J. A. and White, N. J. (2006). "A 20th century acceleration in global sea-level rise." *Geophysical Research Letters* 33(1): L01602.

Costanza, R., Pérez-Maqueo, O., Martinez, M. L., Sutton, P., Anderson, S. J. and Mulder, K. (2008). "The Value of Coastal Wetlands for Hurricane Protection." *AMBIO: A Journal of the Human Environment* 37(4): 241-248.

Donnelly, J. P. and Bertness, M. D. (2001). "Rapid shoreward encroachment of salt marsh cordgrass in response to accelerated sea-level rise." *Proceedings of the National Academy of Sciences* 98(25): 14218-14223.

Edmiston, H. L., Calliston, T., Fahrny, S. A., Lamb, M. A., Levi, L. K., Putland, J. and Wanat, J. M. (2008a). "A River Meets the Bay: A Characterization of the Apalachicola River and Bay System", Apalachicola National Estuarine Research Reserve.

Eleuterius, C. K. and Criss, G. A. (1991). "Point aux Chenes: Past, Present, and Future Persepctive of Erosion". Ocean Springs, Mississippi, Physical Oceanography Section Gulf Coast Research Laboratory

Gabet, E. (1998). "Lateral migration and bank erosion in a saltmarsh tidal channel in San Francisco Bay, California." *Estuaries* 21(4): 745-753.

Hagen, S., Morris, J., Bacopoulos, P. and Weishampel, J. (2013). "Sea-Level Rise Impact on a Salt Marsh System of the Lower St. Johns River." *Journal of Waterway, Port, Coastal, and Ocean Engineering* 139(2): 118-125.

Halpin, P. M. (2000). "Habitat use by an intertidal salt-marsh fish: trade-offs between predation and growth." *Marine Ecology Progress Series* 198: 203-214.

Hughes, R. G. (2001). Biological and Physical Processes That Affect Saltmarsh Erosion and Saltmarsh Restoration: Development of Hypotheses. Ecological Comparisons of Sedimentary Shores. K. Reise, Springer Berlin Heidelberg. **151:** 173-192.

Hughes, R. G. (2004). "Climate change and loss of saltmarshes: consequences for birds." *Ibis* 146: 21-28.

Hughes, R. G. and Paramor, O. A. L. (2004). "On the loss of saltmarshes in south-east England and methods for their restoration." *Journal of Applied Ecology* 41(3): 440-448.

Jørgensen, S. E. and Fath, B. D. (2011). 10 - Structurally Dynamic Models. Developments in Environmental Modelling. J. Sven Erik and D. F. Brian, Elsevier. **Volume 23:** 309-346.

King, S. E. and Lester, J. N. (1995). "The value of salt marsh as a sea defence." *Marine Pollution Bulletin* 30(3): 180-189.

Kirwan, M. L. and Murray, A. B. (2007). "A coupled geomorphic and ecological model of tidal marsh evolution." *Proceedings of the National Academy of Sciences* 104(15): 6118-6122.

Knutson, P. (1987). Role of Coastal Marshes in Energy Dissipation and Shore Protection. The Ecology and Management of Wetlands, Springer US**:** 161-175.

Leonard, L. A. and Luther, M. E. (1995). "Flow hydrodynamics in tidal marsh canopies." *Limnology and Oceanography* 40(8): 1474-1484.

Marani, M., Da Lio, C. and D' Alpaos, A. (2013). "Vegetation engineers marsh morphology through multiple competing stable states." *Proceedings of the National Academy of Sciences* 110(9): 3259-3263.

Mariotti, G. and Fagherazzi, S. (2010). "A numerical model for the coupled long-term evolution of salt marshes and tidal flats." *Journal of Geophysical Research: Earth Surface (2003–2012)* 115(F1).

Miller-Way, T. L., Dardeau, M. and Crozier, G. (1996). "Weeks Bay National Estuarine Research Reserve: An Estuarine Profile and Bibliography", Dauphin Island Sea Lab.

Möller, I. and Spencer, T. (2002). "Wave dissipation over macro-tidal saltmarshes: Effects of marsh edge typology and vegetation change." *Journal of Coastal Research* 36: 506-521.

Morris, J. T., Sundareshwar, P. V., Nietch, C. T., Kjerfve, B. and Cahoon, D. R. (2002). "Responses of coastal wetlands to rising sea level." *Ecology* 83(10): 2869-2877.

Mudd, S. M., Fagherazzi, S., Morris, J. T. and Furbish, D. J. (2004). Flow, sedimentation, and biomass production on a vegetated salt marsh in South Carolina: Toward a predictive

model of marsh morphologic and ecologic evolution. The Ecogeomorphology of Tidal Marshes. Washington, DC, AGU. **59:** 165-188.

Nerem, R. S., Chambers, D. P., Choe, C. and Mitchum, G. T. (2010). "Estimating Mean Sea Level Change from the TOPEX and Jason Altimeter Missions." *Marine Geodesy* 33(sup1): 435-446.

Nicholls, R. J., Leatherman, S. P., Dennis, K. C. and Volante, C. R. (1995). "Impacts and responses to sea-level rise: qualitative and quantitative assessments." *Journal of Coastal Research* SI (14): 26-43.

Pennings, S. C. and Bertness, M. D. (2001). "Salt marsh communities." *Marine community ecology*: 289-316.

Reed, D. J. (1990). "The impact of sea-level rise on coastal salt marshes." *Progress in Physical Geography* 14(4): 465-481.

Reed, D. J. (1995). "The response of coastal marshes to sea-level rise: Survival or submergence?" *Earth Surface Processes and Landforms* 20(1): 39-48.

Schile, L. M., Callaway, J. C., Morris, J. T., Stralberg, D., Parker, V. T. and Kelly, M. (2014). "Modeling tidal marsh distribution with sea-level rise: Evaluating the role of vegetation, sediment, and upland habitat in marsh resiliency." *PLoS ONE* 9(2): e88760.

Schmid, K. (2000). "Shoreline Erosion Analysis of Grand Bay Marsh", Mississippi Department of Environmental Quality, Office of Geology.

Shepard, C. C., Crain, C. M. and Beck, M. W. (2011). "The protective role of coastal marshes: A systematic review and meta-analysis." *PLoS ONE* 6(11): e27374.

Shirley, L. and Battaglia, L. (2006). "Assessing vegetation change in coastal landscapes of the northern Gulf of Mexico." *Wetlands* 26(4): 1057-1070.

Stralberg, D., Brennan, M., Callaway, J. C., Wood, J. K., Schile, L. M., Jongsomjit, D., Kelly, M., Parker, V. T. and Crooks, S. (2011). "Evaluating Tidal Marsh Sustainability in the Face of Sea-Level Rise: A Hybrid Modeling Approach Applied to San Francisco Bay." *PLoS ONE* 6(11): e27388.

Tambroni, N. and Seminara, G. (2012). "A one-dimensional eco-geomorphic model of marsh response to sea level rise: Wind effects, dynamics of the marsh border and equilibrium." *Journal of Geophysical Research: Earth Surface* 117(F3): F03026.

Temmerman, S., Govers, G., Meire, P. and Wartel, S. (2003). "Modelling long-term tidal marsh growth under changing tidal conditions and suspended sediment concentrations, Scheldt estuary, Belgium." *Marine Geology* 193(1–2): 151-169.

Thorne, K. M., Elliott-Fisk, D. L., Wylie, G. D., Perry, W. M. and Takekawa, J. Y. (2014). "Importance of biogeomorphic and spatial properties in assessing a tidal salt marsh vulnerability to sea-level rise." *Estuaries and Coasts* 37(4): 941-951.

Townend, I., Fletcher, C., Knappen, M. and Rossington, K. (2011). "A review of salt marsh dynamics." *Water and Environment Journal* 25(4): 477-488.

Warren, R. S., Fell, P. E., Rozsa, R., Brawley, A. H., Orsted, A. C., Olson, E. T., Swamy, V. and Niering, W. A. (2002). "Salt Marsh Restoration in Connecticut: 20 Years of Science and Management." *Restoration Ecology* 10(3): 497-513.

Warren, R. S. and Niering, W. A. (1993). "Vegetation change on a northeast tidal marsh: Interaction of sea-level rise and marsh accretion." *Ecology* 74(1): 96-103.

Wolters, M., Garbutt, A. and Bakker, J. P. (2005). "Salt-marsh restoration: evaluating the success of de-embankments in north-west Europe." *Biological Conservation* 123(2): 249-268.

CHAPTER 2. REVIEW OF SALT MARSH EVOLUTION MODELS FOR ASSESSING SEA LEVEL RISE EFFECTS ON WETLANDS

2.1 Sea Level Rise Effects on Wetlands

Coastal wetlands are in danger of losing productivity and density under future scenarios; investigating the various parameters impacting these systems provides insight into potential future changes (Nicholls, 2004). It is expected that one of the prominent variables governing future wetland loss will be SLR (Nicholls et al., 1999). The effects of SLR on coastal wetland loss have been studied extensively by a diverse group of researchers. For example, a study on Wequetequock-Pawcatuck tidal marshes in New England over four decades showed that vegetation type and density change as a result of wetland loss in those areas (Warren and Niering, 1993). Another study found that vegetation type change and migration of high-marsh communities will be replaced by cordgrass or inundated if SLR increases significantly (Donnelly and Bertness, 2001). However, other factors and conditions such as removal of sediment by dredging, and sea walls and groyne construction were shown to be influential in the salt marsh productivity variations in southern England (Hughes, 2001). Therefore, it is critical to study an array of variables, including SLR, when assessing the past, present and future productivity of salt marsh systems.

2.2 Importance of Salt Marshes

Salt marshes play an important ecosystem-services role by providing intertidal habitats for many species. These species can be categorized in different ways (Teal, 1962); animals that visit marshes to feed and animals that use marshes as a habitat (Nicol, 1935). Some species are observed in the low tide regions and within the creeks, who travel from regions elsewhere in the estuarine

environment, while others are terrestrial animals that intermittently live in the marsh system. Other species such as crabs live in the marsh surface (Daiber, 1977). Salt marshes protect these animals by providing shelter and acting as a potential growth resource (Halpin, 2000); many of these species have great commercial and economic importance. Marshes also protect shorelines and reduce erosion by dissipating wave energy and increasing friction, both of which subsequently decreases flow energy (Möller and Spencer, 2002). Salt marshes effectively attenuate wave energy by decreasing wave heights per unit distance across salt marsh system, and also significantly affect the mechanical stabilization of shorelines. These processes depend heavily on vegetation density, biomass production, and marsh size (Shepard et al., 2011). Moreover, Knutson (1987) mentioned that the dissipation of energy by salt marsh roots and rhizomes increases the opportunity for sediment deposition and decreases marsh erodibility. During periods of sea level rise, salt marsh systems play an important role in protecting shorelines by both generating and dissipating turbulent eddies at different scales which helps transport and trap fine materials in the marshes (Seginer et al., 1976; Leonard and Luther, 1995; Moller et al., 2014). As a result, understanding changes in vegetation can provide productive restoration planning and coastal management guidance (Bakker et al., 1993).

2.3 Sea Level Rise

Projections of global SLR are important for analyzing coastal vulnerabilities (Parris et al., 2012). Based on studies of historic sea level changes, there were periods of rise, standstill, and fall (Donoghue and White, 1995). Globally, relative SLR is mainly influenced by eustatic sea-level change, which is primarily a function of total water volume in the ocean, and the isostatic

movement of the earth's surface generated by ice sheet mass increase or decrease (Gornitz, 1982). Satellite altimetry data have shown that mean sea level from 1993-2000 increased at a rate of 3.4 ± 0.4 $mm.yr^{-1}$ (Nerem et al., 2010). The total climate related SLR from 1993-2007 is 2.85 ± 0.35 $mm.yr^{-1}$ (Cazenave and Llovel, 2010). Data from long-term tide gauges show that global mean sea level has increased by 1.7 $mm.yr^{-1}$ in the last century (Church and White, 2006). Furthermore, global sea level rise rate has accelerated at 0.01 $mm.yr^{-2}$ in the past 300 years, and if it continues at this rate, SLR with respect to the present will be 34 cm in the year 2100 (Jevrejeva et al., 2008). Additionally, using multiple scenarios for future global SLR while considering different levels of uncertainty can be used develop different potential coastal responses (Walton Jr, 2007).

Unfortunately, there is no universally accepted method for probabilistic projection of global SLR (Parris et al., 2012). However, the four global SLR scenarios for 2100 presented in a National Oceanic and Atmospheric Administration (NOAA) report are considered reasonable and are categorized as low (0.2 m), intermediate-low (0.5 m), intermediate-high (1.2 m) and high (2.0 m). The low scenario is derived from the linear extrapolation of global tide gauge data, beginning in 1900. The intermediate-low projection is developed using the Intergovernmental Panel on Climate Change (IPCC) Fourth Assessment Report (AR4) on SLR. The intermediate-high scenario uses the average of the high statistical projections of SLR from observed data. The high scenario is calculated using projected values of ocean warming and ice sheet melt projection (Parris et al., 2012).

Globally, the acceleration of SLR is not spatially constant (Sallenger et al., 2012). There is no generally accepted method to project SLR at the local scale (Parris et al., 2012); however, a tide

gauge analysis performed in Florida using three different methods forecasted a rise between 0.11 to 0.36 m from present day to the year 2080 (Walton Jr, 2007). The absolute value of the increase of the vertical distance between land and mean sea level is called relative sea level rise (RSLR), and can be defined in marshes as the total value of eustatic SLR, considering deep and shallow subsidence (Rybczyk and Callaway, 2009). The NGOM has generally followed the global eustatic SLR but exceeds the global average rate of RSLR; regional gauges showed RSLR to be about 2 $mm.yr^{-1}$, which varies by location and is higher in Louisiana and Texas because of local subsidence (Donoghue, 2011). RSLR in the western Gulf of Mexico (Texas and Louisiana coasts) is reported to be 5 to 10 $mm.yr^{-1}$ faster than global RSLR because of multi-decadal changes or large basin oceanographic effects (Parris et al., 2012). Concurrently, the U.S. Army Corps of Engineers (USACE) developed three projections of low, intermediate, and high SLR at the local scale. The low curve follows the historic trend of SLR and the intermediate and high curves use NRC curves (United States Army Corps of Engineers (USACE), 2011). These projections are fused with local variations such as subsidence to project local SLR for application in the design of infrastructure (http://www.corpsclimate.us/ccaceslcurves_nn.cfm).

It is very important to consider a dynamic approach when applying SLR scenarios for coastal vulnerability assessments to capture nonlinearities that are unaccounted for by the static or "bathtub" approach (Bacopoulos et al., 2012; Bilskie et al., 2014; Passeri et al., 2014). The static or "bathtub" approach simply elevates the water surface by a given SLR and extrapolates inundation based on the land elevations. A dynamic approach captures the nonlinear feedbacks of the system by considering the interactions between impacted topography and inundation that may lead to an increase or decrease in future tide levels (Hagen and Bacopoulos, 2012; Atkinson et al.,

2013; Bilskie et al., 2014). The static approach also does not consider any future changes in landscape (Murdukhayeva et al., 2013). Additionally, some of the areas that are projected to become inundated using the bathtub approach are not correctly predicted due to the complexities in coastal processes and the changes in coastline and vulnerable areas (Gesch, 2013). Therefore, it is critical to use a dynamic approach that considers these complexities and also includes future changes to these systems such as shoreline morphology.

Estuarine circulation is dominated by tidal and river inflow; understanding the variation in velocity residuals under SLR scenarios can help to understand the potential effects to coastal ecosystems (Valentim et al., 2013). Some estuaries respond to SLR by rapidly filling with more sediment and or by flushing and losing sediment; these responses vary according to the estuary's geometry (Friedrichs et al., 1990). Sediment accumulation in estuaries changes with sediment input, geomorphology, fresh water inflow, tidal condition, and the rate of RSLR (Nichols, 1981). Two parameters that affect an estuary's sediment accumulation status are the potential sediment trapping index and the degree of mixing. The potential sediment trapping index is defined as the ratio of volumetric capacity to the total mean annual inflow (Biggs and Howell, 1984) and the degree of mixing is described as the ratio of mean annual fresh water inflow (during half a tidal cycle) to the tidal prism (the volume of water leaving an estuary between mean high tide and mean low tide) (Nichols, 1989).

2.4 Hydrodynamic Modeling of Sea Level Rise

SLR can alter circulation patterns and sediment transport, which affect the ecosystem and wetlands (Nichols, 1989). The hydrodynamic parameters that SLR can change are tidal range, tidal prism,

surge heights, and inundation of shorelines (National Research Council, 1987). The amount of change for the tidal prism depends on the characteristics of the bay (Passeri et al., 2014). An increase in tidal prism often causes stronger tidal flows in the bays (Boon Iii and Byrne, 1981). Research on the effects of sea level change on hydrodynamic parameters has been investigated using various hydrodynamic models. Reviewing this work accelerates our understanding of how the models that can be applied in coupled hydrodynamic and marsh assessments.

Wolanski and Chappell (1996) applied a calibrated hydrodynamic model to examine the effects of 0.1 m and 0.5 m SLR in three rivers in Australia. Their hydrodynamic model is a one-dimensional, finite difference, implicit, depth-averaged model that solves the full non-linear equations of motion. Results showed changes in channel dimensions under future SLR. In addition, they connected the hydrodynamic model to a sediment transport model and showed that some sediment was transported seaward by two rivers because of the SLR effect resulting in channel widening. The results also indicated transportation of more sediment to the floodplain by another river as a result of SLR.

Liu (1997) used a three-dimensional hydrodynamic model for the China Sea to investigate the effects of one meter sea level rise in near-shore tidal flow patterns and storm surge. The results showed more inundation farther inland due to storm surge. The results also indicated the importance of the dynamic and nonlinear effects of momentum transfer in simulating astronomical tides under SLR and their impact on storm surge modeling. The near-shore transport mechanisms also changed because of nonlinear dynamics and altered depth distribution in shallow near-shore areas. These mechanisms also impact near-shore ecology.

Hearn and Atkinson (2001) studied the effects of local RSLR on Kaneohe Bay in Hawaii using a hydrodynamic model. The model was applied to show the sensitivity of different forcing mechanisms to a SLR of 60 cm. They found circulation pattern changes particularly over the reef which improved the lagoon flushing mechanisms.

French (2008) investigated a managed realignment of an estuarine response to a 0.3 m SLR using a two-dimensional hydrodynamic model (Telemac 2D). The study was done on the Blyth estuary in England, which has hypsometric characteristics (vast intertidal area and a small inlet) that make it vulnerable to SLR. The results showed that the maximum tidal velocity and flow increased by 20% and 28%, respectively under the SLR using present day bathymetry. This research demonstrated the key role of sea wall realignment in protecting the estuary from local flooding. However, the outer estuary hydrodynamics and sediment fluxes were also altered, which could have more unexpected consequences for wetlands.

Leorri et al. (2011) simulated pre-historic water levels and flows in Delaware Bay under SLR during the late Holecene using the Delft3D hydrodynamic model. Sea level was lowered to the level circa 4000 years ago, with present day bathymetry. The authors found that the geometry of the bay changed, which affected the tidal range. The local tidal range changed nonlinearly by 50 cm. They concluded that when projecting sea level rise, coastal amplification (or deamplification) of tides should be considered.

Hagen and Bacopoulos (2012) assessed inundation of Florida's Big Bend Region using a two-dimensional ADCIRC model by comparing maximum envelopes of water against inundated

surfaces. Both static and dynamic approaches were used to demonstrate the nonlinearity of SLR. The results showed an underestimation of the flooded area by 2/3 in comparison with dynamic approach. The authors concluded that it is imperative to implement a dynamic approach when investigating the effects of SLR.

Valentim et al. (2013) employed a two-dimensional hydrodynamic model (MOHID) to study the effects of SLR on tidal circulation patterns in two Portuguese coastal systems. Their results indicated the importance of river inflow in long-term hydrodynamic analysis. Although the difference in residual flow intensity varied between 80 to 100% at the river mouth under a rise of 42 cm based on local projections, it decreased discharge in the bay by 30%. These changes in circulation patterns could affect both biotic and abiotic processes. They concluded that low lying wetlands will be affected by inundation and erosion, making these habitats vulnerable to SLR.

Hagen et al. (2013) studied the effects of SLR on mean low water (MLW) and mean high water (MHW) in a marsh system (particularly tidal creeks) in northeast Florida using an ADCIRC hydrodynamic model. The results showed a higher increase in MHW than the amount of SLR and lower increase in MLW than the amount of SLR. The spatial variability in both of the tidal datums illustrated the nonlinearity in tidal flow and further justified using a dynamic approach in SLR assessments.

2.5 Marsh Response to Sea Level Rise

Research has shown that under extreme conditions, salt marshes will not have time to establish an equilibrium and may migrate landward or convert to open water (Warren and Niering, 1993; Gabet,

1998; Donnelly and Bertness, 2001; Hughes, 2001; Castillo et al., 2002). One method for projecting salt marsh response under different stressors (i.e. SLR) is utilizing ecological models. The dynamics of salt marshes, which are characterized by complex inter-relationships between physics and biology (Townend et al., 2011), requires the coupling of seemingly disparate models to capture sensitivity and feedback processes (Reed, 1990). In particular, these coupled model systems allow researchers to examine marsh response to a projected natural or anthropogenic change in environmental conditions such as SLR. The models can be divided into two groups based on the simulation spatial scales in projecting vegetation productivity: landscape scale models and small scale models with appropriate resolution. Although most studies are categorized based on these scales, the focus on their grouping is more on morphodynamic processes (Rybczyk and Callaway, 2009; Fagherazzi et al., 2012).

2.5.1 Landscape Scale Models

Ecosystem-based landscape models are designed to lower the computational expense by lowering the resolution and simplifying physical processes between ecosystem units (Fagherazzi et al., 2012). These models connect different parameters such as hydrology, hydrodynamics, water nutrients, and environmental inputs, integrating them into a large scale model. Although these models are often criticized for their uncertainty, inaccurate estimation and simplification in their approach (Kirwan and Guntenspergen, 2009), they are frequently used for projecting future wetland states under SLR due to their low computational expense and simple user interface. A few of these models will be discussed herein.

General Ecosystem Model (GEM) is a landscape scale model that directly simulates the hydrologic processes in a grid-cell spatial simulation with a minimum one day time step, and connects processes with water quality parameters to target macrophyte productivity (Fitz et al., 1996). Another direct calculation model is the Coastal Ecological Landscape Spatial Simulation (CELSS) model that interconnects each one square kilometer cell to its four nearest neighbors by exchanging water and suspended sediments using the mass-balance approach and applying other hydrologic forcing like river discharge, sea level, runoff, temperature, and winds. Each cell is checked for a changing ecosystem type until the model reaches the final time (Sklar et al., 1985; Costanza et al., 1990). This model has been implemented in projects to aid in management systems (Costanza and Ruth, 1998).

Reyes et al. (2000) investigated the Barataria and Terrebonne basins of coastal Louisiana for historical land loss and developed Barataria–Terrebonne ecological landscape spatial simulation (BTELSS) model, which is a direct-calculation landscape model. This model framework is similar to CELSS but with interconnections between the hydrodynamic, plant-production, and soil-dynamics modules. Forcing parameters include subsidence, sedimentation, and sea-level rise. After the model was calibrated and validated, it was used to simulate 30 years into the future starting in 1988. They showed that weather variability has more of an impact on land loss than extreme weather. This model was also used for management planning (Martin et al., 2000).

Another landscape model, presented by Martin (2000), was also designed for the Mississippi delta. The Mississippi Delta Model (MDM) is similar to BTELSS, as it transfers data between modules that are working in different time steps. However, it also includes a variable time-step

hydrodynamic element, and mass-balance sediment and marsh modules. This model has higher resolution than BTELSS, which allows river channels to be captured, and results in the building the delta via sediment deposition (Martin et al., 2002).

Reyes et al. (2003) and Reyes et al. (2004) presented two landscape models to simulate land loss and marsh migration in two watersheds in Louisiana. The models include coupled hydrodynamic, biological, and soil dynamic modules. The results from the hydrodynamic and biological modules are fed into the soil dynamic module. The outputs are assessed using a habitat switching module for different time and space scales. The Barataria Basin Model (BBM) and Western Basin Model (WBM) were calibrated to explore SLR effects and river diversion at the Mississippi Delta for 30 and 70-year predictions. The results showed the importance of increasing river inflow to the basins. They also showed that a restriction in water delivery resulted in land loss with a nonlinear trend (Reyes et al., 2003; Reyes et al., 2004).

The same approach as BBM and WBM was applied to develop the Caernarvon Watershed Model in Louisiana, and the Centla Watershed Model for the Biosphere Reserve Centla Swamps in the state of Tabasco in Mexico (Reyes et al., 2004). The first model includes 14,000 cells ranging from 0.25 to 1 km^2 in size used to forecast habitat conditions in 50 years to aid in management planning. The second model illustrated a total habitat loss of 16% in the watershed within 10 years, resulting from increased oil extraction and lack of monitoring (Reyes et al., 2004).

Lastly, the Sea Level Affecting Marshes Model (SLAMM), is a spatial model for projecting sea level rise effects on coastal systems. It implements decision rules to predict the transformation of

different categories of wetlands in each cell of the model (Park et al., 1986). This model assumes each one square-kilometer is covered with one category of wetlands and one elevation, ignoring the development for residential area. In addition, no freshwater inflow is considered where saltwater and freshwater wetlands are distinguishable, and salt marshes in different regions are parameterized with the same characteristics.

The SLAMM model was partially validated in a study where high salt marsh replaced low salt marsh by the year 2075 under low SLR (2.5 ft) in Tuckerton, NJ (Kana et al., 1985). The model input includes a digital elevation model (DEM), SLR, land use land cover (LULC) map, and tidal data (Clough et al., 2010). In the main study using SLAMM in 1986, 57 coastal wetland sites (485,000 ha) were selected for simulation. Results indicated 56% and 22% loss of these wetlands under high and low SLR scenarios, respectively by the year 2100. Most of these losses occurred in the Gulf Coast and in the Mississippi delta (Park et al., 1986). In a more comprehensive study of 93 sites, results showed 17%, 48%, 63%, and 76% of coastal wetland loss for 0.5 m, 1 m, 2 m, and 3 m SLR, respectively (Park et al., 1989).

Another study used measurements, geographic data and SLR in conjunction with simulations from SLAMM to study the effects of SLR on salt marshes along Georgia coast for the year 2100 (Craft et al., 2008). Six sites were selected, including two salt marshes, two brackish marshes, and two fresh water marshes. In the SLAMM version used in this study, salt water intrusion was considered. The results indicated 20% and 45% of salt marshes loss under mean and high SLR, respectively. However, freshwater marshes increased by 2% under mean SLR and decreased by 39% under the maximum SLR scenario. Results showed that marshes in the lower and higher bounds of salinity

are more affected by accelerated SLR, except the ones that have enough accretion or ones that were able to migrate. This model is also applied in other parts of the world (Udo et al., 2013; Wang et al., 2014) and modified to investigate the effects of SLR on other species like Submerged Aquatic Vegetation (SAV) (Lee II et al., 2014).

2.5.2 High Resolution Models

Models with higher resolution, feedback between different parameters in small scales (e.g., salinity level (Spalding and Hester, 2007), CO2 concentration (Langley et al., 2009), temperature (McKee and Patrick, 1988), tidal range (Morris et al., 2002), location (Morris et al., 2002), and marsh platform elevation (Redfield, 1972; Orson et al., 1985)) play an important role in determining salt marsh productivity (Morris et al., 2002; Spalding and Hester, 2007). One of the most significant factors in the ability of salt marshes to maintain equilibrium under accelerated SLR (Morris et al., 2002) is maintaining platform elevation through organic (Turner et al., 2000; Nyman et al., 2006; Neubauer, 2008; Langley et al., 2009) and inorganic (Gleason et al., 1979; Leonard and Luther, 1995; Li and Yang, 2009) sedimentation (Krone, 1987; Morris and Haskin, 1990; Reed, 1995; Turner et al., 2000; Morris et al., 2002). Models with high resolution that investigate marsh vegetation and platform response to SLR are explained herein.

In terms of the seminal work on this topic, Redfield and Rubin (1962) investigated marsh development in New England in response to sea level rise. They showed the dependency of high marshes to sediment deposition and vertical accretion in response to SLR. Randerson (1979) used a holistic approach to build a time-stepping model calibrated by observed data. The model is able to simulate the development of salt marshes considering feedbacks between the biotic and abiotic

elements of the model. However, the author insisted on the dependency of the models on long-term measurements and data. Krone (1985) presented a method for calculating salt marsh platform rise under tidal effects and sea level change, including sediment and organic matter accumulation. Results showed that SLR can have a significant effect on marsh platform elevation. Krone (1987) applied this method to South San Francisco Bay by using historic mean tide measurements, and measuring marsh surface elevation. His results indicated that marsh surface elevation increases in response to SLR and maintains the same rate of increasing, even if the SLR rate becomes constant.

As the study of this topic shifted towards computer modeling, Orr et al. (2003) modified the Krone (1987)'s model by adding a constant organic accretion rate, consistent with French (1993)'s approach. The model was run for SLR scenarios and results indicated that under low SLR, high marshes were projected to keep their elevation, but under higher rates of SLR, the elevation would decrease in 100 years and reach the elevation of low/high marsh. Stralberg et al. (2011) presented a hybrid model that included marsh accretion (sediment and organic), first developed by Krone (1987), and its spatial variation. The model was applied to San Francisco Bay over a 100 year period with SLR assumptions. They concluded that under a high rate of SLR, for minimizing marsh loss, the adjacent upland area should be protected for marsh migration and adding sediments to raise the land and focus more on restoration of the rich-sediment regions.

Allen (1990) presented a numerical model for mudflat-marsh growth that includes minerorganic and organogenic sedimentation rate, sea level rise, sediment compaction parameters and support the model with some published data (Kirby and Britain, 1986; Allen and Rae, 1987; Allen and

Rae, 1988) from Severn estuary in southwest Britain. His results demonstrated a rise in marsh platform elevation, which flattens off afterward in response to the applied SLR scenario.

Chmura et al. (1992) constructed a model for connecting SLR, compaction, sedimentation and platform accretion, and submergence of the marshes. The model was calibrated with long term sedimentation data. The model showed that an equilibrium between the rate of accretion and the rate of SLR can theoretically be reached in Louisiana marshes.

French (1993) applied a one-dimensional model that was based on a simple mass balance to predict marsh growth and marsh platform accretion rate as a function of sedimentation, tidal range, and local subsidence. The model was also applied to assess historical marsh growth and marsh response to nonlinear SLR in Norfolk, UK. His model projected marsh drowning under a dramatic SLR scenario by the year 2100. Allen (1997) also developed a conceptual qualitative model to describe the three-dimensional character of marshes to assess morphostratigraphic evolution of marshes under sea level change. He showed that creek networks grow in cross-section and number in response to SLR, but shrink afterward. He also investigated the effects of great earthquakes on the coastal land and creeks.

van Wijnen and Bakker (2001) studied 100 years of marsh development by developing a simple predictive model that connects changes in surface elevation with SLR. The model was tested in several sites in the Netherlands. Results showed that marsh surface elevation is dependent on accretion rate and continuously increases but with different rates. Their results also indicated that old marshes may subside due to shrinkage of the clay layer in summer.

The Marsh Equilibrium Model (MEM) is a parametric marsh model that showed that there is an optimum range for salt marsh elevation in the tidal frame in order to have the highest biomass productivity (Morris et al., 2002). Based on long-term measurements, Morris et al. (2002) proposed a parabolic function for defining biomass density with respect to nondimensional depth D and parameters a, b, and c that are determined by measurements, differ regionally and depend on salinity, climate, and tide range (Morris, 2007). The accretion rate in this model is a positive function based on organic and inorganic sediment accumulation. The two accretion sources, organic and inorganic, are necessary to maintain marsh productivity under SLR; otherwise marshes might become submerged (Nyman et al., 2006; Blum and Roberts, 2009; Baustian et al., 2012). Organic accretion is a function of the biomass density in the marsh. Inorganic accretion (i.e., mineral sedimentation) also is influenced by the biomass density, which affects the ability of the marsh to 'trap' sediments. Inorganic sedimentation occurs as salt marshes impede flow by increasing friction and the sediments' time of travel, which allows for sediment deposition on the marsh platform (Leonard and Luther, 1995; Leonard and Croft, 2006). The linear function developed by Morris et al. (2002) for the rate of total accretion is a function of nondimensional depth, biomass density and constants q and k. q represents the inorganic portion of accretion that is from the sediment loading rate and k represents the organic and inorganic contributions resulting from the presence of vegetation. The values of the constants q and k differ based on the estuarine system, marsh type, land slope, and other factors (Morris et al., 2002). The accretion rate is positive for salt marshes below MHW; when $D > 0$ no accumulation of sediments will occur for salt marshes above MHW (Morris, 2007). The parameters for this model were derived at North Inlet,

South Carolina where Spartina Alterniflora is the dominant species. However, these constants can be derived for other estuaries.

Temmerman et al. (2003) also generated a zero-dimensional time stepping model using the mass balance approaches from Krone (1987), Allen (1990), and French (1993) . The model was tested and calibrated with historical marsh platform accretion rates in the Scheldt estuary in Belgium. They authors recognize the significance of accounting for long-term elevation change of tidal marshes.

The model developed by Morris et al. (2002) has been utilized in other models for salt marsh evolution (Mudd et al., 2004; D' Alpaos et al., 2006; Kirwan and Murray, 2007). Mudd et al. (2004) suggested a one-dimensional model with hydrodynamic, biomass, and sediment transport (sediment settling and trapping) components. The biomass component is the salt marsh model of Morris et al. (2002) and calculates the evolution of the marsh platform through a transect perpendicular to a tidal creek. The model neglects erosion and the neap-spring tide cycle, models a single marsh species at a time, and only estimates above ground biomass. The hydrodynamic module derives water velocity and level from tidal flow, which serve as inputs for biomass calculation. Sedimentation is divided into particle settling and trapping and also organic deposition. The model showed that the marshes that are more dependent on sediment transport adjust faster to SLR than a marsh that is more dependent on organic deposition.

D' Alpaos et al. (2006) used the marsh model developed by Morris et al. (2002) in a numerical model for the evolution of a salt marsh creek. The model consists of hydrodynamic, sediment

erosion and deposition, and vegetation modules. The modules are connected together in a way that allows tidal flow to affect sedimentation, erosion and marsh productivity and the vegetation to affect drag. The objective of this model was to study vegetation and tidal flow on creek geometry. The results showed that the width-to-depth ratio of the creeks is decreased by increasing vegetation and accreting marsh platform whereas the overall cross section area depends on tidal flow.

Kirwan and Murray (2007) generated a three dimensional model that connects biological and physical processes. The model has a channel network development module that is affected by erosion caused by tidal flow, slope driven erosion, and organic deposition. The vegetation module for this model is based on a simplified version of the parametric marsh model by (Morris et al., 2002). The results indicated that for a moderate SLR, the accretion and SLR are equal, but for a high SLR, the creeks expand and the accretion rate increases and resists against SLR while unvegetated areas are projected to become inundated.

Mariotti and Fagherazzi (2010) also developed a one dimensional model that connects the marsh model by Morris et al. (2002) with tidal flow, wind waves, sediment erosion and deposition. The model was designed to demonstrate marsh boundary change with respect to different scenarios of SLR and sedimentation. This study showed the significance of vegetation on sedimentation in the intertidal zone. Moreover, the results illustrated the expanding marsh boundary under low SLR scenario due to an increase in transported sediment and inundation of the marsh platform and its transformation to a tidal flat under high SLR.

Tambroni and Seminara (2012) investigated salt marsh tendencies for reaching equilibrium by generating a one dimensional model that connects a tidal flow (considering wind driven currents and sediment flux) module with a marsh model. The model captures the growth of creek and marsh structure under SLR scenarios. Their results indicated that a marsh may stay in equilibrium under low SLR, but the marsh boundary may move based on different situations.

Hagen et al. (2013) assessed SLR effects on the lower St. Johns River salt marsh using an integrated model that couples a two dimensional hydrodynamic model, the Morris et al. (2002) marsh model, and an engineered accretion rate. Their hydrodynamic model output is MLW and MHW, which are the inputs for the marsh model. They showed that MLW and MHW in the creeks are highly variable and sensitive to SLR. This variability explains the variation in biomass productivity. Additionally, their study demonstrated how marshes can survive high SLR using an engineered accretion such as thin-layer disposal of dredge spoils.

Marani et al. (2013) studied marsh zonation in a coupled geomorphological-biological model. The model use Exner's equation for calculating variations in marsh platform elevation. They showed that vegetation "engineers" the platform to seek equilibrium through increasing biomass productivity. The zonation of vegetation is due to interconnection between geomorphology and biology. The study also concluded that the resiliency of marshes against SLR depends on their characteristics and abilities and some or all of them may disappear because of changes in SLR.

Schile et al. (2014) calibrated the Marsh Equilibrium Model developed by Morris et al. (2002) for Mediterranean-type marshes and projected marsh distribution and accretion rates for four sites in

the San Francisco Bay Estuary under four SLR scenarios. To better demonstrate the spatial distribution of marshes, the authors applied the results to a high resolution DEM. They concluded that under low SLR, the marshes maintained their productivity, but under intermediate low and high SLR, the area will be dominated by low marsh and no high marsh will remain; under high SLR scenario, the marsh area is projected to become a mudflat.

2.6 References

Allen, J. R. L. (1990). "Salt-marsh growth and stratification: A numerical model with special reference to the Severn Estuary, southwest Britain." *Marine Geology* 95(2): 77-96.

Allen, J. R. L. (1997). "Simulation models of salt-marsh morphodynamics: some implications for high-intertidal sediment couplets related to sea-level change." *Sedimentary Geology* 113(3–4): 211-223.

Allen, J. R. L. and Rae, J. E. (1987). "Late Flandrian Shoreline Oscillations in the Severn Estuary: A Geomorphological and Stratigraphical Reconnaissance." *Philosophical Transactions of the Royal Society of London. Series B, Biological Sciences* 315(1171): 185-230.

Allen, J. R. L. and Rae, J. E. (1988). "Vertical salt-marsh accretion since the Roman Period in the Severn Estuary, southwest Britain." *Marine Geology* 83(1–4): 225-235.

Atkinson, J., McKee Smith, J. and Bender, C. (2013). "Sea-level rise effects on storm surge and nearshore waves on the Texas coast: Influence of landscape and storm characteristics." *Journal of Waterway, Port, Coastal, and Ocean Engineering* 139(2): 98-117.

Bacopoulos, P., Hagen, S. C., Cox, A. T., Dally, W. R. and Bratos, S. M. (2012). "Observation and simulation of winds and hydrodynamics in St. Johns and Nassau Rivers." *Journal of Hydrology* 420–421(0): 391-402.

Bakker, J. P., de Leeuw, J., Dijkema, K. S., Leendertse, P. C., Prins, H. H. T. and Rozema, J. (1993). "Salt marshes along the coast of The Netherlands." *Hydrobiologia* 265(1-3): 73-95.

Baustian, J. J., Mendelssohn, I. A. and Hester, M. W. (2012). "Vegetation's importance in regulating surface elevation in a coastal salt marsh facing elevated rates of sea level rise." *Global Change Biology* 18(11): 3377-3382.

Biggs, R. B. and Howell, B. A. (1984). "Estuary as a Sediment Trap: Alternate Approaches to Estimating Its Filtering Efficiency." *The Estuary as a Filter*: 107-129.

Bilskie, M. V., Hagen, S. C., Medeiros, S. C. and Passeri, D. L. (2014). "Dynamics of sea level rise and coastal flooding on a changing landscape." *Geophysical Research Letters* 41(3): 927-934.

Blum, M. D. and Roberts, H. H. (2009). "Drowning of the Mississippi Delta due to insufficient sediment supply and global sea-level rise." *Nature Geoscience* 2(7): 488-491.

Boon Iii, J. D. and Byrne, R. J. (1981). "On basin hyposmetry and the morphodynamic response of coastal inlet systems." *Marine Geology* 40(1–2): 27-48.

Castillo, J., Rubio-Casal, A., Luque, C., Nieva, F. and Figueroa, M. (2002). "Wetland loss by erosion in Odiel Marshes (SW Spain)." *Journal of Coastal Research* 36: 134-138.

Cazenave, A. and Llovel, W. (2010). "Contemporary Sea Level Rise." *Annual Review of Marine Science* 2(1): 145-173.

Chmura, G. L., Costanza, R. and Kosters, E. C. (1992). "Modelling coastal marsh stability in response to sea level rise: a case study in coastal Louisiana, USA." *Ecological Modelling* 64(1): 47-64.

Church, J. A. and White, N. J. (2006). "A 20th century acceleration in global sea-level rise." *Geophysical Research Letters* 33(1): L01602.

Clough, J. S., Park, R. A. and Fuller, R. (2010). "SLAMM 6 beta technical documentation." *Waitsfield, VT*.

Costanza, R. and Ruth, M. (1998). "Using Dynamic Modeling to Scope Environmental Problems and Build Consensus." *Environmental Management* 22(2): 183-195.

Costanza, R., Sklar, F. H. and White, M. L. (1990). "Modeling Coastal Landscape Dynamics." *BioScience* 40(2): 91-107.

Craft, C., Clough, J., Ehman, J., Joye, S., Park, R., Pennings, S., Guo, H. and Machmuller, M. (2008). "Forecasting the effects of accelerated sea-level rise on tidal marsh ecosystem services." *Frontiers in Ecology and the Environment* 7(2): 73-78.

D' Alpaos, A., Lanzoni, S., Mudd, S. M. and Fagherazzi, S. (2006). "Modeling the influence of hydroperiod and vegetation on the cross-sectional formation of tidal channels." *Estuarine, Coastal and Shelf Science* 69(3–4): 311-324.

Daiber, F. (1977). "Salt marsh animals: Distributions related to tidal flooding, salinity and vegetation." *Ecosystems of the world*.

Donnelly, J. P. and Bertness, M. D. (2001). "Rapid shoreward encroachment of salt marsh cordgrass in response to accelerated sea-level rise." *Proceedings of the National Academy of Sciences* 98(25): 14218-14223.

Donoghue, J. (2011). "Sea level history of the northern Gulf of Mexico coast and sea level rise scenarios for the near future." *Climatic Change* 107(1-2): 17-33.

Donoghue, J. F. and White, N. M. (1995). "Late Holocene Sea-Level Change and Delta Migration, Apalachicola River Region, Northwest Florida, U.S.A." *Journal of Coastal Research* 11(3): 651-663.

Fagherazzi, S., Kirwan, M. L., Mudd, S. M., Guntenspergen, G. R., Temmerman, S., D'Alpaos, A., van de Koppel, J., Rybczyk, J. M., Reyes, E., Craft, C. and Clough, J. (2012). "Numerical models of salt marsh evolution: Ecological, geomorphic, and climatic factors." *Reviews of Geophysics* 50(1): RG1002.

Fitz, H. C., DeBellevue, E. B., Costanza, R., Boumans, R., Maxwell, T., Wainger, L. and Sklar, F. H. (1996). "Development of a general ecosystem model for a range of scales and ecosystems." *Ecological Modelling* 88(1–3): 263-295.

French, J. R. (1993). "Numerical simulation of vertical marsh growth and adjustment to accelerated sea-level rise, North Norfolk, U.K." *Earth Surface Processes and Landforms* 18(1): 63-81.

French, J. R. (2008). "Hydrodynamic Modelling of Estuarine Flood Defence Realignment as an Adaptive Management Response to Sea-Level Rise." *Journal of Coastal Research*: 1-12.

Friedrichs, C., Aubrey, D. and Speer, P. (1990). Impacts of Relative Sea-level Rise on Evolution of Shallow Estuaries. Residual Currents and Long-term Transport. R. T. Cheng, Springer New York. **38:** 105-122.

Gabet, E. (1998). "Lateral migration and bank erosion in a saltmarsh tidal channel in San Francisco Bay, California." *Estuaries* 21(4): 745-753.

Gesch, D. B. (2013). "Consideration of Vertical Uncertainty in Elevation-Based Sea-Level Rise Assessments: Mobile Bay, Alabama Case Study." *Journal of Coastal Research*: 197-210.

Gleason, M. L., Elmer, D. A., Pien, N. C. and Fisher, J. S. (1979). "Effects of Stem Density upon Sediment Retention by Salt Marsh Cord Grass, Spartina alterniflora Loisel." *Estuaries* 2(4): 271-273.

Gornitz, V., Lebedeff, S., Hansen, J. (1982). "Global Sea Level Trend in the Past Century." *Science* 215(4540): 1611-1614.

Hagen, S., Morris, J., Bacopoulos, P. and Weishampel, J. (2013). "Sea-Level Rise Impact on a Salt Marsh System of the Lower St. Johns River." *Journal of Waterway, Port, Coastal, and Ocean Engineering* 139(2): 118-125.

Hagen, S. C. and Bacopoulos, P. (2012). "Coastal Flooding in Florida's Big Bend Region with Application to Sea Level Rise Based on Synthetic Storms Analysis." *Terr. Atmos. Ocean. Sci.* 23: 481-500.

Halpin, P. M. (2000). "Habitat use by an intertidal salt-marsh fish: trade-offs between predation and growth." *Marine Ecology Progress Series* 198: 203-214.

Hearn, C. J. and Atkinson, M. J. (2001). "Effects of sea-level rise on the hydrodynamics of a coral reef lagoon: Kaneohe Bay, Hawaii." *Sea-level Changes and Their Effects*: 25.

Hughes, R. G. (2001). Biological and Physical Processes That Affect Saltmarsh Erosion and Saltmarsh Restoration: Development of Hypotheses. Ecological Comparisons of Sedimentary Shores. K. Reise, Springer Berlin Heidelberg. **151:** 173-192.

Jevrejeva, S., Moore, J. C., Grinsted, A. and Woodworth, P. L. (2008). "Recent global sea level acceleration started over 200 years ago?" *Geophysical Research Letters* 35(8): L08715.

Kana, T., Eiser, W., Baca, B. and Williams, M. (1985). "Potential impacts of sea level rise on wetlands around southcentral New Jersey." *Report to US Environmental Protection Agency* 30.

Kirby, R. and Britain, G. (1986). Suspended fine cohesive sediment in the Severn Estuary and inner Bristol Channel, UK, Energy Technology Support Unit (ETSU).

Kirwan, M. L. and Guntenspergen, G. R. (2009). "Accelerated sea-level rise – a response to Craft et al." *Frontiers in Ecology and the Environment* 7(3): 126-127.

Kirwan, M. L. and Murray, A. B. (2007). "A coupled geomorphic and ecological model of tidal marsh evolution." *Proceedings of the National Academy of Sciences* 104(15): 6118-6122.

Knutson, P. (1987). Role of Coastal Marshes in Energy Dissipation and Shore Protection. The Ecology and Management of Wetlands, Springer US**:** 161-175.

Krone, R. (1985). "Simulation of marsh growth under rising sea levels." *Hydraulics and Hydrology in the Small Computer Age*, ASCE.

Krone, R. (1987). "A method for simulating historic marsh elevations." *Coastal Sediments (1987)*, ASCE.

Langley, J. A., McKee, K. L., Cahoon, D. R., Cherry, J. A. and Megonigal, J. P. (2009). "Elevated CO2 stimulates marsh elevation gain, counterbalancing sea-level rise." *Proceedings of the National Academy of Sciences* 106(15): 6182-6186.

Lee II, H., Reusser, D. A., Frazier, M. R., McCoy, L. M., Clinton, P. J. and Clough, J. S. (2014). "Sea Level Affecting Marshes Model (SLAMM)-New Functionality for Predicting Changes in Distribution of Submerged Aquatic Vegetation in Response to Sea Level Rise. Version 1.0."

Leonard, L. A. and Croft, A. L. (2006). "The effect of standing biomass on flow velocity and turbulence in Spartina alterniflora canopies." *Estuarine, Coastal and Shelf Science* 69(3–4): 325-336.

Leonard, L. A. and Luther, M. E. (1995). "Flow hydrodynamics in tidal marsh canopies." *Limnology and Oceanography* 40(8): 1474-1484.

Leorri, E., Mulligan, R., Mallinson, D. and Cearreta, A. (2011). "Sea-level rise and local tidal range changes in coastal embayments: An added complexity in developing reliable sea-level index points." *Journal of Integrated Coastal Zone Management* 11: 307-314.

Li, H. and Yang, S. L. (2009). "Trapping Effect of Tidal Marsh Vegetation on Suspended Sediment, Yangtze Delta." *Journal of Coastal Research* 25(4): 915-930.

Liu, S. K. (1997). "Using coastal models to estimate effects of sea level rise." *Ocean & Coastal Management* 37(1): 85-94.

Marani, M., Da Lio, C. and D' Alpaos, A. (2013). "Vegetation engineers marsh morphology through multiple competing stable states." *Proceedings of the National Academy of Sciences* 110(9): 3259-3263.

Mariotti, G. and Fagherazzi, S. (2010). "A numerical model for the coupled long-term evolution of salt marshes and tidal flats." *Journal of Geophysical Research: Earth Surface (2003–2012)* 115(F1).

Martin, J. (2000). "Manipulations of natural system functions within the Mississippi Delta: A simulation-modeling study."

Martin, J. F., Reyes, E., Kemp, G. P., Mashriqui, H. and Day, J. W. (2002). "Landscape modeling of the Mississippi Delta: using a series of landscape models, we examined the survival and creation of Mississippi Delta marshes and the impact of altered riverine inputs, accelerated sea-level rise, and management proposals on these marshes." *BioScience* 52(4): 357-365.

Martin, J. F., White, M. L., Reyes, E., Kemp, G. P., Mashriqui, H. and Day, J. J. W. (2000). "PROFILE: Evaluation of Coastal Management Plans with a Spatial Model: Mississippi Delta, Louisiana, USA." *Environmental Management* 26(2): 117-129.

McKee, K. and Patrick, W. H. (1988). "The relationship of smooth cordgrass (Spartina alterniflora) to tidal datums: A review." *Estuaries* 11(3): 143-151.

Moller, I., Kudella, M., Rupprecht, F., Spencer, T., Paul, M., van Wesenbeeck, B. K., Wolters, G., Jensen, K., Bouma, T. J., Miranda-Lange, M. and Schimmels, S. (2014). "Wave attenuation over coastal salt marshes under storm surge conditions." *Nature Geosci* 7(10): 727-731.

Möller, I. and Spencer, T. (2002). "Wave dissipation over macro-tidal saltmarshes: Effects of marsh edge typology and vegetation change." *Journal of Coastal Research* 36: 506-521.

Morris, J. (2007). "Ecological engineering in intertidial saltmarshes." *Hydrobiologia* 577(1): 161-168.

Morris, J. T. and Haskin, B. (1990). "A 5-yr Record of Aerial Primary Production and Stand Characteristics of Spartina Alterniflora." *Ecology* 71(6): 2209-2217.

Morris, J. T., Sundareshwar, P. V., Nietch, C. T., Kjerfve, B. and Cahoon, D. R. (2002). "Responses of coastal wetlands to rising sea level." *Ecology* 83(10): 2869-2877.

Mudd, S. M., Fagherazzi, S., Morris, J. T. and Furbish, D. J. (2004). Flow, sedimentation, and biomass production on a vegetated salt marsh in South Carolina: Toward a predictive model of marsh morphologic and ecologic evolution. The Ecogeomorphology of Tidal Marshes. Washington, DC, AGU. **59:** 165-188.

Murdukhayeva, A., August, P., Bradley, M., LaBash, C. and Shaw, N. (2013). "Assessment of Inundation Risk from Sea Level Rise and Storm Surge in Northeastern Coastal National Parks." *Journal of Coastal Research*: 1-16.

National Research Council (1987). Responding to Changes in Sea Level: Engineering Implications. Washington, DC, The National Academies Press.

Nerem, R. S., Chambers, D. P., Choe, C. and Mitchum, G. T. (2010). "Estimating Mean Sea Level Change from the TOPEX and Jason Altimeter Missions." *Marine Geodesy* 33(sup1): 435-446.

Neubauer, S. C. (2008). "Contributions of mineral and organic components to tidal freshwater marsh accretion." *Estuarine, Coastal and Shelf Science* 78(1): 78-88.

Nicholls, R. J. (2004). "Coastal flooding and wetland loss in the 21st century: changes under the SRES climate and socio-economic scenarios." *Global Environmental Change* 14(1): 69-86.

Nicholls, R. J., Hoozemans, F. M. J. and Marchand, M. (1999). "Increasing flood risk and wetland losses due to global sea-level rise: regional and global analyses." *Global Environmental Change* 9, Supplement 1(0): S69-S87.

Nichols, M. a. A., G. (1981). "Sedimentary processes in coastal lagoons". UNESCO Technical Papers in Marine Science (UNESCO), UNESCO. **33:** 27-80.

Nichols, M. M. (1989). "Sediment accumulation rates and relative sea-level rise in lagoons." *Marine Geology* 88(3–4): 201-219.

Nicol, A. T. (1935). "The Ecology of a Salt–Marsh." *Journal of the Marine Biological Association of the United Kingdom (New Series)* 20(02): 203-261.

Nyman, J. A., Walters, R. J., Delaune, R. D. and Patrick Jr, W. H. (2006). "Marsh vertical accretion via vegetative growth." *Estuarine, Coastal and Shelf Science* 69(3–4): 370-380.

Orr, M., Crooks, S. and Williams, P. B. (2003). "Will Restored Tidal Marshes Be Sustainable?" *San Francisco Estuary and Watershed Science* 1(1).

Orson, R., Panageotou, W. and Leatherman, S. P. (1985). "Response of Tidal Salt Marshes of the U.S. Atlantic and Gulf Coasts to Rising Sea Levels." *Journal of Coastal Research* 1(1): 29-37.

Park, R. A., Armentano, T. V. and Cloonan, C. L. (1986). "Predicting the effects of sea level rise on coastal wetlands." *Effects of changes in stratospheric ozone and global climate* 4: 129-152.

Park, R. A., Trehan, M. S., Mausel, P. W., Howe, R. C. and Titus, J. G. (1989). The effects of sea level rise on US coastal wetlands and lowlands, Office of Policy, Planning and Evaluation, US Environmental Protection Agency.

Parris, A., Bromirski, P., Burkett, V., Cayan, D., Culver, M., Hall, J., Horton, R., Knuuti, K., Moss, R., Obeysekera, J., Sallenger, A. and Weiss, J. (2012). "Global Sea Level Rise Scenarios for the US National Climate Assessment." *NOAA Tech Memo OAR CPO*: 1-37.

Passeri, D., Hagen, S., Bilskie, M. and Medeiros, S. (2014). "On the significance of incorporating shoreline changes for evaluating coastal hydrodynamics under sea level rise scenarios." *Natural Hazards*: 1-19.

Randerson, P. (1979). "A simulation model of salt-marsh development and plant ecology." *Estuarine and coastal land reclamation and water storage*: 48-67.

Redfield, A. C. (1972). "Development of a New England Salt Marsh." *Ecological Monographs* 42(2): 201-237.

Redfield, A. C. and Rubin, M. (1962). "The age of salt marsh peat and its relation to recent changes in sea level at Barnstable, Massachusetts." *Proceedings of the National Academy of Sciences of the United States of America* 48(10): 1728.

Reed, D. J. (1990). "The impact of sea-level rise on coastal salt marshes." *Progress in Physical Geography* 14(4): 465-481.

Reed, D. J. (1995). "The response of coastal marshes to sea-level rise: Survival or submergence?" *Earth Surface Processes and Landforms* 20(1): 39-48.

Reyes, E., Day, J. W., Lara-Domínguez, A. L., Sánchez-Gil, P., Lomelí, D. Z. and Yáñez-Arancibia, A. (2004). "Assessing coastal management plans using watershed spatial models for the Mississippi delta, USA, and the Ususmacinta–Grijalva delta, Mexico." *Ocean & Coastal Management* 47(11–12): 693-708.

Reyes, E., Martin, J., Day, J., Kemp, G. P. and Mashriqui, H. (2004). "River forcing at work: ecological modeling of prograding and regressive deltas." *Wetlands Ecology and Management* 12(2): 103-114.

Reyes, E., Martin, J. F., Day Jr, J. W., Kemp, G. P. and Mashriqui, H. (2003). Impacts of sea-level rise on coastal landscapes. INTEGRATED ASSESSMENT OF THE CLIMATE CHANGE IMPACTS ON THE GULF COAST REGION. Z. H. Ning, R. E. Turner, T. Doyle and K. Abdollahi, GCRCC and LSU Graphic Services**:** 105–114.

Reyes, E., White, M. L., Martin, J. F., Kemp, G. P., Day, J. W. and Aravamuthan, V. (2000). "Landscape modeling of coastal habitat change in the Mississippi Delta." *Ecology* 81(8): 2331-2349.

Rybczyk, J. and Callaway, J. (2009). "Surface elevation models." *Coastal wetlands: an integrated ecosystem approach. Amsterdam, Boston: Elsevier*: 835-853.

Sallenger, A. H., Doran, K. S. and Howd, P. A. (2012). "Hotspot of accelerated sea-level rise on the Atlantic coast of North America." *Nature Clim. Change* 2(12): 884-888.

Schile, L. M., Callaway, J. C., Morris, J. T., Stralberg, D., Parker, V. T. and Kelly, M. (2014). "Modeling tidal marsh distribution with sea-level rise: Evaluating the role of vegetation, sediment, and upland habitat in marsh resiliency." *PLoS ONE* 9(2): e88760.

Seginer, I., Mulhearn, P. J., Bradley, E. F. and Finnigan, J. J. (1976). "Turbulent flow in a model plant canopy." *Boundary-Layer Meteorology* 10(4): 423-453.

Shepard, C. C., Crain, C. M. and Beck, M. W. (2011). "The protective role of coastal marshes: A systematic review and meta-analysis." *PLoS ONE* 6(11): e27374.

Sklar, F. H., Costanza, R. and Day Jr, J. W. (1985). "Dynamic spatial simulation modeling of coastal wetland habitat succession." *Ecological Modelling* 29(1–4): 261-281.

Spalding, E. A. and Hester, M. W. (2007). "Interactive effects of hydrology and salinity on oligohaline plant species productivity: Implications of relative sea-level rise." *Estuaries and Coasts* 30(2): 214-225.

Stralberg, D., Brennan, M., Callaway, J. C., Wood, J. K., Schile, L. M., Jongsomjit, D., Kelly, M., Parker, V. T. and Crooks, S. (2011). "Evaluating Tidal Marsh Sustainability in the Face of Sea-Level Rise: A Hybrid Modeling Approach Applied to San Francisco Bay." *PLoS ONE* 6(11): e27388.

Tambroni, N. and Seminara, G. (2012). "A one-dimensional eco-geomorphic model of marsh response to sea level rise: Wind effects, dynamics of the marsh border and equilibrium." *Journal of Geophysical Research: Earth Surface* 117(F3): F03026.

Teal, J. M. (1962). "Energy Flow in the Salt Marsh Ecosystem of Georgia." *Ecology* 43(4): 614-624.

Temmerman, S., Govers, G., Meire, P. and Wartel, S. (2003). "Modelling long-term tidal marsh growth under changing tidal conditions and suspended sediment concentrations, Scheldt estuary, Belgium." *Marine Geology* 193(1–2): 151-169.

Townend, I., Fletcher, C., Knappen, M. and Rossington, K. (2011). "A review of salt marsh dynamics." *Water and Environment Journal* 25(4): 477-488.

Turner, R. E., Swenson, E. M. and Milan, C. S. (2000). Organic and inorganic contributions to vertical accretion in salt marsh sediments. Concepts and Controversies in Tidal Marsh Ecology. M. Weinstein and D. Kreeger, Springer Netherlands**:** 583-595.

Udo, K., Takeda, Y., Yoshida, J. and Mano, A. (2013). "Long-term area change of two tidal flats in Japan and its future projection due to sea level rise." *Journal of Coastal Research, Special Issue No. 65*: 1975-1980.

United States Army Corps of Engineers (USACE) (2011). "Sea-level change considerations for civil works programs " *EC 1165-2-212*.

Valentim, J. M., Vaz, L., Vaz, N., Silva, H., Duarte, B., Cacador, I. and Dias, J. (2013). "Sea level rise impact in residual circulation in Tagus estuary and Ria de Aveiro lagoon." *Journal of Coastal Research* Special Issue No. 65: 1981-1986.

van Wijnen, H. J. and Bakker, J. P. (2001). "Long-term Surface Elevation Change in Salt Marshes: a Prediction of Marsh Response to Future Sea-Level Rise." *Estuarine, Coastal and Shelf Science* 52(3): 381-390.

Walton Jr, T. L. (2007). "Projected sea level rise in Florida." *Ocean Engineering* 34(13): 1832-1840.

Wang, H., Ge, Z., Yuan, L. and Zhang, L. (2014). "Evaluation of the combined threat from sea-level rise and sedimentation reduction to the coastal wetlands in the Yangtze Estuary, China." *Ecological Engineering* 71(0): 346-354.

Warren, R. S. and Niering, W. A. (1993). "Vegetation change on a northeast tidal marsh: Interaction of sea-level rise and marsh accretion." *Ecology* 74(1): 96-103.

Wolanski, E. and Chappell, J. (1996). "The response of tropical Australian estuaries to a sea level rise." *Journal of Marine Systems* 7(2–4): 267-279.

CHAPTER 3. METHODS AND VALIDATION

The content in this chapter is published as: Alizad, K., Hagen, S. C., Morris, J. T., Bacopoulos, P., Bilskie, M. V., Weishampel, J. F. and Medeiros, S. C. 2016. A coupled, two-dimensional hydrodynamic-marsh model with biological feedback." *Ecological Modelling* 327: 29-43, 10.1016/j.ecolmodel.2016.01.013.

3.1 Introduction

Coastal salt marsh systems provide intertidal habitats for many species (Halpin, 2000; Pennings and Bertness, 2001), many of which (e.g., crabs and fish) have significant commercial importance. Marshes also protect shorelines by dissipating wave energy and increasing friction, processes which subsequently decrease flow energy (Knutson, 1987; Leonard and Luther, 1995; Möller and Spencer, 2002; Shepard et al., 2011). Salt marsh communities are classic examples of systems that are controlled by and in turn influence physical processes (Silliman and Bertness, 2002).

Studying the dynamics of salt marshes, which are characterized by complex inter-relationships between physics and biology (Townend et al., 2011), requires the coupling of seemingly disparate models to capture their sensitivity and feedback processes (Reed, 1990). Furthermore, coastal ecosystems need to be examined using dynamic models, because biophysical feedbacks change topography and bottom friction with time (Jørgensen and Fath, 2011). Such coupled models allow researchers to examine marsh responses to natural or anthropogenic changes in environmental conditions. The models can be divided into landscape scale and fine scale models based on the scales for projecting vegetation productivity. Ecosystem-based landscape models are designed to lower the computational expense by expanding the resolution to the order of kilometers and simplifying physical processes between ecosystem units (Fagherazzi et al., 2012). These models

connect different drivers including hydrology, hydrodynamics, water nutrients, environmental inputs and integrate them in a large scale model (Sklar et al., 1985; Park et al., 1986; Park et al., 1989; Costanza et al., 1990; Fitz et al., 1996; Costanza and Ruth, 1998; Martin et al., 2000; Reyes et al., 2000; Martin et al., 2002; Craft et al., 2008; Clough et al., 2010). However, fine scale models with resolutions on the order of meters can provide more realistic results by including different feedback mechanisms. Most relevant to this work is their ability to model the response in marsh productivity to a change in forcing mechanisms (e.g., sea-level rise-SLR) (Reed, 1995; Allen, 1997; Morris et al., 2002; Temmerman et al., 2003; Mudd et al., 2004; Kirwan and Murray, 2007; Mariotti and Fagherazzi, 2010; Stralberg et al., 2011; Tambroni and Seminara, 2012; Hagen et al., 2013; Marani et al., 2013; Schile et al., 2014).

Previous studies have shown that salt marshes possess biological feedbacks that change relative marsh elevation by accreting organic and inorganic material (Patrick and DeLaune, 1990; Reed, 1995; Turner et al., 2000; Morris et al., 2002; Baustian et al., 2012; Kirwan and Guntenspergen, 2012). SLR also will cause salt marshes to transgress, but extant marshes may be unable to accrete at a sufficient rate in response to high SLR (Warren and Niering, 1993; Donnelly and Bertness, 2001) leading to their complete submergence and loss (Nyman et al., 1993).

Salt marsh systems adapt to changing mean sea level through continuous adjustment of the marsh platform elevation toward an equilibrium (Morris et al., 2002). Based on long-term measurements of sediment accretion and marsh productivity, Morris et al. (2002) developed the Marsh Equilibrium Model (MEM) that links sedimentation, biological feedback, and the relevant time scale for SLR. Marsh equilibrium theory holds that a dynamic equilibrium exists, and that marshes

are continuously moving in the direction of that equilibrium. MEM uses a polynomial formulation for salt marsh productivity and accounts explicitly for inputs of suspended sediments and implicitly for the in situ input of organic matter to the accreting salt marsh platform. The coupled model presented in this manuscript incorporates biological feedback by including the MEM accretion formulation as well as implementing a friction coefficient effect that varies between subtidal and intertidal states. The resulting model not only has the capability of capturing biophysical feedback that modifies relative elevation, but it also includes the biological feedback on hydrodynamics.

Since the time scale for SLR is on the order of decades to centuries, models that are based on long-term measurements, like MEM, are able to capture a fuller picture of the governing long-term processes than physical models that use temporary physical processes to extrapolate long-term results (Fagherazzi et al., 2012). MEM has been applied to a number of investigations on the interaction of hydrodynamics and salt marsh productivity. Mudd et al. (2004) used MEM coupled with a one-dimensional hydrodynamic component to investigate the effect of SLR on sedimentation and productivity in salt marshes at the North Inlet estuary, South Carolina. MEM has also been used to simulate the effects of vegetation on sedimentation, flow resistance, and channel cross section change (D' Alpaos et al., 2006), as well as in a three-dimensional model of salt marsh accretion and channel network evolution based on a physical model for sediment transport (Kirwan and Murray, 2007). Hagen et al. (2013) coupled a two-dimensional hydrodynamic model with the zero-dimensional biomass production formula of Morris et al. (2002) to capture SLR effects on biomass density and simulated human-enhanced marsh accretion.

Coupling a two-dimensional hydrodynamic model with a point-based parametric marsh model that incorporates biological feedback, such as MEM, has not been previously achieved. Such a model is necessary because results from short-term limited hydrodynamic studies cannot be used for long-term or extreme events in ecological and sedimentary interaction applications. Hence, there is a need for integrated models, which incorporate both hydrodynamic and biological components for long time scales (Thomas et al., 2014). Additionally, models that ignore the spatial variability of the accretion mechanism may not accurately capture the dynamics of a marsh system (Thorne et al., 2014), and it is important to model the distribution at the correct scale for spatial modeling (Jørgensen and Fath, 2011).

Ecological models that integrate physics and biology provide a means of examining the responses of coastal systems to various possible scenarios of environmental change. D' Alpaos et al. (2007) employed simplified shallow water equations in a coupled model to study SLR effects on marsh productivity and accretion rates. Temmerman et al. (2007) applied a more physically complicated shallow water model to couple it with biological models to examine landscape evolution within a limited domain. These coupled models have shown the necessity of the interconnection between physics and biology; however, the applied physical models were simplified or the study area was small. This paper presents a practical framework with a novel application of MEM that enables researchers to forecast the fate of coastal wetlands and their responses to SLR using a physically more complicated hydrodynamic model and a larger study area. The coupled HYDRO-MEM model is based on the model originally presented by Hagen et al. (2013). This model has since been enhanced to include: spatially dependent marsh platform accretion, a bottom friction roughness coefficient (Manning's *n*) using temporal and spatial variations in habitat state, a

"coupling time step" to incrementally advance and update the solution, and changes in biomass density and hydroperiod via biophysical feedbacks. The presented framework can be employed in any estuary or coastal wetland system to assess salt marsh productivity regardless of tidal range by updating an appropriate biomass curve for the dominant salt marsh species in the estuary. In this study, the coupled model was applied to the Timucuan marsh system located in northeast Florida under high and low SLR scenarios. The objectives of this study were to (1) develop a spatially-explicit model by linking a hydrodynamic-physical model and MEM using a coupling time step and (2) assess a salt marsh system long-term response to projected SLR scenarios.

3.2 Methods

3.2.1 Study Area

The study area is the Timucuan salt marsh, located along the lower St. Johns River in Duval County in northeastern Florida (Figure 3.1). The marsh system is located to the north of the lower 10–20 km of the St. Johns River, where the river is engineered and the banks are hardened for support of shipping traffic and port utility. The creeks have changed little from 1929 to 2009 based on surveyed data from National Ocean Service (NOS) and the United States Army Corps of Engineers (USACE), which show the creek layout to have remained essentially the same since 1929. The salt marsh of the Timucuan preserve, which was designated the Timucuan Ecological and Historic Preserve in 1988, is among the most pristine and undisturbed marshes found along the southeastern United States seaboard (United States National Park Service (Denver Service Center), 1996). Maintaining the health of the approximately 185 square km of salt marsh, which cover roughly

75% of the preserve, is important for the survival of migratory birds, fish, and other wildlife that rely on this area for food and habitat.

The primary habitats of these wetlands are salt marshes and the tidal creek edges between the north bank and Sisters Creek are dominated by low marsh, where *S. alterniflora* thrives (DeMort, 1991). A sufficient biomass density of *S. alterniflora* in the marsh is integral to its survival, as the grass aids in shoreline protection, erosion control, filtering of suspended solids, and nutrient uptake of the marsh system (Bush and Houck, 2002). *S. alterniflora* covers most of the southern part of the watershed and east of Sisters Creek up to the primary dunes on the north bank, and is also the dominant species on the Black Hammock barrier island (DeMort, 1991). The low marsh is the more tidally vulnerable region of the study area. Our focus is on the areas that are directly exposed to SLR and where *S. alterniflora* is dominant. However, we also extended our salt marsh study area 11 miles to the south, 17 miles to the north, and 18 miles to the west of the mouth of the St. Johns River. The extension of the model boundary allows enough space to study the potential for salt marsh migration.

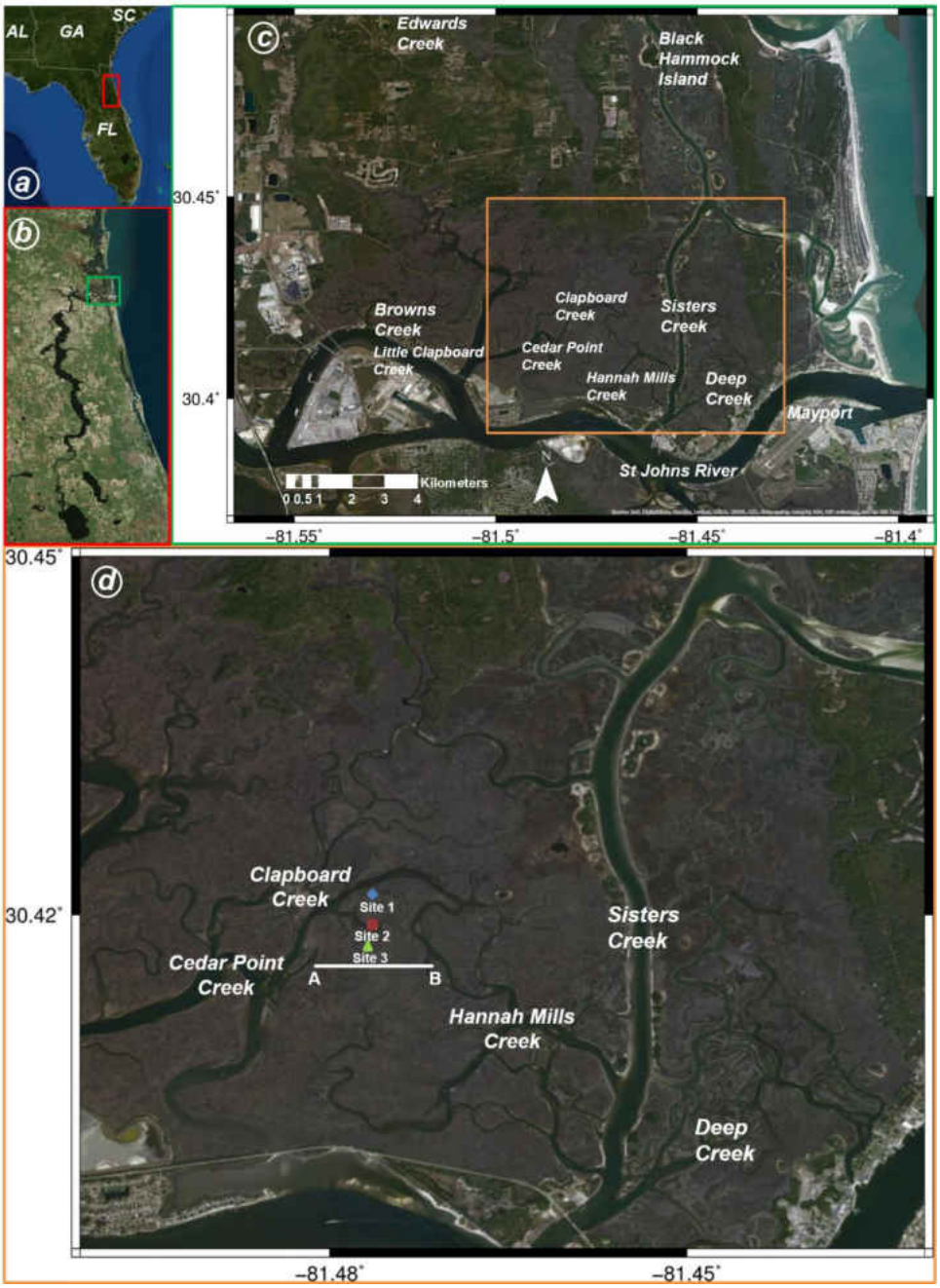

Figure 3.1: Study area and progressive insets. (a) Location of St. Johns river; (b) Location of Timucuan salt marsh system and lower St. Johns river; (c) Timucuan salt marsh system and tidal creeks. (d) Sub-region of Timucuan including the location of example transect AB and three biomass sample sites. Site 1 (blue) is in a low biomass productivity region, site 2 (red) is in a medium biomass productivity region, and site 3 (green) is in a high biomass productivity region. The maps are screen captures of world imagery in ArcGIS (ESRI, 2012).

3.2.2 Overall Model Description

The flowchart shown in Figure 3.2 illustrates the dynamic coupling of the physical and biological processes in the model. The framework to run the HYDRO-MEM model consists of two main elements: the hydrodynamic model, and a marsh model with biological feedback (MEM) in the form of an ArcGIS toolbox. The two model components provide inputs for one another at a specified time step within the loop structure, referred to as the coupling time step. The coupling time step refers to the length of the time interval between updating the hydrodynamics based on the output of MEM, which was always integrated with an annual time step. The length of the coupling time step (Δt) governs the frequency of exchange of information from one model component to the other. The choice of coupling time step size affects the accuracy and computational expense of the HYDRO-MEM model which is an important consideration if extensive areas are simulated. The model's initial conditions include astronomic tides, bottom friction, and elevation, which consist of the marsh surface elevations, creek geometry, and sea level. The hydrodynamic model is then run using the initial conditions and its results are processed to derive tidal constituents.

The tidal constituents are fed into the ArcGIS toolbox, which contains two components that were designed to work independently. The "Tidal Datums" element of the ArcGIS toolbox computes Mean Low Water (MLW) and Mean High Water (MHW) in regions that were always classified as wetted during the hydrodynamic simulation. The second component of the toolbox, "Biomass Density," uses the MLW and MHW calculated in the previous step and extrapolates those values across the marsh platform using the Inverse Distance Weighting (IDW) method of extrapolation

in ArcGIS (i.e., from the areas that were continuously wetted during the hydrodynamic simulation), computes biomass density for the marsh platform, and establishes a new marsh platform elevation based on the computed accretion.

The simulation terminates and outputs the final results if the target time has been reached, otherwise time is incremented by the coupling time step, data are transferred and model inputs are modified, and another incremental simulation is performed. After each time advancement of the MEM and after updating the topography, the hydrodynamic model is re-initialized using the current elevations, water levels, and updated bottom friction parameters calculated in the previous iteration.

The size of the coupling time step, i.e. the time elapsed in executing MEM before updating the hydrodynamic model, was selected based on desired accuracy and computational expense. The coupling time step was adjusted in this work to minimize numerical error associated with biomass calculations (the difference between using two different coupling time steps) while also minimizing the run time.

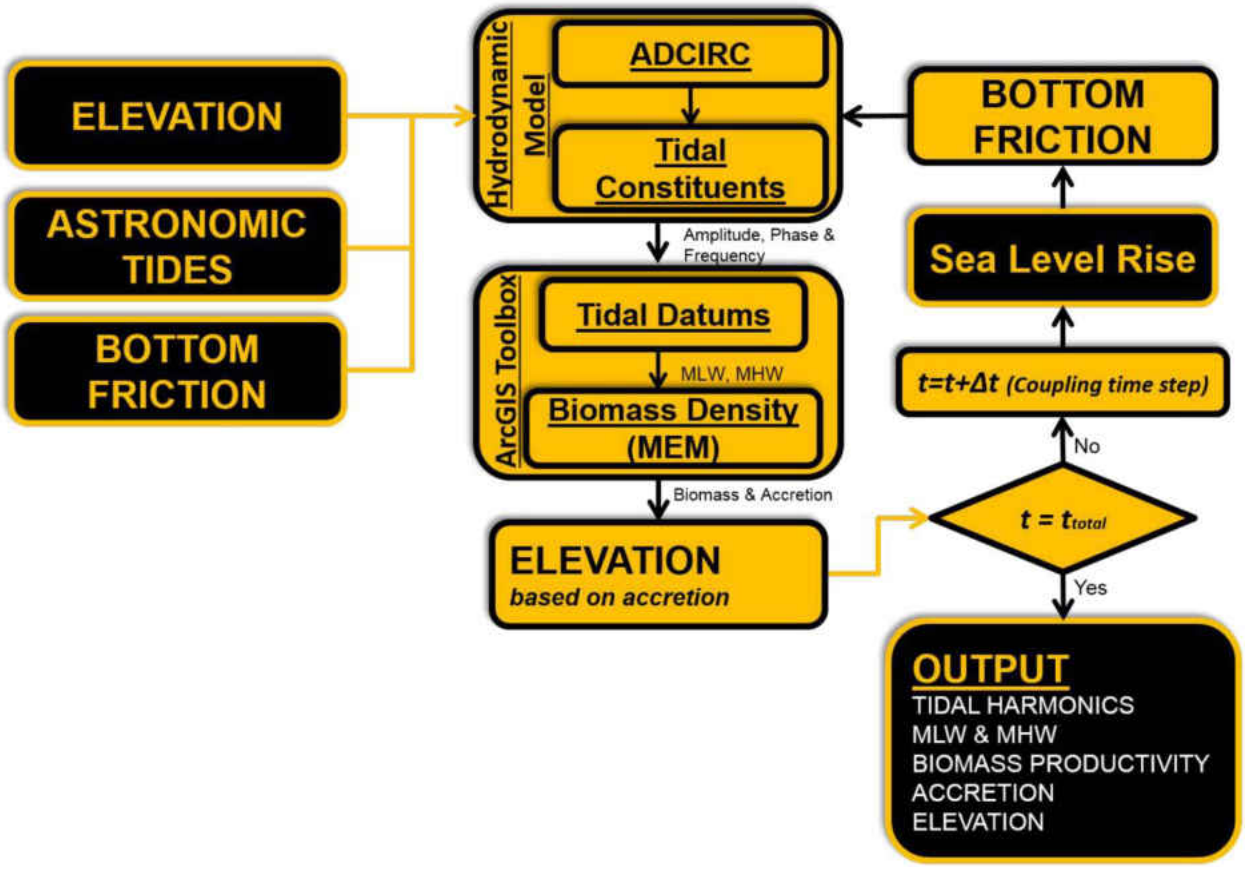

Figure 3.2: HYRDO-MEM model flowchart. The black boxes show the parameters that are not being changed and the gold boxes are the parameters that are being changed through simulation. The two main elements are the big gold boxes which are labeled as hydrodynamic model and ArcGIS toolbox. The black boxes on the left represent the initial conditions.

3.2.2.1 Hydrodynamic Model

We used the two-dimensional, depth-integrated ADvanced CIRCulation (ADCIRC) finite element model to simulate tidal hydrodynamics (Luettich et al., 1992). ADCIRC is one of the main components of the HYDRO-MEM model due to its capability to simulate the highly variable tidal response throughout the creeks and marsh platform. ADCIRC solves the shallow water equations

for water levels and currents using continuous Galerkin finite elements in space. ADCIRC based models have been used extensively to model long wave processes such as astronomic tides and hurricane storm surge (Bacopoulos and Hagen, 2009; Bunya et al., 2010) and SLR impacts (Atkinson et al., 2013; Bilskie et al., 2014). A value-added feature of using ADCIRC within the HYDRO-MEM model is its ability to capture a two-dimensional field of the tidal flow and hydroperiod within the intertidal zone. ADCIRC contains a robust wetting and drying algorithm that allows elements to turn on (wet) or turn off (dry) during run-time, enabling the swelling of tidal creeks and overtopping of channel banks (Medeiros and Hagen, 2013). A least-squares harmonic analysis routine within ADCIRC computes the amplitudes and phases for a specified set of tidal constituents at each computational point in the model domain (global water levels). The tidal constituents are then sent to the ArcGIS toolbox for further processing.

Full hydrodynamic model description including elevation sources and boundary conditions can be found in Bacopoulos et al. (2012) and Hagen et al. (2013). The model is forced with the seven dominating tidal constituents along the open ocean boundary located on the continental shelf that account for more than 90% of the offshore tidal activity (Bacopoulos et al., 2012; Hagen et al., 2013). Placement of the offshore tidal boundary allows tides to propagate through the domain and into the tidal creeks and intertidal zones, and simulate non-linear interactions that occur in the tidal flow.

To model future conditions, sea level was increased by applying an offset of the initial sea surface equal to the SLR across the model domain to the initial conditions. Previous studies introduced SLR by applying an additional tidal constituent to the offshore boundary (Hagen et al., 2013). Both

methods produce an equivalent solution; however, we offset the initial sea surface across the entire domain as the method of choice in order to reduce computational time.

There is no accepted method to project SLR at the local scale (Parris et al., 2012); however, a tide gauge analysis performed in Florida using three different methods gave a most probable range of rise between 0.11 and 0.36 m from present to the year 2080 (Walton Jr, 2007). The U.S. Army Corps of Engineers (USACE) developed low, intermediate, and high SLR projections at the local scale, based on long-term tide gage records (http://www.corpsclimate.us/ccaceslcurves_nn.cfm). The low curve follows the historic trend of SLR and the intermediate and high curves use the National Research Council (NRC) curves (United States Army Corps of Engineers (USACE), 2011). Both methodologies account for local subsidence. We based our SLR scenarios on the USACE projections at Mayport, FL (Figure 3.1c), which accelerates to 11 cm and 48 cm for the low and high scenarios, respectively, in the year 2050. The low and high SLR scenarios display linear and nonlinear trends, respectively and using the time step approach helps to capture the rate of SLR in the modeling.

The hydrodynamic model uses Manning's *n* coefficients for bottom friction, which have been assessed for present-day conditions of the lower St. Johns River (Bacopoulos et al., 2012). Bottom friction must be continually updated by the model due to temporal changes in the SLR and biomass accretion. To compute Manning's *n* at each coupling time step, the HYDRO-MEM model utilizes the wet/dry area output of the hydrodynamic model as well as biomass density and accreted marsh platform elevation to find the regions that changed from marsh (dry) to channel (wet). This process is a part of the biofeedback process in the model: Manning's *n* is adjusted using the accretion,

which changes the hydrodynamics, which in turn changes the biomass density in the next time step. The hydrodynamic model, along with the main digital elevation model (Figure 3.3) and bottom friction parameter (Manning's *n*) inputs, was previously validated in numerous studies (Bacopoulos et al., 2009; Bacopoulos et al., 2011; Giardino et al., 2011; Bacopoulos et al., 2012; Hagen et al., 2013) and specifically Hagen et al. (2013) validated the MLW and MHW generated by this model.

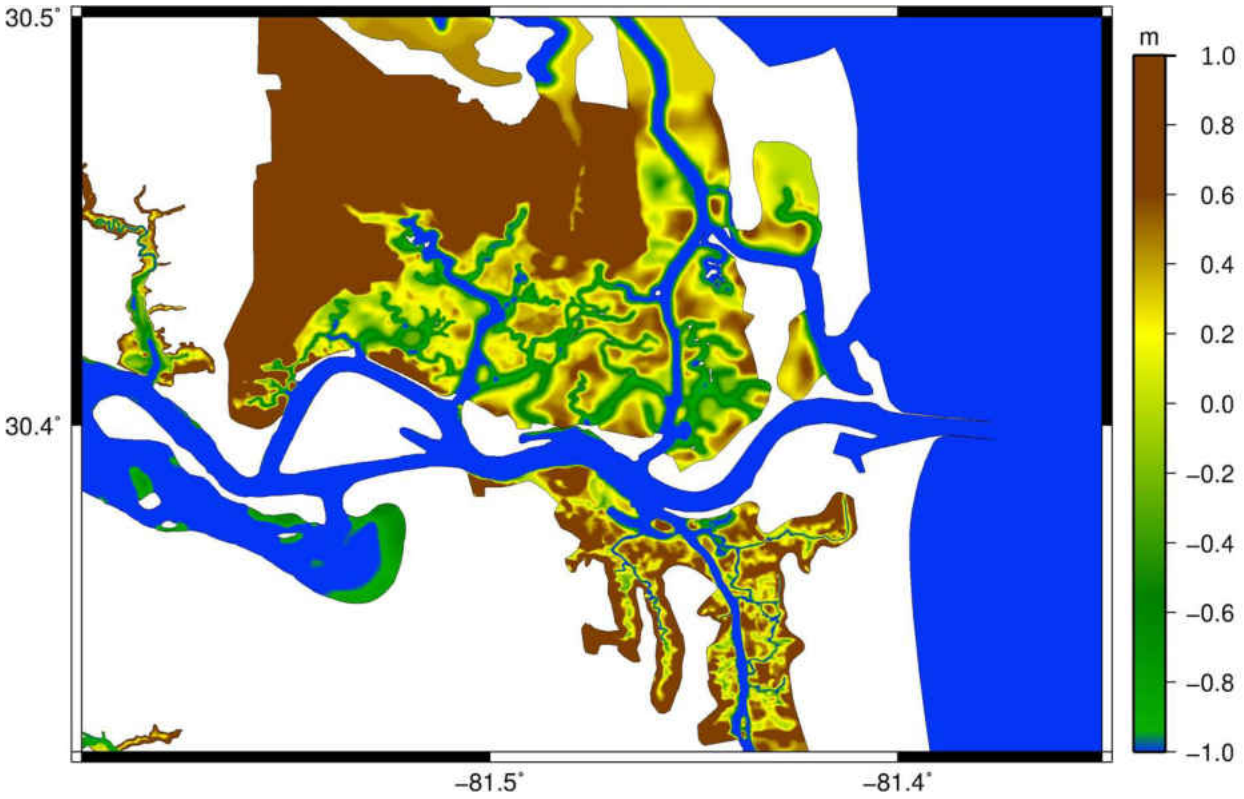

Figure 3.3: ADCIRC model input of the Timucuan salt marsh surface elevations. Elevations are referenced to NAVD88 in meters with blue representing water depths greater than 1 m, greens indicating depths between 0 m and 1 m, and yellows and browns representative of elevations above 0 m NAVD88.

3.2.2.2 ArcGIS Toolbox

This element of the HYDRO-MEM model is designed as a user interface toolbox in ArcGIS (ESRI, 2012). The toolbox consists of two separate tools that were coded in Python v2.7. The first, "Tidal Datums," uses tidal constituents from the preceding element of the HYDRO-MEM model loop, the hydrodynamic model, to generate MLW and MHW in the river and tidal creeks. MLW and MHW represent the average low and high tides at a point (Hagen et al., 2013). The flooding frequency and duration are considered in the calculation of MLW and MHW. These values are necessary for the MEM-based tool in the model. The Tidal Datums tool produces raster files of MLW and MHW using the data from ADCIRC simulation and a 10 m Digital Elevation Model (DEM). These feed into the second tool, "Biomass Density," to calculate MLW and MHW within the marsh areas that were not continuously wet during the ADCIRC simulation, which is done by interpolating MLW and MHW values from the creeks and river areas across the marsh platform using IDW. This interpolation technique is necessary because very small creeks that are important in flooding the marsh surface are not resolved in the hydrodynamic model. IDW calculates MLW and MHW at each computational point across the marsh platform based on its distance from the tidal creeks, where the number of the nearest sample points for the IDW interpolation based on the default setting in ArcGIS is twelve. This method was used in this work for the marsh interpolation due to its accuracy and acceptable computational time. The method produces lower water levels for points farther from the source, which in turn results in lower sedimentation and accretion in the MEM-based part of the model. Interpolated MLW and MHW, biomass productivity, and accretion are displayed as rasters in ArcGIS. The interpolated values of MLW and MHW in the

marsh are used by MEM in each raster cell to compute the biomass density and accretion rate across the marsh platform.

The zero-dimensional implementation of MEM has been demonstrated to successfully capture salt marsh response to SLR (Morris et al., 2002; Morris, 2015). MEM predicts two salt marsh variables: biomass productivity and accretion rate. These processes are related; the organic component of the accretion is dependent on biomass productivity, and the updated marsh platform elevation is generated using the computed accretion rate. The coupling of the two parts of MEM is incorporated dynamically in the HYDRO-MEM model. MEM approximates salt marsh productivity as a parabolic function

$$B = aD + bD^2 + c \tag{3.1}$$

where B is the biomass density ($g \cdot m^{-2}$), a = 1000 $g.m^{-2}$, b = -3718 $g.m^{-2}$, and c = 1021 $g.m^{-2}$ are coefficients derived from bioassay data collected at North Inlet, SC (Morris et al., 2013) and where the variable D is the non-dimensional depth, given by

$$D = \frac{MHW - E}{MHW - MLW} \tag{3.2}$$

and variable E is the relative marsh surface elevation (NAVD 88). Relative elevation is a proxy for other variables that directly regulate growth, such as soil salinity (Morris, 1995) and hypoxia, and Equation (3.1) actually represents a slice through n-dimensional niche space (Hutchinson, 1957).

The coefficients *a*, *b*, and *c* may change with marsh species, estuary type (fluvial, marine, mixed), climate, nutrients, and salinity (Morris, 2007), but Equation (3.1) should be independent of tide range because it is calibrated to dimensionless depth *D*, consistent with the meta-analysis of Mckee and Patrick (1988) documenting a correlation between the growth range of *S. alterniflora* and mean tide range. The coefficients *a*, *b*, and *c* in Equation (3.1) give a maximum biomass of 1088 $g.m^{-2}$, which is generally consistent with biomass measurements from other southeastern salt marshes (Hopkinson et al., 1980; Schubauer and Hopkinson, 1984; Dame and Kenny, 1986; Darby and Turner, 2008), and since our focus is on an area where *S. alterniflora* is dominant, these constants are used. Additionally, because many tidal marsh species occupy a vertical range within the upper tidal frame, but sorted along a salinity gradient, the model is able to qualitatively project the wetland area coverage including other marsh species in low, medium, and high productivity. The framework has the capability to be applied to other sites with different dominant salt marsh species by using experimentally-derived coefficients to generate the biomass curves (Kirwan and Guntenspergen, 2012).

The first derivative of the biomass density function with respect to non-dimensional depth is a linear function, which will be used in analyzing the HYDRO-MEM model results, is given by

$$\frac{dB}{dD} = 2bD + a \tag{3.3}$$

The first derivative values are close to zero for the points around the optimal point of the biomass density curve. These values become negative for the points on the right (sub-optimal) side and positive for the points on the left (super-optimal) side of the biomass density curve.

The accretion rate determined by MEM is a positive function based on organic and inorganic sediment accumulation (Morris et al., 2002). These two accretion sources, organic and inorganic, are necessary to maintain marsh productivity against rising sea level; otherwise marshes might become submerged (Nyman et al., 2006; Blum and Roberts, 2009; Baustian et al., 2012). Sediment accretion is a function of the biomass density in the marsh and relative elevation. Inorganic accretion (i.e., mineral sedimentation) is influenced by the biomass density, which affects the ability of the marsh to 'trap' sediments (Mudd et al., 2010). Inorganic sedimentation also occurs as salt marshes impede flow by increasing friction, which enhances sediment deposition on the marsh platform (Leonard and Luther, 1995; Leonard and Croft, 2006). The linear function developed by Morris et al. (2002) for the rate of total accretion is given by

$$\frac{dY}{dt} = (q + kB)D \quad \text{for} \quad D>0 \tag{3.4}$$

where dY is the total accretion (cm/yr), dt is the time interval, q represents the inorganic contribution to accretion from the suspended sediment load and k represents the organic and inorganic contributions due to vegetation. The values of the constants q (0.0018) and k (2.5×10^{-5}) are from a fit of MEM to a time-series of marsh elevations at North Inlet (Morris et al., 2002) modified for a high sedimentary environment. These constants take both autochthonous organic matter and trapping of allochthonous mineral particles into account for biological feedback. The accretion rate is positive for salt marshes below MHW; when $D < 0$ no accumulation of sediments will occur for salt marshes above MHW (Morris, 2007). The marsh platform elevation change is then calculated using the following equation

$$Y(t+\Delta t) = Y(t) + dY \tag{3.5}$$

where the marsh platform elevation Y is raised by dY meters every Δt years.

3.3 Results

3.3.1 Coupling Time Step

In this study, coupling time steps of 50, 10, and 5 years were used for both the low and high SLR scenarios. The model was run for one 50-year coupling time step, five 10-year coupling time steps, and ten 5-year coupling time steps for each SLR scenario. The average differences for biomass density in Timucuan marsh between using one 50-year coupling time step and five 10-year coupling time steps for low and high SLR scenarios were 37 and 57 $g \cdot m^{-2}$, respectively. Decreasing the coupling time step to 5 years indicated convergence within the marsh system when compared to a 10-year coupling time step (Table 3.1). The average difference for biomass density between using five 10-year coupling time steps and ten 5-year coupling time steps in the same area for low and high SLR were 6 and 11 $g \cdot m^{-2}$, which implied convergence using smaller coupling time steps. The HYDRO-MEM model did not fully converge using a coupling time step of 10 years for the high SLR scenario, and a 5 year coupling time step was required (Table 3.1) because of the acceleration in rate of SLR. However, the model was able to simulate reasonable approximations of low, medium, or high productivity of the salt marshes when applying a single coupling time step of 50 years when SLR is small and linear. For this case, the model was run for the current condition and the feedback mechanism is subsequently applied using 50-year coupling time step. The next run produces the results for salt marsh productivity after 50 years using the SLR scenario.

Table 3.1: Model convergence as a result of various coupling time steps.

Number of coupling time steps	Coupling time step (years)	Biomass density for a sample point* at low SLR (11cm) ($g.m^{-2}$)	Biomass density for a sample point* at high SLR (48cm) ($g.m^{-2}$)	Convergence at low SLR (11 cm)	Convergence at high SLR (48 cm)
1	50	1053	928	No	No
5	10	1088	901	Yes	No
10	5	1086	909	Yes	Yes

*The sample point is located at longitude = -81.4769 and latitude = 30.4167.

3.3.2 Hydrodynamic Results

MLW and MHW demonstrated spatial variability throughout the creeks and over the marsh platform. The water surface across the estuary varied from -0.85 m to -0.3 m (NAVD 88) for MLW and from 0.65 m to 0.85 m for MHW in the present day simulation (Figure 3.4a, Figure 3.4). The range and spatial distribution of MHW and MLW exhibited a non-linear response to future SLR scenarios. Under the low SLR (11 cm) scenario, MLW ranged from -0.74 m in the ocean to -0.25 m in the creeks (Figure 3.4b), while MHW varied from 1 m to 0.75 m (Figure 3.4e). Under the high SLR (48 cm) scenario, the MLW ranged from -0.35 m in the ocean to 0.05 m in the creeks (Figure 3.4c), and from 1.35 m to 1.15 m for MHW (Figure 3.4f).

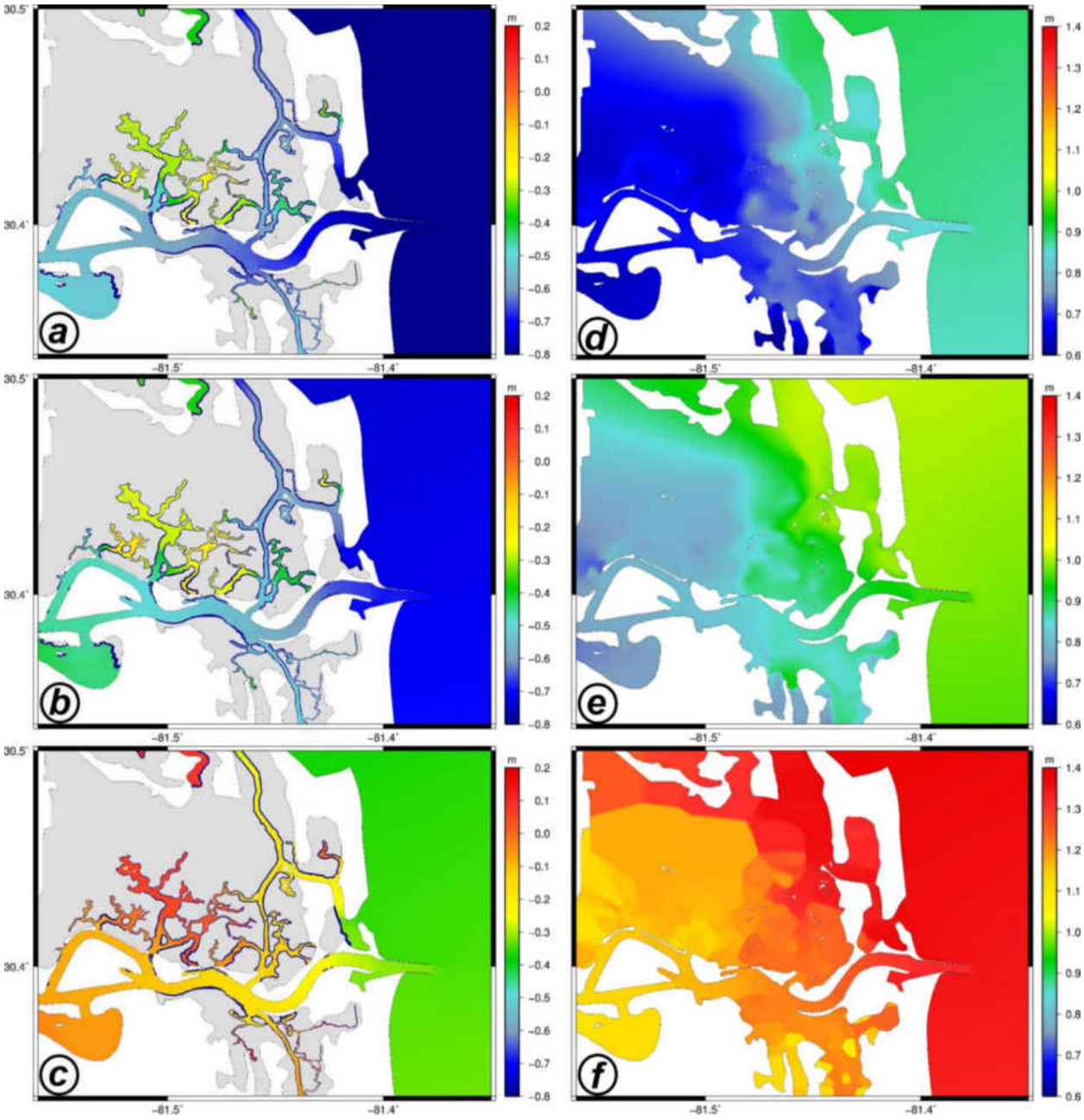

Figure 3.4: MLW (left column) and MHW (right column) results for the year 2000 (a and d), and for the year 2050 under low (11 cm) (b and e) and high (48 cm) (c and f) SLR scenarios. Results are referenced to NAVD88.

The same spatial pattern of water level was exhibited on the marsh platform for both present-day and future conditions with the low SLR scenario, but with future conditions showing slightly higher values consistent with the 11 cm increase in MSL (Figure 3.4d, Figure 3.4e). The MHW values in both cases were within the same range as those in the creeks. However, the spatial pattern of MHW changed under the high SLR scenario; the water levels in the creeks increased significantly and were more evenly distributed relative to the present-day conditions and low SLR scenario (Figure 3.4d, Figure 3.4e, Figure 3.4f). As a result, the spatial variation of MHW in the creeks and marsh area was lower than that of the present in the high SLR scenario (Figure 3.4f).

3.3.3 Marsh Dynamics

Simulations of biomass density demonstrated a wide range of spatial variation in the year 2000 (Figure 3.5a), and in the two future scenarios (Figure 3.5b-Figure 3.5c), depending on the pre-existing elevations of the marsh surface and their change relative to future MHW and MLW. The maps showed an increase in biomass density under low SLR in 90% of the marshes and a decrease in 80% of the areas under the high SLR scenario. The average biomass density increased from 804 $g \cdot m^{-2}$ in the present to 994 $g \cdot m^{-2}$ in the year 2050 with low SLR, and decreased to 644 $g \cdot m^{-2}$ under the high SLR scenario.

Recall that the derivative of biomass density under low SLR scenario varies linearly with respect to non-dimensional depth. Figure 3.6 illustrates the aboveground biomass density curve with respect to non-dimensional depth and three sample points with low, medium, and high productivity. The slope of the curve at the sample points is also shown, depicting the first derivative of biomass density. The derivative is negative if a point is located on the right side of the biomass

density curve, and is positive if it is on the left side. In addition, values close to zero indicate a higher productivity, whereas large negative values indicate low productivity (Figure 3.6). The average biomass density derivative under the low SLR scenario increased from -2000 $g \cdot m^{-2}$ to -700 $g \cdot m^{-2}$ and decreased to -2400 $g \cdot m^{-2}$ in the high SLR case.

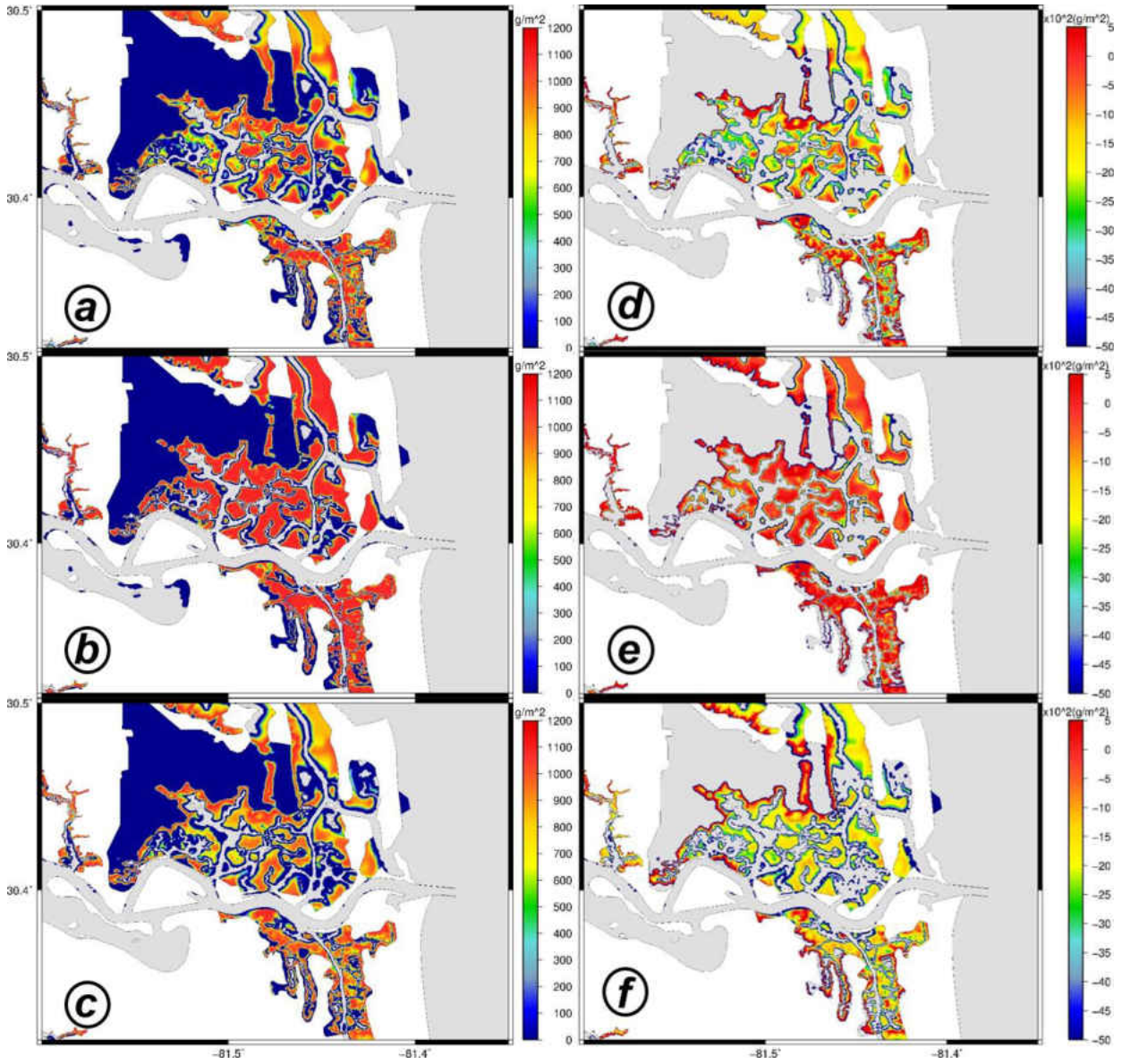

Figure 3.5: Biomass density patterns (left column) and its first derivative (right column) in the Timucuan marsh system. (a) Biomass density in the year 2000; (b) Biomass density in the year 2050 under a low SLR (11 cm) scenario; (c) Biomass density in the year 2050 under a high SLR (48 cm) scenario. Dark blue represents no biomass density (0 $g \cdot m^{-2}$), yellows are medium biomass density (~700 $g \cdot m^{-2}$), and reds indicate biomass density of 1000 $g \cdot m^{-2}$ or greater. (d) Biomass density first derivative in the year 2000; (e) Biomass density first derivative in the year 2050 under the low SLR (11 cm) scenario; (f) Biomass density first derivative in the year 2050 under the high SLR (48 cm) scenario.

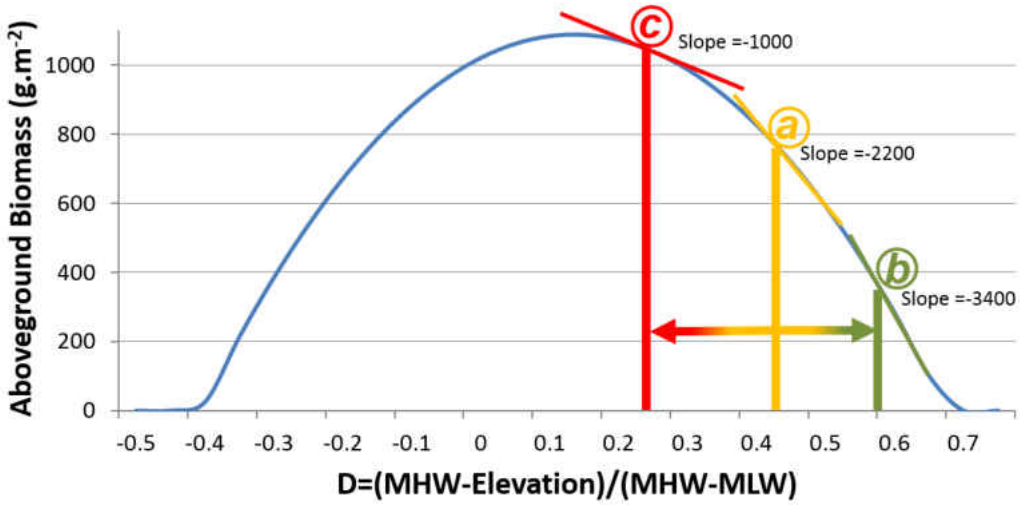

Figure 3.6: Change in the biomass productivity curve under different SLR scenarios. The colors selected are based on the scale in Figure 3.5. (a) is a selected geographical point from the Timucuan marsh system in the year 2000 that falls within the medium productivity range of the curve; (b) is the same geographical location (a), in the year 2050 under high SLR (48 cm) and has moved to the low productivity range of the curve; (c) is the same geographical location (a) in the year 2050 and under low SLR (11 cm) and has moved to the high productivity region.

Sediment accretion in the marsh varied spatially and temporally under different SLR scenarios. Under the low SLR scenario (11 cm), the average salt marsh accretion totaled 19 cm or 0.38 cm per year (Figure 3.7a). The average salt marsh accretion increased by 20% under the high SLR scenario (48 cm) due to an increase in sedimentation (Figure 3.7b). Though the magnitudes are different, the general spatial patterns of the low and high SLR scenarios were similar.

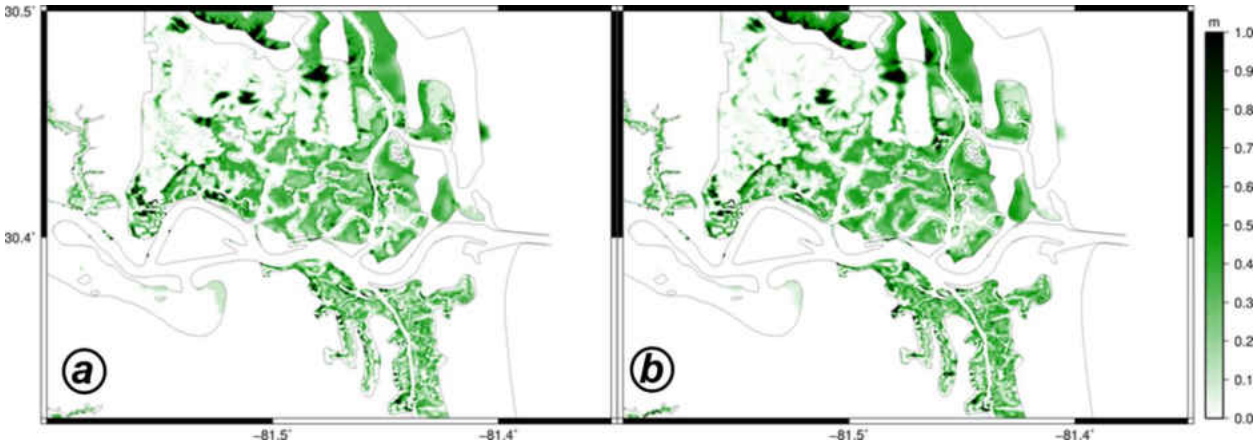

Figure 3.7: Fifty years (year 2050) of salt marsh platform accretion following (a) 11 cm of SLR and (b) 48 cm of SLR.

Comparisons of marsh platform accretion, MHW, and biomass density across transect AB spanning over Cedar Point Creek, Clapboard Creek, and Hannah Mills Creek (Figure 3.1d) between present and future time demonstrated that acceleration of SLR from 11 cm to 48 cm in 50 years reduced the overall biomass, but the effect depended on the initial elevation (Figure 3.8aFigure 3.8d). Under the low SLR, accretion was maximum at the edge of the creeks, 25 to 30 cm, and decreased to 15 cm with increasing distance from the edge of the creek (Figure 3.8a). Analyzing the trend and variation of MHW between future and present across the transect under low and high SLR showed that it is not uniform across the marsh and varied with distance from creek channels and underlying topography (Figure 3.8a, Figure 3.8c). MHW increased slightly in response to a rapid rise in topography (Figure 3.8a, Figure 3.8c).

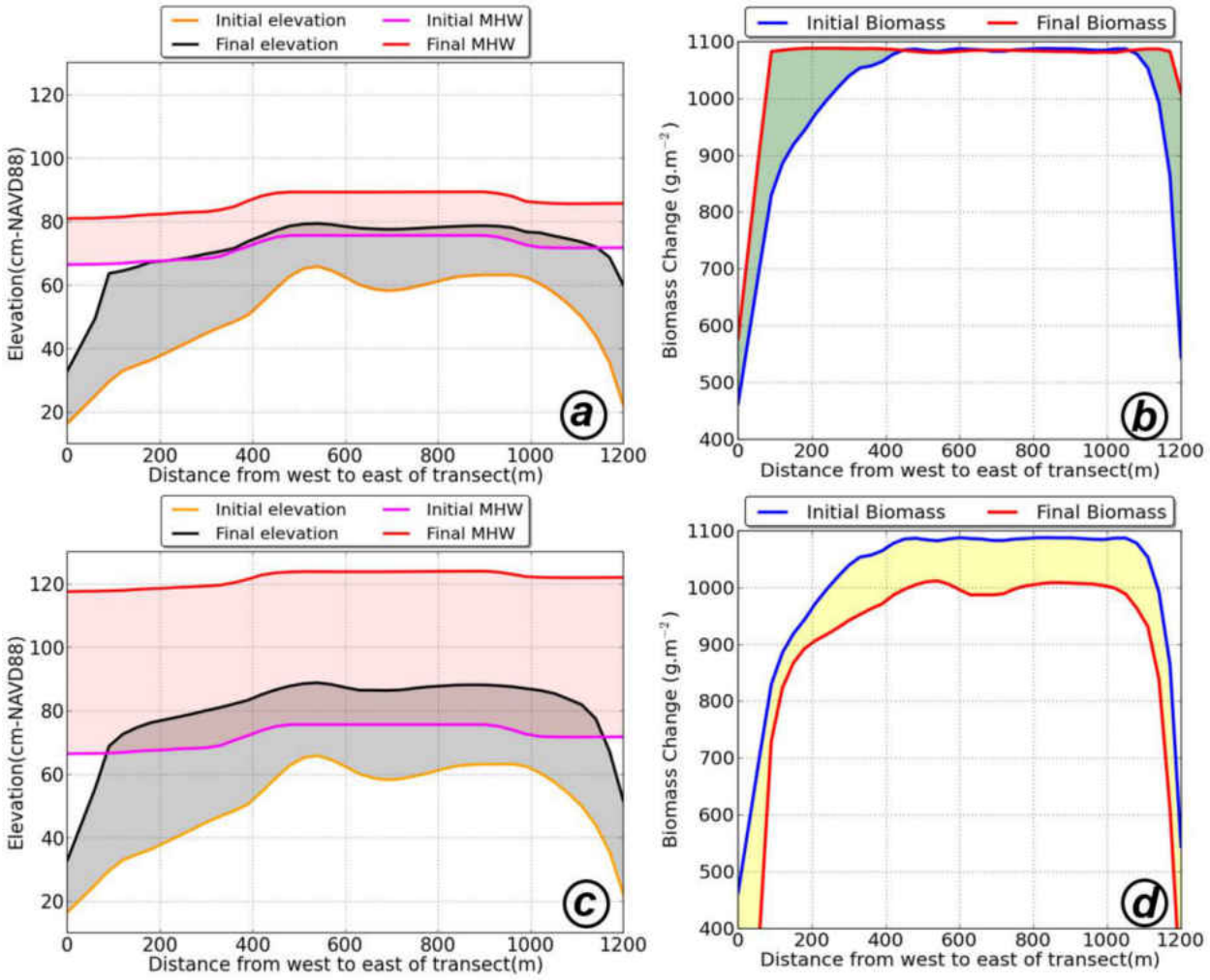

Figure 3.8: Changes in elevation, MHW, and biomass along a transect (see Figure 3.1d for location of transect) for the low (11 cm) (a and b) and the high (48 cm) (c and d) scenarios. (a and c) Gray shaded area shows the elevation change between years 2000 (orange line) and 2050 (black line); red shaded area represents the increase in MHW between years 2000 (magenta line) and 2050 (red line). (b and d) The dark green (yellow) shaded area shows an increase (decrease) in biomass density between years 2000 (blue line) and 2050 (red line).

The change in MHW, which is a function of the changing hydrodynamics and marsh topography, was nearly uniform across space when SLR was high, but when SLR was low, marsh topography

continued to influence MHW, which can be seen in the increase between years 2020 and 2030 (Figure 3.9c, Figure 3.9d). This is due to the accretion of the marsh platform keeping pace with the change in MHW. The change in biomass was a function of the starting elevation as well as the rate of SLR (Figure 3.9e, Figure 3.9f). When the starting marsh elevation was low, as it was for sites 1 and 2, biomass increased significantly over the 50 yr simulation, corresponding to a rise in the relative elevation of the marsh platform that moved them closer to the optimum. The site that was highest in elevation at the start, site 3, was essentially in equilibrium with sea level throughout the simulation and remained at a nearly optimum elevation (Figure 3.9e). When the rate of SLR was high, the site lowest in elevation at the start, site 1, ultimately lost biomass and was close to extinction (Figure 3.9f). Likewise, the site highest in elevation, site 3, also lost biomass, but was less sensitive to SLR than site 1. The site with intermediate elevation, site 2, actually gained biomass by the end of the simulation when SLR was high (Figure 3.9f).

Biomass density was generally affected by rising mean sea level and varying accretion rates. A modest rate of SLR apparently benefitted these marshes, but high SLR was detrimental (Figure 3.9e, Figure 3.9f). This is further explained by looking at the derivatives. The first-derivative change of biomass density under low SLR (shaded red) demonstrated an increase toward the zero (Figure 3.10). Biomass density rose to the maximum level and was nearly uniform across transect AB under the low SLR scenario (Figure 3.8b), but with 48 cm of SLR biomass declined (Figure 3.8d). The biomass derivative across the transect decreased from year 2000 to year 2050 under the high SLR scenario (Figure 3.10), which indicated a move to the right side of the biomass curve (Figure 3.6).

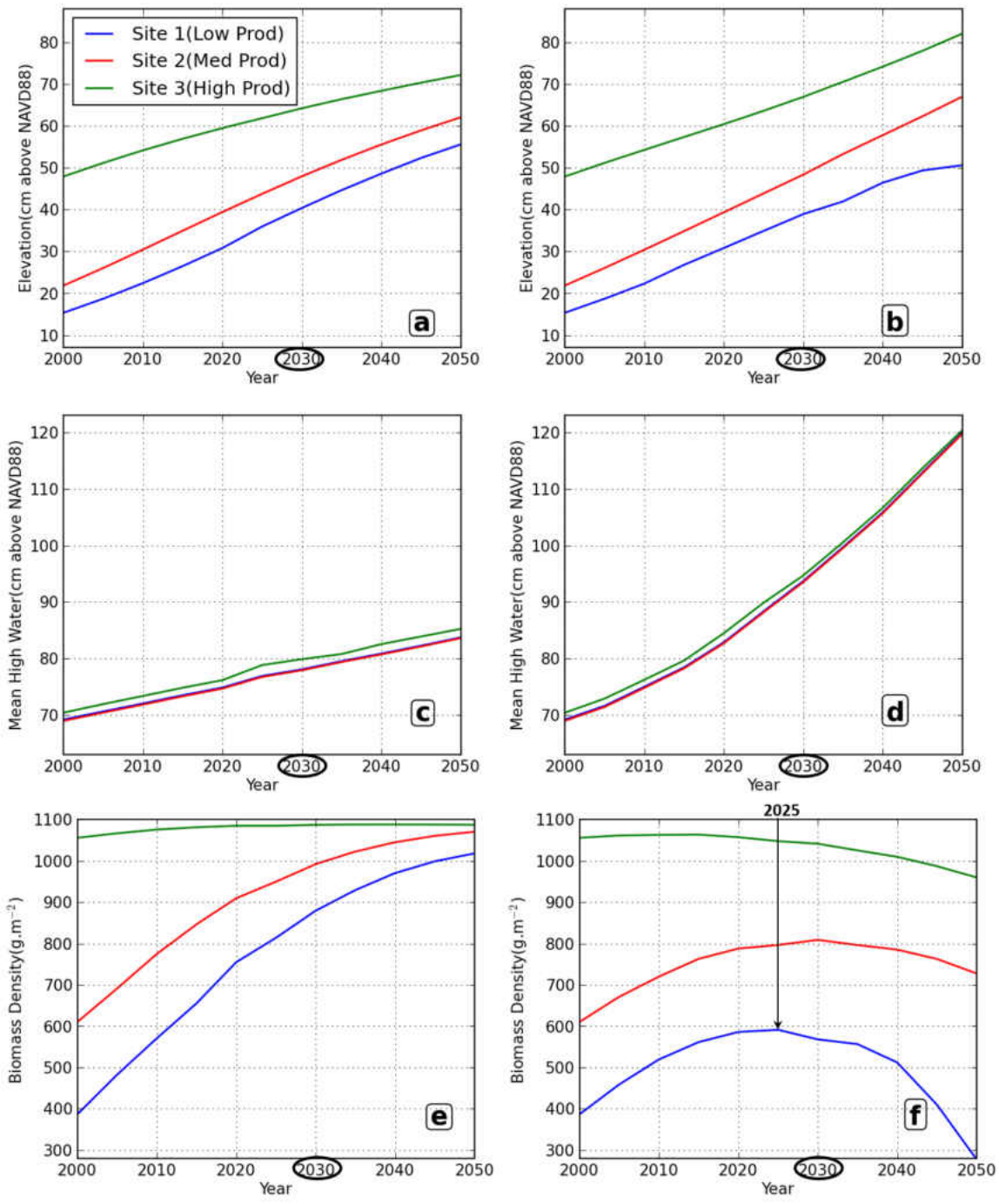

Figure 3.9: Changes in salt marsh platform elevation in (a) and (b), MHW in (c) and (d), and biomass density in (e) and (f) are displayed, for the low SLR (11 cm) and the high SLR (48 cm) scenarios respectively, for locations of low, medium, and high productivity as shown in Figure 3.1d (indicated as Sites 1, 2, and 3).

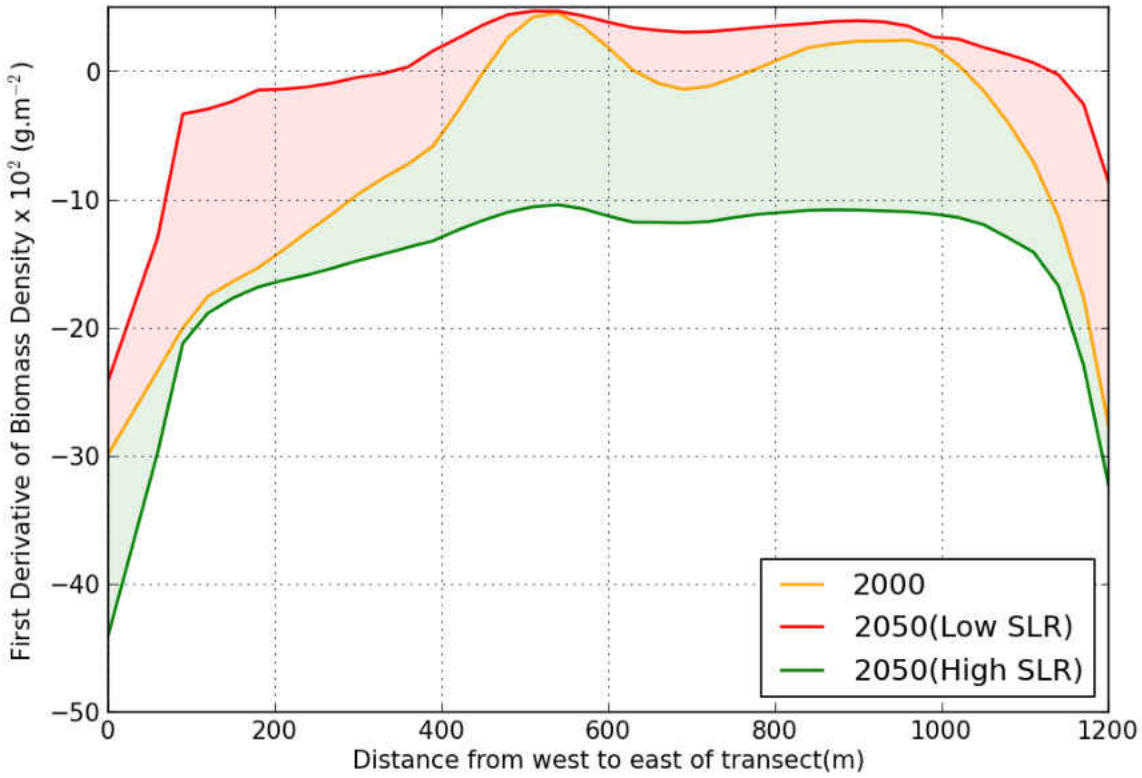

Figure 3.10: Changes in the first derivative of biomass density along a transect between years 2000 and 2050. Red shaded area shows the change of the first derivative of biomass density between the year 2000 (yellow line) and the year 2050 (red line) under a low SLR (11 cm) scenario; green shaded area demonstrates the change in the first derivative of biomass between the year 2000 (yellow line) and the year 2050 (green line) under a high SLR (48 cm) scenario.

Comparisons between using the coupled model and MEM in isolation are given in Table 3.2 according to total wetland area and marsh productivity for both the coupled HYDRO-MEM model and MEM. The HYDRO-MEM model exhibited more spatial variation of low and medium productivity for both the low and high SLR scenarios (Figure 3.11). Under the low SLR scenario there was less open water and more low and medium productivity, while under the high SLR scenario there was less high productivity and more low and medium productivity.

Table 3.2: Comparisons of areal coverage by landscape classifications following 50-yr simulations with high and low SLR using a coupled HYDRO-MEM model vs. a direct application of a spatially-distributed marsh equilibrium model (MEM) run without hydrodynamics. The marshes with productivity less than 370 g·m^{-2} are categorized as low, between 370 g.m^{-2} and 750 g.m^{-2} are categorized as medium, and more than 750 g.m^{-2} are categorized as high productivity.

Models	Area Percentage by landscape classification			
	Water	Low productivity	Medium productivity	High productivity
HYDRO-MEM (low SLR)	54.4	5.2	6.3	34.1
MEM (low SLR)	62.6	1.2	1.3	34.9
HYDRO-MEM (high SLR)	62.1	6.7	8.8	22.4
MEM (high SLR)	61.0	1.2	1.1	36.7

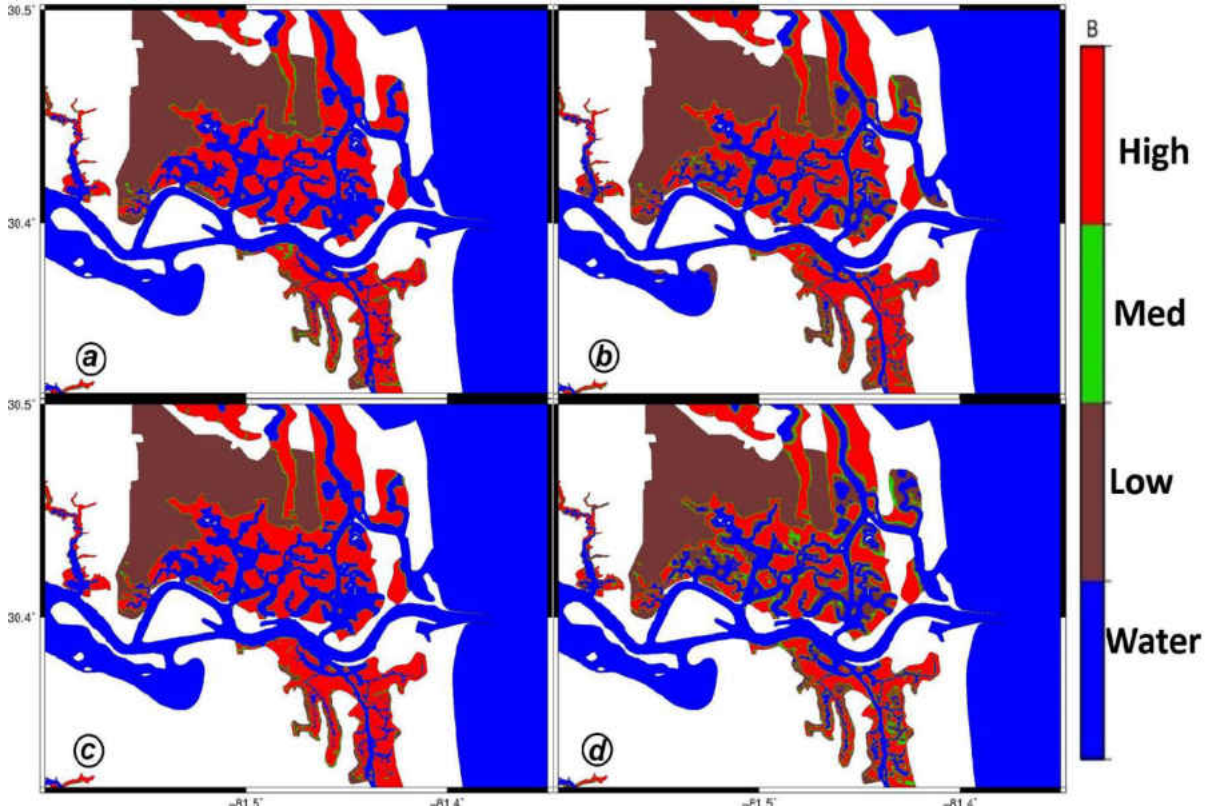

Figure 3.11: Biomass density patterns between using MEM (a and c) and HYDRO-MEM model (b and d) under the low SLR scenario (a and b) and the high SLR scenario (c and d). The marshes with productivity less than 370 g·m^{-2} are categorized as low, between 370 g.m^{-2} and 750 g.m^{-2} are categorized as medium, and more than 750 g.m^{-2} are categorized as high productivity.

To qualitatively validate the model result, infrared aerial imagery and land cover data from the National Land Cover Database for the year 2001 (NLCD2001) (Homer et al., 2007) were compared with the low, medium, and high productivity map (Figure 3.12). Within the box marked (a) in the aerial image (leftmost figure), the boundaries for the major creeks were captured in the model results (middle figure). Additionally, smaller creeks in boxes (a), (b) and (c) in the NLCD map (rightmost figure) also were represented well in the model results. The model identified the NLCD wetland areas corresponding to box (a) as highly productive marshes. Box (b) highlights an area with higher elevations, shown as forest land in the aerial map, and categorized as non-wetland in the NLCD map. These regions had low or no productivity in the model results. The border of the brown (low productivity) region in the model results generally mirrors the forested area in the aerial and the non-wetland area of the NLCD data. A low elevation area identified by box (c) consists of a drowning marsh flat with a dendritic layout of shallow tidal creeks. The model identified this area as having low or no productivity, but with a productive area marsh in the southeast corner. Collectively, comparison of the model results in these areas to ancillary data demonstrates the capability of the model to realistically characterize the estuarine landscape.

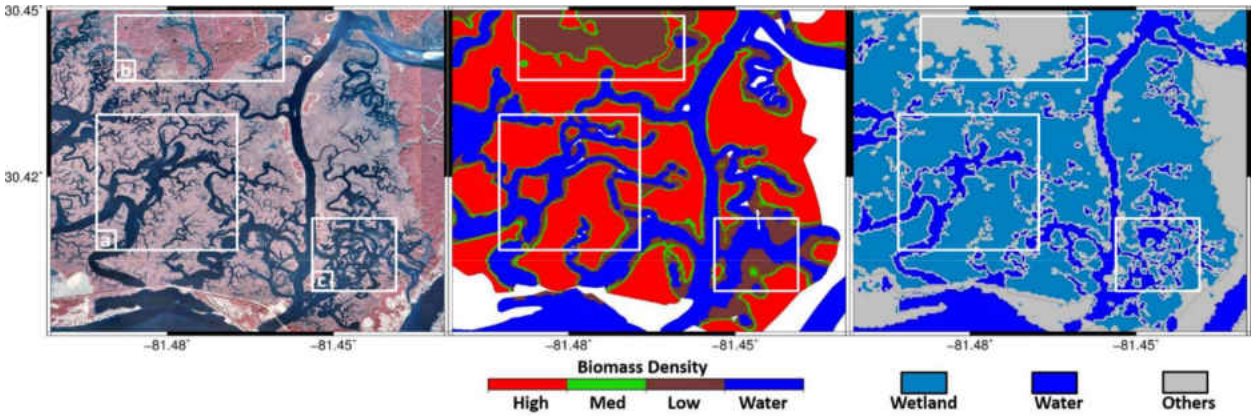

Figure 3.12: Qualitative comparison maps. From left to right, infrared aerial map of Timucuan sub-region (Figure 3.1d) from January 7, 1999 (USGS Digital Orthophoto Quadrangles), model generated map of open water, and low, medium, and high productivity regions, and wetland coverage area in the National Land Cover Database for the year 2001 (NLCD2001).

3.4 Discussion

Geomorphic variation on the marsh platform as well as variation in marsh biomass and their interactions with tidal flow play a key role in the spatial and temporal distribution of tidal constants, MLW and MHW, across an estuarine landscape. Tidal flow is affected because salt marsh systems increase momentum dissipation through surface friction, which is a function of vegetation growth (Möller et al., 1999; Möller and Spencer, 2002). Furthermore, the productivity and accretion of sediment in marshes affect the total area of wetted zones and, as a result of higher SLR projections, may increase the width of the tidal creeks, and some areas that are currently covered by marshes might convert to open water. Also, as the level of water increases, water can flow with lower resistance in the tidal creeks and circulate more freely through the marshes, thus leading to less spatial variability in tidal constants within the creeks and over the marsh platform.

During the high SLR scenario, water levels and flow rates increased and bottom friction was reduced. This reduced the spatial variability in MHW in the creeks and across the marshes. Further, as SLR increased, MHW in the marshes and creeks converged as energy dissipation from the marshes decreased. These energy controls are fundamental to the geomorphological feedbacks that maintain stable marshes. At the upper end of SLR, the tidal constants are in more dynamic equilibrium, where at the lower end of SLR, the tidal constants are sensitive to subtle changes where they are in adjustment towards dynamic equilibrium.

Marsh productivity is primarily a function of relative elevation, MHW, and accretion relative to SLR. SLR affects future marsh productivity by altering elevation, relative MHW, and their distributions across the marsh platform (i.e., hydroperiod). SLR also affects the accretion rate due to the biological feedback mechanisms of the system. The HYDRO-MEM model captured this relationship by updating accretion at each coupling time step based on data-derived biomass curve (MEM). Biomass density increased under the low SLR scenario as a result of the dynamic interactions between SLR and sedimentation. In this case, the low SLR scenario and the marsh system worked together to increase productivity and are in agreement with the predicted changes for salt marsh productivity in response to suggested ranges of SLR in recent study (Cadol et al., 2014).

For the low SLR scenario, the numerator in Equation 3.2 decreased with increasing accretion while the denominator increased; the point on the horizontal axis of the biomass curve moved to the left, closer to the optimum part of the curve (Figure 3.6). For the high SLR scenario, the numerator's growth outpaced that of the denominator in Equation 3.2, and the non-dimensional depth increased

to a higher value on the right side of the graph (Figure 3.6). This move illustrates the decrease in salt marsh productivity from the medium to the low region on the biomass density curve. In our study, most of the locations for the year 2000 were positioned on the right side of the biomass curve (Figure 3.6, Figure 3.5d). If the location is positioned on the far right or left sides of the biomass curve, the first derivative of biomass productivity is a small negative or large positive number, respectively (Figure 3.6). This number characterizes the slope of the tangent line to the curve at that point on the curve. The slope will approach zero at the optimal point of the curve (parabolic maximum). Therefore, if the point transitions to the right side of the curve, the first derivative will become smaller, and if the point moves to the left side of the curve, the first derivative will become larger. Under the low SLR scenario, the first derivative showed higher values generally approaching the optimal point (Figure 3.5e). As shown in Figure 3.6, the biomass density decreased under the high SLR scenario and the first derivative also decreased as it shifted to the right side of the biomass density curve (Figure 3.5f).

D' Alpaos et al. (2007) found that the inorganic sedimentation portion of the accretion decreases with increasing distance from the creek, which in this study is observed throughout a majority of the marsh system, thus indicating good model performance (Figure 3.7a, Figure 3.7b). Figure 3.8a and Figure 3.8c further illustrate this finding for the transect AB (Figure 3.1d), showing that the minimum accretion was in the middle of the transect (at a distance from the creeks) and the maximum was close to creeks. This model result is a consequence of the higher elevation of inland areas, and decreased inundation time of the marsh surface, rather than a result of a decrease in the mass of sediment transport.

Spatial and temporal variation in the tidal constants had a dynamic effect on accretion and also biomass density (Figure 3.8a, Figure 3.8b). The coupling between the hydrodynamic model and MEM, which included the dynamics of SLR, also helped to better capture the salt marsh's movements toward a dynamic equilibrium. This change in condition is exemplified by the red area in Figure 3.10 that depicted the movement toward the optimum point on the biomass density curve.

Although the salt marsh platform showed increased rates of accretion under high SLR, the salt marsh was not able to keep up with MHW. Salt marsh productivity declined along the edge of the creeks (Figure 3.8d); if this trend were to continue, the marsh would drown. The decline depends on the underlying topography as well as the tidal metrics, neither of which are uniform across the marsh. The first derivative curve for high SLR (shaded green) in Figure 3.10 illustrates a decline in biomass density; however, marshes with medium productivity due to higher accretion rates had minimal losses (Figure 3.9f) and the marsh productivity remained in the intermediate level. The marshes in the high productivity zone descended to the medium zone as the marshes in the lower level were exposed to more frequent and extended inundation. As a result, in the year 2050 under the high SLR scenario, the total salt marsh area was projected to decrease, with salt marshes mostly in the medium productivity level surviving (Figure 3.5c, Figure 3.5f). The high SLR scenario also exhibits a tipping point in biomass density that occurs at different times based on low, medium or high productivity, where biomass density declines beyond the tipping point.

The complex dynamics introduced by marsh biogeomorphological feedbacks as they influence hydrodynamic, biological, and geomorphological processes across the marsh landscape can be appreciated by examination of the time series from a few different positions within the marshes

(Figure 3.9). The interactions of these processes are reciprocal. That is, relative elevations affect biology, biology affects accretion of the marsh platform, which affects hydrodynamics and accretion, which affects biology, and so on. Furthermore, to add even more complexity to the biofeedback processes, the present conditions affect the future state. For example, the response of marsh platform elevation to SLR depends on the current elevation as well as the rate of SLR (Figure 3.9a, Figure 3.9b). The temporal change of accretion for the low productivity point under the high SLR scenario after 2030 can be explained by the reduction in salt marsh productivity and the resulting decrease in accretion. These marshes, which were typically near the edge of creeks, were prone to submersion under the high SLR scenario. However, the higher accretion rates for the medium and high productivity points under the high SLR compared to the low SLR scenario were due to the marsh's adaptive capability to capture sediment. The increasing temporal rate of biomass density change for the high, medium, and low productivity points under the low SLR scenario was due to the underlying rates of change of salt marsh platform and MHW (Figure 3.9). The decreasing rate of change for biomass density under the high SLR after 2030 for the medium and high productivity points, and after 2025 for the low productivity point was mainly because of the drastic change in MHW (Figure 3.9f).

The sensitivity of the coupled HYDRO-MEM model to the coupling time step length varied between the low and high SLR scenarios. The high SLR case required a shorter coupling time step due to the non-linear trend in water level change over time. However, the increased accuracy with a smaller coupling time step comes at the price of increased computational time. The run time for a single run of the hydrodynamic model across 120 cores (Intel Xeon quad core @ 3.0 GHz) was four wallclock hours, and with the addition of the ArcGIS portion of the HYDRO-MEM model

framework, the total computational time was noteworthy for this small marsh area and should be considered when increasing the number of the coupling time steps and the calculation area. Therefore, the optimum of the tested coupling time steps for the low and high SLR scenarios were determined to be 10 and 5 years, respectively.

As shown in Figure 3.11 and Table 3.2, the incorporation of the hydrodynamic component in the HYDRO-MEM model leads to different results in simulated wetland area and biomass productivity relative to the results estimated by the marsh model alone. Under the low SLR scenario, there was an 8.2% difference in predicted total wetland area between using the coupled HYDRO-MEM model vs. MEM alone (Table 3.2), and the low and medium productivity regions were both underestimated. Generally, MEM alone predicted higher productivity than the HYDRO-MEM model results. These differences are in part attributed to the fact that such an application of MEM applies fixed values for MLW and MHW in the wetland areas and uses a bathtub approach for simulating SLR, whereas the HYDRO-MEM model simulates the spatially varying MLW and MHW across the salt marsh landscape and accounts for non-linear response of MLW and MHW due to SLR (Figure 3.11). Secondly, the coupling of the hydrodynamics and salt marsh platform accretion processes influences the results of the HYDRO-MEM model.

A qualitative comparison of the model results to aerial imagery and NLCD data provided a better understanding of the biomass density model performance. The model results illustrated in areas representative of the sub-optimal, optimal and super-optimal regions of the biomass productivity curve were reasonably well captured compared with the above-mentioned ancillary data. This provided a final assessment of the model ability to produce realistic results.

The HYDRO-MEM model is the first spatial model that includes (1) the dynamics of SLR and its nonlinear (Passeri et al., 2015) effects on biomass density, and (2) SLR rate by employing a time step approach in the modeling rather than using a constant value for SLR. The time step approach used here also helped to capture the complex feedbacks between vegetation and hydrodynamics. This model can be applied in other estuaries to aid resource managers in their planning for potential changes or restoration acts under climate change and SLR scenarios. The outputs of this model can be used in storm surge or hydrodynamic simulations to provide an updated friction coefficient map. The future of this model should include more complex physical processes including inflows for fluvial systems, sediment transport (Mariotti and Fagherazzi, 2010) and biologically mediated resuspension, and a realistic depiction of more accurate geomorphological changes in the marsh system.

3.5 Acknowledgments

This research is funded partially under Award No. NA10NOS4780146 from the National Oceanic and Atmospheric Administration (NOAA) Center for Sponsored Coastal Ocean Research (CSCOR) and the Lousiana Sea Grant Laborde Chair endowment. The development of MEM was supported by a grant from the National Science Foundation to J.T. Morris. The STOKES Advanced Research Computing Center (ARCC) (webstokes.ist.ucf.edu) provided computational resources for the hydrodynamic model simulations. Earlier versions of the model were developed by James J. Angelo. The statements and conclusions do not necessarily reflect the views of NOAA-CSCOR, NSF, STOKES ARCC, Louisiana Sea Grant, or their affiliates.

3.6 References

Allen, J. R. L. (1997). "Simulation models of salt-marsh morphodynamics: some implications for high-intertidal sediment couplets related to sea-level change." *Sedimentary Geology* 113(3–4): 211-223.

Atkinson, J., McKee Smith, J. and Bender, C. (2013). "Sea-level rise effects on storm surge and nearshore waves on the Texas coast: Influence of landscape and storm characteristics." *Journal of Waterway, Port, Coastal, and Ocean Engineering* 139(2): 98-117.

Bacopoulos, P., Funakoshi, Y., Hagen, S. C., Cox, A. T. and Cardone, V. J. (2009). "The role of meteorological forcing on the St. Johns River (Northeastern Florida)." *Journal of Hydrology* 369(1–2): 55-70.

Bacopoulos, P. and Hagen, S. (2009). "Tidal Simulations for the Loxahatchee River Estuary (Southeastern Florida): On the Influence of the Atlantic Intracoastal Waterway versus the Surrounding Tidal Flats." *Journal of Waterway, Port, Coastal, and Ocean Engineering* 135(6): 259-268.

Bacopoulos, P., Hagen, S. C., Cox, A. T., Dally, W. R. and Bratos, S. M. (2012). "Observation and simulation of winds and hydrodynamics in St. Johns and Nassau Rivers." *Journal of Hydrology* 420–421(0): 391-402.

Bacopoulos, P., Parrish, D. M. and Hagen, S. C. (2011). "Unstructured mesh assessment for tidal model of the South Atlantic Bight and its estuaries." *Journal of Hydraulic Research* 49(4): 487-502.

Baustian, J. J., Mendelssohn, I. A. and Hester, M. W. (2012). "Vegetation's importance in regulating surface elevation in a coastal salt marsh facing elevated rates of sea level rise." *Global Change Biology* 18(11): 3377-3382.

Bilskie, M. V., Hagen, S. C., Medeiros, S. C. and Passeri, D. L. (2014). "Dynamics of sea level rise and coastal flooding on a changing landscape." *Geophysical Research Letters* 41(3): 927-934.

Blum, M. D. and Roberts, H. H. (2009). "Drowning of the Mississippi Delta due to insufficient sediment supply and global sea-level rise." *Nature Geoscience* 2(7): 488-491.

Bunya, S., Dietrich, J. C., Westerink, J. J., Ebersole, B. A., Smith, J. M., Atkinson, J. H., Jensen, R., Resio, D. T., Luettich, R. A., Dawson, C., Cardone, V. J., Cox, A. T., Powell, M. D., Westerink, H. J. and Roberts, H. J. (2010). "A High-Resolution Coupled Riverine Flow, Tide, Wind, Wind Wave, and Storm Surge Model for Southern Louisiana and Mississippi. Part I: Model Development and Validation." *Monthly Weather Review* 138(2): 345-377.

Bush, T. and Houck, M. (2002). "Plant fact sheet. Smooth Cordgrass Spartina alterniflora Loisel." *USDA Natural Resources Conservation Service*.

Cadol, D., Engelhardt, K., Elmore, A. and Sanders, G. (2014). "Elevation-dependent surface elevation gain in a tidal freshwater marsh and implications for marsh persistence." *Limnology and Oceanography* 59(3): 1065-1080.

Clough, J. S., Park, R. A. and Fuller, R. (2010). "SLAMM 6 beta technical documentation." *Waitsfield, VT*.

Costanza, R. and Ruth, M. (1998). "Using Dynamic Modeling to Scope Environmental Problems and Build Consensus." *Environmental Management* 22(2): 183-195.

Costanza, R., Sklar, F. H. and White, M. L. (1990). "Modeling Coastal Landscape Dynamics." *BioScience* 40(2): 91-107.

Craft, C., Clough, J., Ehman, J., Joye, S., Park, R., Pennings, S., Guo, H. and Machmuller, M. (2008). "Forecasting the effects of accelerated sea-level rise on tidal marsh ecosystem services." *Frontiers in Ecology and the Environment* 7(2): 73-78.

D' Alpaos, A., Lanzoni, S., Marani, M. and Rinaldo, A. (2007). "Landscape evolution in tidal embayments: Modeling the interplay of erosion, sedimentation, and vegetation dynamics." *Journal of Geophysical Research: Earth Surface* 112(F1): F01008.

D' Alpaos, A., Lanzoni, S., Mudd, S. M. and Fagherazzi, S. (2006). "Modeling the influence of hydroperiod and vegetation on the cross-sectional formation of tidal channels." *Estuarine, Coastal and Shelf Science* 69(3–4): 311-324.

Dame, R. and Kenny, P. D. (1986). "Variability of Spartina-Alterniflora Primary Production in the Euhaline North Inlet Estuary." *Marine Ecology Progress Series* 32(1): 71-80.

Darby, F. and Turner, R. E. (2008). "Below- and Aboveground Biomass of Spartina alterniflora: Response to Nutrient Addition in a Louisiana Salt Marsh." *Estuaries and Coasts* 31(2): 326-334.

DeMort, C. L. (1991). The St. Johns River System. The Rivers of Florida. R. Livingston, Springer New York. **83:** 97-120.

Donnelly, J. P. and Bertness, M. D. (2001). "Rapid shoreward encroachment of salt marsh cordgrass in response to accelerated sea-level rise." *Proceedings of the National Academy of Sciences* 98(25): 14218-14223.

ESRI (2012). "ArcMap 10.1". ESRI, Redlands, California.

Fagherazzi, S., Kirwan, M. L., Mudd, S. M., Guntenspergen, G. R., Temmerman, S., D'Alpaos, A., van de Koppel, J., Rybczyk, J. M., Reyes, E., Craft, C. and Clough, J. (2012). "Numerical models of salt marsh evolution: Ecological, geomorphic, and climatic factors." *Reviews of Geophysics* 50(1): RG1002.

Fitz, H. C., DeBellevue, E. B., Costanza, R., Boumans, R., Maxwell, T., Wainger, L. and Sklar, F. H. (1996). "Development of a general ecosystem model for a range of scales and ecosystems." *Ecological Modelling* 88(1–3): 263-295.

Giardino, D., Bacopoulos, P. and Hagen, S. (2011). "Tidal Spectroscopy of the Lower St. Johns River from a High-Resolution Shallow Water Hydrodynamic Model." *The International Journal of Ocean and Climate Systems* 2(1): 1-18.

Hagen, S., Morris, J., Bacopoulos, P. and Weishampel, J. (2013). "Sea-Level Rise Impact on a Salt Marsh System of the Lower St. Johns River." *Journal of Waterway, Port, Coastal, and Ocean Engineering* 139(2): 118-125.

Halpin, P. M. (2000). "Habitat use by an intertidal salt-marsh fish: trade-offs between predation and growth." *Marine Ecology Progress Series* 198: 203-214.

Homer, C., Dewitz, J., Fry, J., Coan, M., Hossain, N., Larson, C., Herold, N., McKerrow, A., VanDriel, J. N. and Wickham, J. (2007). "Completion of the 2001 national land cover database for the counterminous United States." *Photogrammetric Engineering and Remote Sensing* 73(4): 337.

Hopkinson, C. S., Gosselink, J. G. and Parrondo, R. T. (1980). "Production of Coastal Louisiana Marsh Plants Calculated from Phenometric Techniques." *Ecology* 61(5): 1091-1098.

Hutchinson, G. (1957). "Concluding remarks.: Cold Sprig Harbor Symposia on Quantitative Biology", Yale University New Haven.

Jørgensen, S. E. and Fath, B. D. (2011). 10 - Structurally Dynamic Models. Developments in Environmental Modelling. J. Sven Erik and D. F. Brian, Elsevier. **Volume 23:** 309-346.

Jørgensen, S. E. and Fath, B. D. (2011). 11 - Spatial Modelling. Developments in Environmental Modelling. J. Sven Erik and D. F. Brian, Elsevier. **Volume 23:** 347-368.

Kirwan, M. L. and Guntenspergen, G. R. (2012). "Feedbacks between inundation, root production, and shoot growth in a rapidly submerging brackish marsh." *Journal of Ecology* 100(3): 764-770.

Kirwan, M. L. and Murray, A. B. (2007). "A coupled geomorphic and ecological model of tidal marsh evolution." *Proceedings of the National Academy of Sciences* 104(15): 6118-6122.

Knutson, P. (1987). Role of Coastal Marshes in Energy Dissipation and Shore Protection. The Ecology and Management of Wetlands, Springer US**:** 161-175.

Leonard, L. A. and Croft, A. L. (2006). "The effect of standing biomass on flow velocity and turbulence in Spartina alterniflora canopies." *Estuarine, Coastal and Shelf Science* 69(3–4): 325-336.

Leonard, L. A. and Luther, M. E. (1995). "Flow hydrodynamics in tidal marsh canopies." *Limnology and Oceanography* 40(8): 1474-1484.

Luettich, R. A., Westerink, J. J. and Scheffner, N. W. (1992). "ADCIRC : an advanced three-dimensional circulation model for shelves, coasts, and estuaries. I: Theory and methodology of ADCIRC-2DD1 and ADCIRC-3DL." *Technical Rep. No. DRP-92-6, U.S. Army Engineer Waterways Experiment Station, Vicksburg, Miss.*(Technical Rep. No. DRP-92-6).

Marani, M., Da Lio, C. and D' Alpaos, A. (2013). "Vegetation engineers marsh morphology through multiple competing stable states." *Proceedings of the National Academy of Sciences* 110(9): 3259-3263.

Mariotti, G. and Fagherazzi, S. (2010). "A numerical model for the coupled long-term evolution of salt marshes and tidal flats." *Journal of Geophysical Research: Earth Surface (2003–2012)* 115(F1).

Martin, J. F., Reyes, E., Kemp, G. P., Mashriqui, H. and Day, J. W. (2002). "Landscape modeling of the Mississippi Delta: using a series of landscape models, we examined the survival and creation of Mississippi Delta marshes and the impact of altered riverine inputs, accelerated sea-level rise, and management proposals on these marshes." *BioScience* 52(4): 357-365.

Martin, J. F., White, M. L., Reyes, E., Kemp, G. P., Mashriqui, H. and Day, J. J. W. (2000). "PROFILE: Evaluation of Coastal Management Plans with a Spatial Model: Mississippi Delta, Louisiana, USA." *Environmental Management* 26(2): 117-129.

Mckee, K. L. and Patrick, W. (1988). "The relationship of smooth cordgrass (Spartina alterniflora) to tidal datums: a review." *Estuaries* 11(3): 143-151.

Medeiros, S. C. and Hagen, S. C. (2013). "Review of wetting and drying algorithms for numerical tidal flow models." *International Journal for Numerical Methods in Fluids* 71(4): 473-487.

Möller, I. and Spencer, T. (2002). "Wave dissipation over macro-tidal saltmarshes: Effects of marsh edge typology and vegetation change." *Journal of Coastal Research* 36: 506-521.

Möller, I., Spencer, T., French, J. R., Leggett, D. J. and Dixon, M. (1999). "Wave transformation over salt marshes: a field and numerical modelling study from North Norfolk, England." *Estuarine, Coastal and Shelf Science* 49(3): 411-426.

Morris, J. (1995). "The mass balance of salt and water in intertidal sediments: Results from North Inlet, South Carolina." *Estuaries* 18(4): 556-567.

Morris, J. (2007). "Ecological engineering in intertidial saltmarshes." *Hydrobiologia* 577(1): 161-168.

Morris, J. T. (2015). "Marsh equilibrium theory." *ICI-Spartina symposium 2014*.

Morris, J. T., Sundareshwar, P. V., Nietch, C. T., Kjerfve, B. and Cahoon, D. R. (2002). "Responses of coastal wetlands to rising sea level." *Ecology* 83(10): 2869-2877.

Morris, J. T., Sundberg, K. and Hopkinson, C. S. (2013). "Salt marsh primary production and its responses to relative sea level and nutrients in estuaries at Plum Island, Massachusetts, and North Inlet, South Carolina, USA." *Oceanography* 26(3): 78-84.

Mudd, S. M., D'Alpaos, A. and Morris, J. T. (2010). "How does vegetation affect sedimentation on tidal marshes? Investigating particle capture and hydrodynamic controls on biologically mediated sedimentation." *Journal of Geophysical Research: Earth Surface* 115(F3): F03029.

Mudd, S. M., Fagherazzi, S., Morris, J. T. and Furbish, D. J. (2004). Flow, sedimentation, and biomass production on a vegetated salt marsh in South Carolina: Toward a predictive model of marsh morphologic and ecologic evolution. The Ecogeomorphology of Tidal Marshes. Washington, DC, AGU. **59:** 165-188.

Nyman, J. A., DeLaune, R., Roberts, H. and Patrick Jr, W. (1993). "Relationship between vegetation and soil formation in a rapidly submerging coastal marsh." *Marine ecology progress series. Oldendorf* 96(3): 269-279.

Nyman, J. A., Walters, R. J., Delaune, R. D. and Patrick Jr, W. H. (2006). "Marsh vertical accretion via vegetative growth." *Estuarine, Coastal and Shelf Science* 69(3–4): 370-380.

Park, R. A., Armentano, T. V. and Cloonan, C. L. (1986). "Predicting the effects of sea level rise on coastal wetlands." *Effects of changes in stratospheric ozone and global climate* 4: 129-152.

Park, R. A., Trehan, M. S., Mausel, P. W., Howe, R. C. and Titus, J. G. (1989). The effects of sea level rise on US coastal wetlands and lowlands, Office of Policy, Planning and Evaluation, US Environmental Protection Agency.

Parris, A., Bromirski, P., Burkett, V., Cayan, D., Culver, M., Hall, J., Horton, R., Knuuti, K., Moss, R., Obeysekera, J., Sallenger, A. and Weiss, J. (2012). "Global Sea Level Rise Scenarios for the US National Climate Assessment." *NOAA Tech Memo OAR CPO*: 1-37.

Passeri, D. L., Hagen, S. C., Medeiros, S. C. and Bilskie, M. V. (2015). "Impacts of historic morphological changes and sea level rise on tidal hydrodynamics in the Grand Bay, Mississippi estuary." *Estuarine, Coastal and Shelf Science*: Submitted.

Patrick, W. H. and DeLaune, R. D. (1990). "Subsidence. accretion. and sea level rise in south San Francisco Bay marshes." *Limnology and Oceanography* 35(6): 1389-1395.

Pennings, S. C. and Bertness, M. D. (2001). "Salt marsh communities." *Marine community ecology*: 289-316.

Reed, D. J. (1990). "The impact of sea-level rise on coastal salt marshes." *Progress in Physical Geography* 14(4): 465-481.

Reed, D. J. (1995). "The response of coastal marshes to sea-level rise: Survival or submergence?" *Earth Surface Processes and Landforms* 20(1): 39-48.

Reyes, E., White, M. L., Martin, J. F., Kemp, G. P., Day, J. W. and Aravamuthan, V. (2000). "Landscape modeling of coastal habitat change in the Mississippi Delta." *Ecology* 81(8): 2331-2349.

Schile, L. M., Callaway, J. C., Morris, J. T., Stralberg, D., Parker, V. T. and Kelly, M. (2014). "Modeling tidal marsh distribution with sea-level rise: Evaluating the role of vegetation, sediment, and upland habitat in marsh resiliency." *PLoS ONE* 9(2): e88760.

Schubauer, J. P. and Hopkinson, C. S. (1984). "Above- and belowground emergent macrophyte production and turnover in a coastal marsh ecosystem, Georgia1." *Limnology and Oceanography* 29(5): 1052-1065.

Shepard, C. C., Crain, C. M. and Beck, M. W. (2011). "The protective role of coastal marshes: A systematic review and meta-analysis." *PLoS ONE* 6(11): e27374.

Silliman, B. R. and Bertness, M. D. (2002). "A trophic cascade regulates salt marsh primary production." *Proceedings of the National Academy of Sciences* 99(16): 10500-10505.

Sklar, F. H., Costanza, R. and Day Jr, J. W. (1985). "Dynamic spatial simulation modeling of coastal wetland habitat succession." *Ecological Modelling* 29(1–4): 261-281.

Stralberg, D., Brennan, M., Callaway, J. C., Wood, J. K., Schile, L. M., Jongsomjit, D., Kelly, M., Parker, V. T. and Crooks, S. (2011). "Evaluating Tidal Marsh Sustainability in the Face of Sea-Level Rise: A Hybrid Modeling Approach Applied to San Francisco Bay." *PLoS ONE* 6(11): e27388.

Tambroni, N. and Seminara, G. (2012). "A one-dimensional eco-geomorphic model of marsh response to sea level rise: Wind effects, dynamics of the marsh border and equilibrium." *Journal of Geophysical Research: Earth Surface* 117(F3): F03026.

Temmerman, S., Bouma, T. J., Van de Koppel, J., Van der Wal, D., De Vries, M. B. and Herman, P. M. J. (2007). "Vegetation causes channel erosion in a tidal landscape." *Geology* 35(7): 631-634.

Temmerman, S., Govers, G., Meire, P. and Wartel, S. (2003). "Modelling long-term tidal marsh growth under changing tidal conditions and suspended sediment concentrations, Scheldt estuary, Belgium." *Marine Geology* 193(1–2): 151-169.

Thomas, R. E., Johnson, M. F., Frostick, L. E., Parsons, D. R., Bouma, T. J., Dijkstra, J. T., Eiff, O., Gobert, S., Henry, P.-Y., Kemp, P., McLelland, S. J., Moulin, F. Y., Myrhaug, D., Neyts, A., Paul, M., Penning, W. E., Puijalon, S., Rice, S. P., Stanica, A., Tagliapietra, D., Tal, M., Tørum, A. and Vousdoukas, M. I. (2014). "Physical modelling of water, fauna and flora: knowledge gaps, avenues for future research and infrastructural needs." *Journal of Hydraulic Research* 52(3): 311-325.

Thorne, K. M., Elliott-Fisk, D. L., Wylie, G. D., Perry, W. M. and Takekawa, J. Y. (2014). "Importance of biogeomorphic and spatial properties in assessing a tidal salt marsh vulnerability to sea-level rise." *Estuaries and Coasts* 37(4): 941-951.

Townend, I., Fletcher, C., Knappen, M. and Rossington, K. (2011). "A review of salt marsh dynamics." *Water and Environment Journal* 25(4): 477-488.

Turner, R. E., Swenson, E. M. and Milan, C. S. (2000). Organic and inorganic contributions to vertical accretion in salt marsh sediments. Concepts and Controversies in Tidal Marsh Ecology. M. Weinstein and D. Kreeger, Springer Netherlands**:** 583-595.

United States Army Corps of Engineers (USACE) (2011). "Sea-level change considerations for civil works programs " *EC 1165-2-212*.

United States National Park Service (Denver Service Center) (1996). Timucuan Ecological and Historic Preserve, Florida: general management plan, development concept plans, US National Park Service, Denver Service Center.

Walton Jr, T. L. (2007). "Projected sea level rise in Florida." *Ocean Engineering* 34(13): 1832-1840.

Warren, R. S. and Niering, W. A. (1993). "Vegetation change on a northeast tidal marsh: Interaction of sea-level rise and marsh accretion." *Ecology* 74(1): 96-103.

CHAPTER 4. APPLICATION OF THE MODEL IN A FLUVIAL ESTUARINE SYSTEM

The content in this chapter is under review as: Alizad, K., Hagen, S. C., Morris, J. T., Medeiros, S. C., Bilskie, M. V., Weishampel, J. F. 2016. Coastal Wetland Response to Sea Level Rise in a Fluvial Estuarine System." *Earth's Future*.

4.1 Introduction

The fate of coastal wetlands may be in danger due to climate change and sea-level-rise (SLR) in particular. Identifying and investigating factors that influence the productivity of coastal wetlands may provide insight into the potential future salt marsh landscape and to identify tipping points (Nicholls, 2004). It is expected that one of the most prominent drivers of coastal wetland loss will be SLR (Nicholls et al., 1999). Salt marsh systems play an important role in coastal protection by attenuating waves and providing shelters and habitats for various species (Daiber, 1977; Halpin, 2000; Moller et al., 2014). A better understanding of salt marsh evolution under SLR supports more effective coastal restoration, planning, and management (Bakker et al., 1993).

Plausible projections of global SLR, including its's rate, are critical to effectively analyze coastal vulnerability (Parris et al., 2012). In addition to increasing local mean tidal elevations, SLR alters circulation patterns and sediment transport, which can affect the ecosystem as a whole and wetlands in particular (Nichols, 1989). Studies have shown that adopting a dynamic modeling approach is preferred over static modeling when conducting coastal vulnerability assessments under SLR scenarios. Dynamic modeling includes nonlinearities that are unaccounted for by simply increasing water levels. The static or "bathtub" approach simply elevates the present-day water surface by the amount of SLR and projects new inundation using a digital elevation model

(DEM). On the other hand, a dynamic approach incorporates the various nonlinear feedbacks in the system and considers interactions between topography and inundation that can lead to an increase or decrease in tidal amplitudes and peak storm surge, changes to tidal phases and timing of maximum storm surge, and modify depth-averaged velocities (magnitude and direction) (Hagen and Bacopoulos, 2012; Atkinson et al., 2013; Bilskie et al., 2014; Passeri et al., 2015; Bilskie et al., 2016; Passeri et al., 2016).

Previous research has investigated the effects of sea-level change on hydrodynamics and coastal wetland changes using a variety of modeling tools (Wolanski and Chappell, 1996; Liu, 1997; Hearn and Atkinson, 2001; French, 2008; Leorri et al., 2011; Hagen and Bacopoulos, 2012; Hagen et al., 2013; Valentim et al., 2013). Several integrated biological models have been developed to assess the effect of SLR on coastal wetland changes. They employed hydrodynamic models in conjunction with marsh models to capture the changes in marsh productivity as a result of variations in hydrodynamics (D' Alpaos et al., 2007; Kirwan and Murray, 2007; Temmerman et al., 2007; Hagen et al., 2013). However, these models were designed for small marsh systems or simplified complex processes. Alizad et al. (2016) coupled a hydrodynamic model with Marsh Equilibrium Model (MEM) to include the biological feedback in a time stepping framework that incorporates the dynamic interconnection between hydrodynamics and marsh system by updating inputs including topography and bottom roughness in each time step.

Lidar-derived DEMs are a generally-accepted means to generate accurate topographic surfaces over large areas (Medeiros et al., 2011; Bilskie and Hagen, 2013). While the ability to cover vast geographic regions at relatively low cost make lidar an attractive proposition, there are well

documented topographic errors, especially in coastal marshes, when compared to Real Time Kinematic (RTK) topographic survey data (Hsing-Chung et al., 2004; Hladik and Alber, 2012; Medeiros et al., 2015). The accuracy of lidar DEMs in salt marsh systems is limited primarily because of the inability of the laser to penetrate through the dense vegetation to the true marsh surface (Hladik and Alber, 2012). Filters, such as slope-based or photogrammetric techniques applied in post processing, are able to reduce but not eliminate these errors (Kraus and Pfeifer, 1998; Lane, 2000; Vosselman, 2000; Carter et al., 2001; Hicks et al., 2002; Sithole and Vosselman, 2004; James et al., 2006). The amount of adjustment required to correct the lidar-derived marsh DEM varies on the marsh system, its location, the season of data collection, and instrumentation (Montane and Torres, 2006; Yang et al., 2008; Wang et al., 2009; Chassereau et al., 2011; Hladik and Alber, 2012). In this study, the lidar-derived marsh table elevation is adjusted based on RTK topographic measurements and remotely sensed data (Medeiros et al., 2015).

Sediment deposition is a critical component in sustaining marsh habitats (Morris et al., 2002). The most important factor that promotes sedimentation is the existence of vegetation that increases residence time within the marsh allowing sediment to settle out (Fagherazzi et al., 2012). Research has shown that salt marshes maintain their state (*i.e.* equilibrium) under SLR by accreting sediments and organic materials (Reed, 1995; Turner et al., 2000; Morris et al., 2002; Baustian et al., 2012). Salt marshes need these two sources of accretion (sediment and organic materials) to survive in place (Nyman et al., 2006; Baustian et al., 2012) or to migrate to higher land (Warren and Niering, 1993; Elsey-Quirk et al., 2011).

The Apalachicola River (Figure 4.1), situated in the Florida Panhandle, is formed by the confluence of the Chattahoochee and Flint Rivers, and has the largest volumetric discharge of any river in Florida, which drains the second largest watershed in Florida (Isphording, 1985). Its wide and shallow microtidal estuary is centered on Apalachicola Bay in the northeastern Gulf of Mexico (GOM). Apalachicola Bay is bordered by East Bay to the northeast, St. Vincent Sound to the west, and St. George Sound to the east. The river feeds into an array of salt marsh systems, tidal flats, oyster bars, and submerged aquatic vegetation (SAV) as it empties into Apalachicola Bay, which has an area of 260 km^2 and a mean depth of 2.2 m (Mortazavi et al., 2000). Offshore, the barrier islands (St. Vincent, Little St. George, St. George and Dog Islands) shelter the bay from the Gulf of Mexico. Approximately 17% of the estuary is comprised of marsh systems that provide habitats for many species, including birds, crabs, and fish (Halpin, 2000; Pennings and Bertness, 2001). Approximately 90% of Florida's annual oyster catch, which amounts to 10% of the nation's, comes from Apalachicola Bay, and 65% of workers in Franklin County are or have been employed in the commercial fishing industry (FDEP, 2013). Therefore, accurate assessments regarding this ecosystem can provide insights to environmental and economic management decisions.

It is projected that SLR may shift tidal boundaries upstream in the river, which may alter inundation patterns and remove coastal vegetation or change its spatial distribution (Florida Oceans and Coastal Council, 2009; Passeri et al., 2016). Apalachicola salt marshes may lose productivity with increasing SLR due to the microtidal nature of the estuary (Livingston, 1984). Therefore, the objective of this study is to assess the response of the Apalachicola salt marsh for various SLR scenarios using a high-resolution Hydro-MEM model for the region

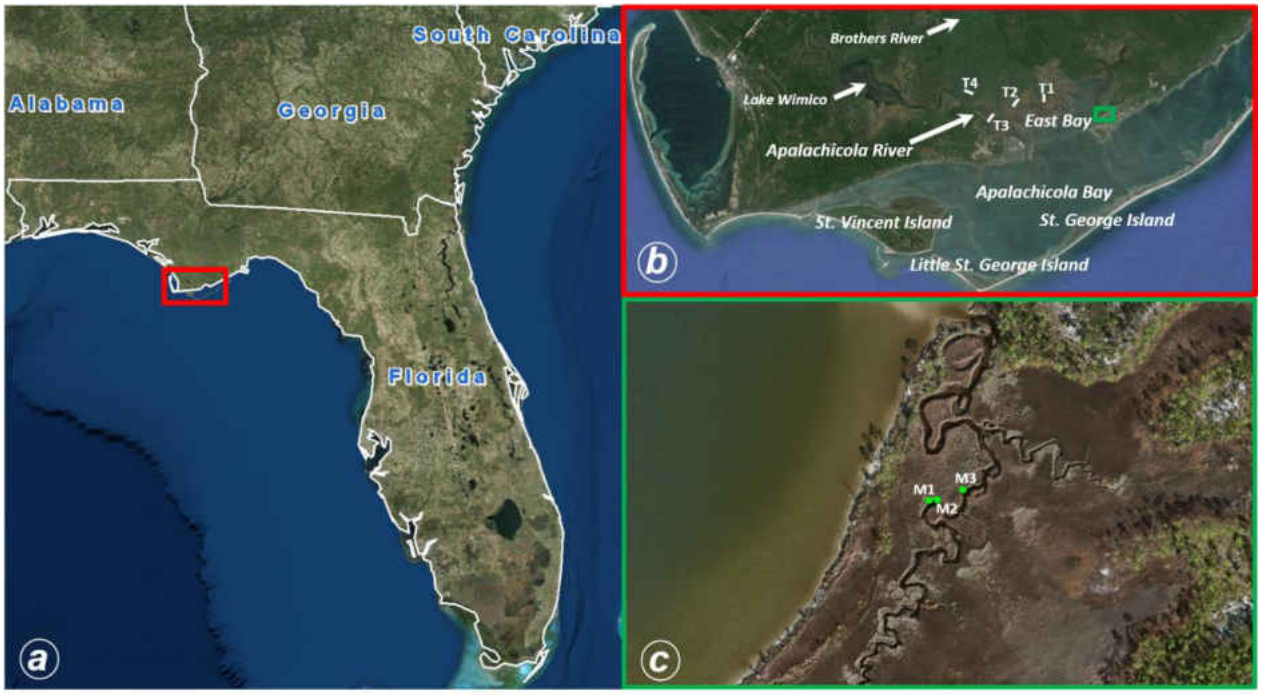

Figure 4.1: Study area and marsh organ locations. (a) Location of the Apalachicola estuarine system in Florida; (b) The Apalachicola River, Bay, and other locations including the transects for assessing velocity variations in the estuarine system; (c) The marsh organ experimental sets in the estuarine system.

4.2 Methods

4.2.1 HYDRO-MEM Model

The integrated Hydro-MEM model was used to assess the response of the Apalachicola salt marsh under SLR scenarios. The hydrodynamic and biologic components are coupled and exchange information at discrete coupling intervals (time steps). Incorporating multiple feedback points along the simulation timeline via a coupling time step permits a nonlinear rate of SLR to be modeled. This contrasts with other techniques that apply the entire SLR amount in one single step.

This procedure better describes the physical and biological interactions between hydrodynamics and salt marsh systems over time. The coupling time step, considering the desired level of accuracy and computational expense, depends on the rate of SLR and governs the frequency of information exchange between the hydrodynamic and biological models (Alizad et al., 2016).

The model was initialized from the present day marsh surface elevations and sea level. First, the hydrodynamic model computes water levels and depth-averaged currents and yields astronomic tidal constituent amplitudes and phases. From these results, mean high water (MHW) was computed and passed to the parametric marsh model, and along with field/laboratory analyzed biomass curve parameters, the spatial distribution of biomass density and accretion was calculated. Accretion was applied to the marsh elevations and the bottom friction was updated based on the biomass distribution and passed back to the hydrodynamic model to initialize the next time step. Additional details in the Hydro-MEM model can be found in Alizad et al. (2016). The next two sections provide specific details to each portion of the Hydro-MEM framework, the hydrodynamic model and the marsh model.

4.2.1.1 Hydrodynamic Model

Hydrodynamic simulations were performed using the two dimensional, depth-integrated, ADvanced CIRCulation (ADCIRC) finite element based shallow water equations model to solve for water levels and depth-averaged currents. An unstructured mesh for the Apalachicola estuary was developed with focus on simulating water level variations within the river, tidal creeks, and daily wetting and drying across the marsh surface. The mesh was constructed from manual digitization using recent aerial imagery of the River, distributaries, tidal creeks, estuarine

impoundments, and intertidal zones. To facilitate numerical stability of the model with respect to wetting and drying, the number of triangular elements within the creeks was restricted to three or more to represent a trapezoidal cross-section (Medeiros and Hagen, 2013). Therefore, the width of the smallest captured creek was approximately 40 m. For smaller creeks, the computational nodes located inside the digitized creek banks were assigned a lower bottom friction value to allow the water to flow more readily, thus keeping lower resistance of the creek (compared to marsh grass vegetation). The mesh extends to the 60^{o} west meridian (the location of the tidal boundary forcing) in the western North Atlantic and encompasses the Caribbean Sea and the Gulf of Mexico (Hagen et al., 2006). Overall, the triangular elements range from a minimum of 15 m within the creeks and marsh platform, 300 m in Apalachicola Bay, and 136 km in the open ocean.

The source data for topography and bathymetry consisted of the online accessible lidar-derived digital elevation model (DEM) provided by the Northwest Florida Water Management District (http://www.nwfwmdlidar.com/) and Apalachicola River surveyed bathymetric data from the U.S. Army Corps of Engineers, Mobile District. Medeiros et al. (2015) showed that the lidar topographic data for this salt marsh contained high bias and required correction to increase the accuracy of the marsh surface elevation and facilitate wetting of the marsh platform during normal tidal cycles. The DEM was adjusted using biomass density estimated by remote sensing; however a further adjustment was also implemented. The biomass adjusted DEM in that study (Figure 4.2) reduced the high bias of the lidar-derived marsh platform elevation from 0.65 m to 0.40 m. This remaining 0.40 m of bias was removed by lowering the DEM by this amount at the southeastern salt marsh shoreline where the vegetation is densest and linearly decreasing the adjustment value to zero moving upriver (i.e. to the northwest). This method was necessary in order to properly

capture the cyclical tidal flooding of the marsh platform; without removing this remaining bias, the majority of the platform was incorrectly specified to be above MHW and was unable to become wet in the model during high tide.

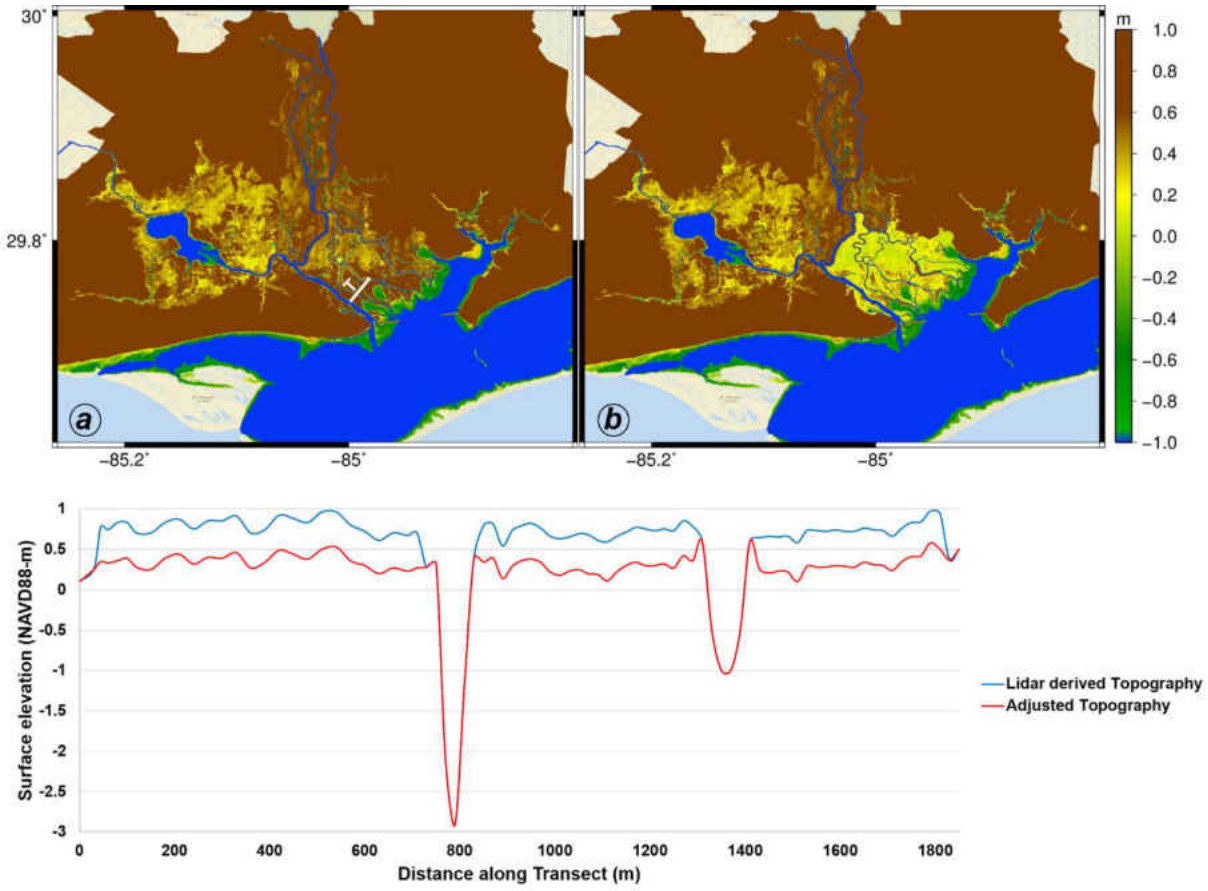

Figure 4.2: Topographic model input of the Apalachicola estuarine system and the elevation change along the transect "T" shown in Figure 4.2a. Color bar elevations are referenced to NAVD88 in meters. (a) Adjusted marsh platform elevation; (b) lidar data elevation without any correction.

Bottom friction was included in the model as spatially varying Manning's n and were assigned based on the National Land-Cover Database 2001 (Homer et al., 2004; Bilskie et al., 2015). Three values for low, medium, and high biomass densities in each land cover class were defined as 0.035, 0.05, and 0.07, respectively (Arcement and Schneider, 1989; Medeiros, 2012; Medeiros et al., 2012). At each coupling time step, using the computed biomass density and hydrodynamics, Manning's n values for specific computational nodes were converted to open water (permanently submerged due to SLR) or if their biomass density changed.

In this study, the four global SLR scenarios for the year 2100 presented by Parris et al. (2012) were applied; low (0.2 m), intermediate-low (0.5 m), intermediate-high (1.2 m) and high (2.0 m). The coupling time step was 10 years for the low and intermediate-low SLR scenarios and 5 years for the intermediate-high and high SLR scenarios. This protocol effectively discretizes the SLR curves into linear segments that adequately capture the projected SLR acceleration for the purposes of this study (Alizad et al., 2016). Thus, the total number of hydrodynamic simulations used in this study are 60: 10 (100 years divided by 10 coupling steps) for the low and intermediate-low scenarios and 20 (100 years divided by 20 coupling steps) for the intermediate-high and high scenarios.

The hydrodynamic model is forced with astronomic tides at the 60° meridian (open ocean boundary of the WNAT model domain) and river inflow for the Apalachicola River. The tidal forcing is comprised of time varying water surface elevations of the seven principal tidal constituents (M_2, S_2, N_2, K_1, O_1, K_2, and Q_1) (Egbert et al., 1994; Egbert and Erofeeva, 2002). The river inflow boundary forcing was obtained from the United States Geological Survey (USGS)

gage near Sumatra, FL in the Apalachicola River (USGS 02359170). The mean discharge value from 38 years of record for this gage (http://waterdata.usgs.gov/nwis/uv?02359170) was 670.17 cubic meters per second as of February 2016. The discharge at the upper (northern) extent of the Apalachicola River is controlled at the Jim Woodruff Dam near the Florida – Georgia border and was considered to be fixed for all simulations. Two separate hyperbolic tangent ramping functions were applied at the model start, one for tidal forcing and the other for the river inflow boundary condition. The main outputs from the hydrodynamic model used in this study were the amplitude and phase harmonic tidal constituents, which were then used as input to the Hydro-MEM model. This hydrodynamic model has been extensively validated for astronomic tides in this region (Bilskie et al., 2016; Passeri et al., 2016).

4.2.1.2 Marsh Model

The parametric marsh model employed was the Marsh Equilibrium Model (MEM), which quantifies biomass density (B) (g.m^{-2}.yr^{-1}) using a parabolic curve (Morris et al., 2002) :

$$B = aD + bD^2 + c$$
$$D = MHW - Elevation \tag{4.1}$$

The biomass density curve includes data for three different marsh grass species of *S. cynosuroides*, *J. romerianus*, and *S. alterniflora*. These curves were divided into left (sub-optimal) and right (super-optimal) branches that meet at the maximum biomass density point. The left and right curve coefficients used were a_l = 197.5 g.m^{-3}.yr^{-1}, b_l = -9870 g.m^{-4}.yr^{-1}, c_l =1999 g.m^{-2}.yr^{-1}, and a_r = 326.5 g.m^{-3}.yr^{-1}, b_r = -1633 g.m^{-4}.yr^{-1}, c_r =1998 g.m^{-2}.yr^{-1}, respectively. They were derived using

field bio-assay experiments, commonly referred to as "marsh organs", which consisted of planted marsh species in an array of PVC pipes cut to different elevations in the tidal frame. The pipes each contain approximately the same amount of biomass at the start of the experiment and are allowed to flourish or die off based on their natural response to the hydroperiod of their row (Morris et al., 2013). They were installed at three sites in Apalachicola estuary (Figure 4.1) in 2011 and inspected regularly for two years by qualified staff from the Apalachicola National Estuarine Research Reserve (ANERR).

The accretion rate in the coupled model included the accumulation of both organic and inorganic materials and was based on the MEM accretion rate formula found in (Morris et al., 2002). The total accretion (dY) (cm/yr) during the study time (dt) was calculated by incorporating the amount of inorganic accumulation from sediment load (q) and the vegetation effect on organic and inorganic accretion (k):

$$\frac{dY}{dt} = (q + kB)D \qquad \text{for} \qquad D>0 \tag{4.2}$$

where the parameters q (0.0018 yr^{-1}) and k (1.5 x $10^{-5} g^{-1}.m^2$) (Morris et al., 2002) were used to calculate the total accretion at each computational point and update the DEM at each coupling time step. The accretion was calculated for the points with positive relative depth, where average mean high tide is above the marsh platform (Morris, 2007).

4.3 Results

4.3.1 Hydrodynamic Results

The MHW results for future SLR scenarios predictably showed higher water levels and altered inundation patterns. The water level change in the creeks was spatially variable under the low and intermediate-low SLR scenario. However, the water level in the higher scenarios were more spatially uniform. The warmer colors in Figure 4.3 indicate higher water levels; however, please note that to capture the variation in water level for each scenario the range of each scale bar was adjusted. In the low SLR scenario, the water level changed from 10 to 40 cm in the river and creeks, but the wetted area remained similar to the current condition (Figure 4.3a, Figure 4.3b). The water level and wetted area increased under the intermediate-low SLR scenario and some of the forested area became inundated (Figure 4.3c). Under the intermediate-high and high SLR scenarios, all of the wetlands were inundated, water level increased by more than a meter, and the bay extended to the uplands (Figure 4.3d, Figure 4.3e).

The table in Figure 4.3 shows the inundated area for each SLR scenario in the Apalachicola region including the bay, rivers and creeks. Under the intermediate-low SLR the wetted area increased by 12 km^2, an increase by 2 percent. However, the flooded area for the intermediate-high and high SLR scenarios drastically increased to 255 km^2 and 387 km^2, which is a 45 and 68 percent increase in the wetted area, respectively.

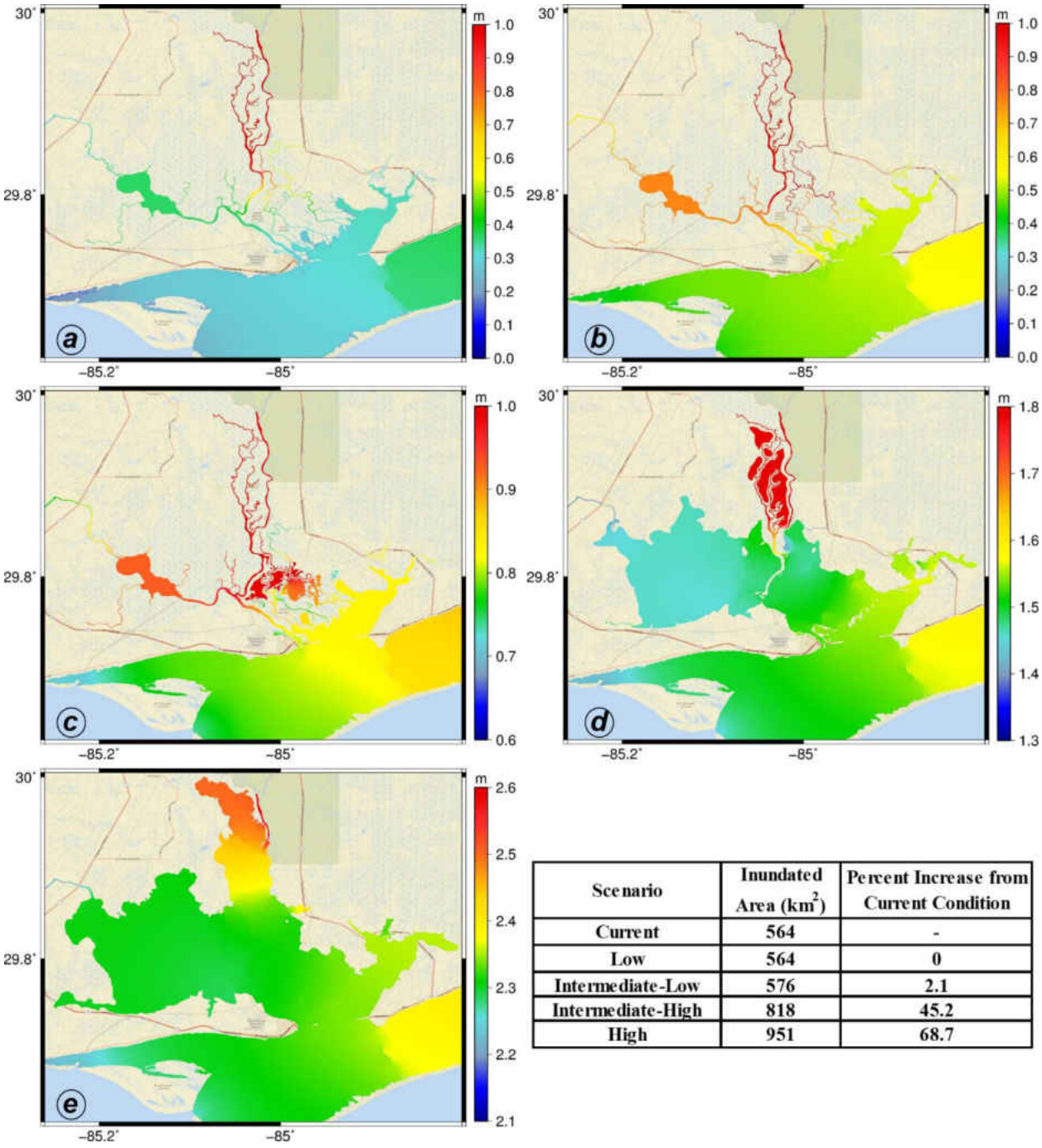

Scenario	Inundated Area (km^2)	Percent Increase from Current Condition
Current	564	-
Low	564	0
Intermediate-Low	576	2.1
Intermediate-High	818	45.2
High	951	68.7

Figure 4.3: MHW results for projected SLR scenarios and projected wetted area. MHW projection under (a) Current condition; (b) low SLR scenario (0.2 m); (c) intermediate-low SLR scenario (0.5 m); (d) intermediate-high SLR scenario (1.2 m); (e) high SLR scenario (2 m).

4.3.2 Biomass Density

Biomass density is a function of both topography and MHW and is herein categorized as low, medium, and high. The biomass density map for the current condition (Figure 4.4b) displays a biomass concentration in the lower part of the East Bay islands. The black boxes in the map (Figure 4.4a, Figure 4.4b) draw attention to areas of interest for comparison with satellite imagery (Medeiros et al., 2015). The three boxes qualitatively illustrate that our model reasonably captured the low, medium, and high productivity distributions in these key areas. The simulated categorized (low, medium, and high) biomass density (Figure 4.4b) was compared with the biomass density derived from satellite imagery over both the entire satellite imagery coverage area (Figure 4.4a, n = 61202 pixels) as well as over the highlighted areas (n = 6411 pixels). The confusion matrices for these two sets of predictions are shown in Table 4.1.

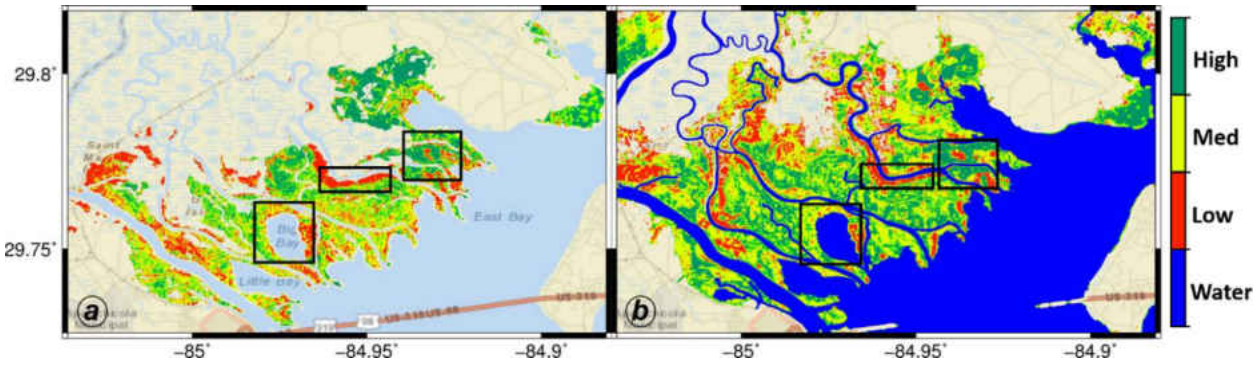

Figure 4.4: Biomass density maps focused on the wetland area in the islands between the Apalachicola River and the East Bay categorized into low, medium, and high productive regions represented by red, yellow, and green, respectively and blue shows the wet regions. (a) The IfSAR data (Medeiros et al., 2015) with black boxes highlights three selected regions for comparison; (b) Biomass density results under current conditions and the black boxes for comparison.

Table 4.1: Confusion Matrices for Biomass Density Predictions

	Entire Coverage Area			Highlighted Areas		
Predicted / True	**Low**	**Medium**	**High**	**Low**	**Medium**	**High**
Low	4359	7112	4789	970	779	576
Medium	1764	10331	7942	308	809	647
High	2129	8994	7266	396	728	1198

These confusion matrices indicate a true positive rate over the entire coverage area of 23.5%, 46.0%, and 35.9% for low, medium and high, respectively, and an overall weighted true positive rate of 35.9%. For comparison, a neutral model where the biomass category was assigned randomly (stratified to match the distribution of the true data derived from satellite imagery) produced true positive rates of 30.5%, 36.8% and 32.8% for low, medium and high, respectively, and an overall weighted true positive rate of 33.6%. For the highlighted areas, the true positive rates were 41.7%, 45.8%, 51.6% for low, medium and high, respectively, and an overall weighted true positive rate of 46.4%.

Temporal changes in the biomass density are demonstrated in the four columns (a), (b), (c), and (d) of Figure 4.5 for the years 2020, 2050, 2080, and 2100. The rows from top to bottom show biomass density results for the low, intermediate-low, intermediate-high, and high SLR scenarios, respectively. For the year 2020 (Figure 4.5a), under the low SLR scenario, the salt marsh productivity yields little , but for the other SLR scenarios the medium and low biomass density are getting more dominant, specifically in the intermediate-high and high SLR scenarios marsh lands were lost. In Figure 4.5b, the first row from top displays a higher productivity for the year 2050

under the low SLR scenario, whereas in the intermediate-high and high SLR (third and fourth column) the salt marsh is losing productivity and marsh lands were drowned. This trend continues in the year 2080 (Figure 4.5c). In the year 2100 (Figure 4.5d), as shown for the low SLR scenario (first row), the biomass density is more spatially uniform. Some salt marsh areas lost productivity whereas some areas with no productivity became productive, where the model captured marsh migration. Regions in the lower part of the islands between the Apalachicola River and East Bay shifted to more productive regions while most of the other marshes converted to medium productivity and some areas with no productivity near Lake Wimico became productive. Under the intermediate-low SLR scenario (second row of Figure 4.5d), the upper part of the islands became flooded and most of the salt marshes lost productivity while some migrated to higher lands. Salt marsh migration was more evident in the intermediate-high and high SLR scenarios (third and fourth row of Figure 4.5d). The productive band around the extended bay under higher scenarios implied the possibility for productive wetlands in those regions. It is shown in the intermediate-high and high SLR scenarios (third and fourth row) from 2020 to 2100 (column (a) to (d)) that the flooding direction started from regions of no productivity and extended to low productivity areas. Under higher SLR, the inundation stretched over the marsh platform until it was halted by the higher topography.

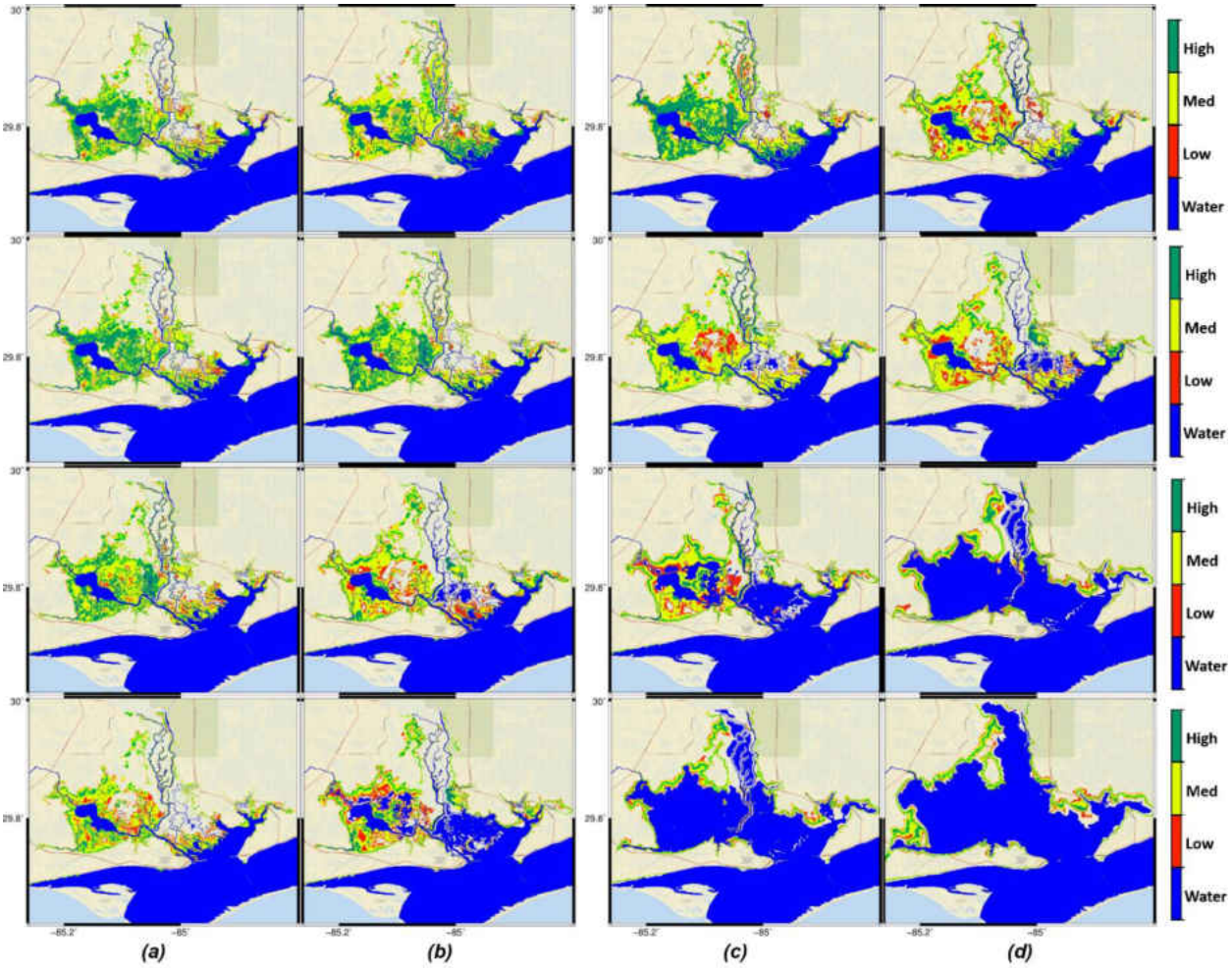

Figure 4.5: Temporal changes in biomass density under future SLR scenarios. Biomass density is categorized into low, medium, and high productive regions represented by red, yellow, and green, respectively and blue shows the wet regions. For column (a), (b), (c), and (d) shows biomass density for the years 2020, 2050, 2080, and 2100, respectively and the rows from top to bottom displays the results for the low (0.2 m), intermediate-low (0.5 m), intermediate-high (1.2 m), and high (2 m) SLR.

4.4 Discussion

The salt marsh response to SLR is dynamic and strongly depends on both MHW and geomorphology of the marsh system. The hydrodynamic results for the SLR scenarios are a function of the rate of SLR and its magnitude, the subsequent topographic changes resulting from marsh platform accretion, and the change in flow resistance induced by variations in biomass density. This was demonstrated in the low and intermediate-low SLR scenarios, where the water level varies in the creeks, in the marsh platform and where the flooding started from no marsh productivity regions (Figure 4.3b, Figure 4.3c). In the intermediate-high and high SLR scenarios, the overwhelming extent of inundation damped the impact of topography and flow resistance and the new hydrodynamic patterns were mostly dependent on SLR magnitude.

Using the adjusted marsh platform and river inflow forcing in the hydrodynamic simulations, the model results demonstrated good agreement with the remotely sensed data (Figure 4.4a, Figure 4.4b). If we focus on the three black boxes highlighted in the Figure 4.3a and Figure 4.3b, in the first box from left, the model predicted the topographically lower lands as having low productivity whereas the higher lands were predicted to have medium productivity. Some higher lands near the bank of the river (middle box in the Figure 4.4a) were correctly predicted as a low productivity (Figure 4.4b). The right box in Figure 4.4a also depicts areas of both high and mixed productivity patterns. The model also predicted the vast expanse of area with no productivity. Although the model prediction shows a qualitatively successful results, the quantitative results indicated that over the entire coverage area, slightly more than one third of the cells were correctly captured. This represents a slight performance increase over the neutral model, with weighted true

positive rates over the entire coverage area of 35.9% and 33.6% for the proposed model and the neutral model, respectively. However, the results from the highlighted areas indicated much better performance with 46.4% of the cells being correctly identified. This indicates the promise of the method to capture the biomass density distribution in key areas.

In both cases, as shown in Table 4.1, there is a noticeable pattern of difficulty in differentiating between medium and high classifications. This may be attributed to saturation in satellite imagery based coverage where at high levels of "greenness" and canopy height, the satellite imagery can no longer differentiate subtle differences in biomass density, especially at fine spatial resolutions. As such, the incorrectly classified cells are primarily located throughout the high resolution part of the model domain where the spacing is 15 m on average. This error may be mitigated by coarsening the resolution of the biomass density predictions using a spatial filter; predictions at this fine of a resolution are admittedly ambitious. This would reduce the "speckled" appearance of the predictions and likely lead to better results.

Another of the main error sources that decrease the prediction accuracy likely originate from the remotely sensed, experimental, and elevation data. The remotely sensed biomass density is primarily based on IfSAR and ASTER data which have inherent uncertainty (Andersen et al., 2005). In addition, the remotely sensed biomass density estimation was constrained to areas classified as Emergent Herbaceous Wetland (95) by the National Land Cover Dataset 2011. This explains the difference in coverage area and may have excluded areas where the accuracy of the proposed biomass density prediction model was better. Other errors are likely generated by the variability in planting, harvesting, and processing of biomass that is minimized, but unavoidable,

in any field experiment of this nature. These data were used to train the satellite imagery based biomass density prediction method and errors in their computation, while minimized by sample replication and outlier removal, may have propagated into the coverage used as the ground truth for comparison (Figure 4.4a). Another source of error occurs in the topography adjustment process in the marsh system. The true marsh topography is highly nonlinear and any adjustment algorithm cannot include all of the nonlinearities and microtopographic changes in the system. Considering all of these factors and the capability of the model to capture the low, medium, and high productive regions qualitatively as well as the difficulty to model the complicated processes within salt marsh systems, the Hydro-MEM model was successful in computing the marsh productivity. In order to improve the predictions and correctly identify additional regions with limited or no salt marsh productivity, future versions of the Hydro-MEM model will include salinity and additional geomorphology, such as shoreline accretion and erosion.

Lastly, investigating the temporal changes in biomass density helps to understand the interaction between the flow physics and biology used in the coupled Hydro-MEM model. In the year 2020 (Figure 4.5a), under the low (linear projected) SLR case, the accretion aids the marshes to maintain their position in the tidal frame, thus enabling them to remain productive. However, under higher SLR scenarios, the magnitude and rate of inundation prevented this adaptation and salt marshes began to lose their productivity. The sediment accretion rate in the SLR scenarios also affects the biomass density. The accretion and SLR rate associated with the low SLR scenario in the years 2050 and 2080 (first row from top in Figure 4.5b and Figure 4.5c) increased productivity. The higher water levels associated with the intermediate-low SLR scenario lowered marsh productivity and generated new impoundments in the upper islands between the Apalachicola River and East

Bay (second row of Figure 4.5b and Figure 4.5c). Under the intermediate-high and high SLR, the trend continued and salt marshes lost productivity, drowned or disappeared altogether. It also caused the disappearance or productivity loss and inundation of salt marshes in other parts near Lake Wimico.

The inundation direction under the intermediate-low SLR scenario began from regions of no productivity, extended over low productivity areas, and stopped at higher productivity regions due to an increased organic and inorganic accretion rates and larger bottom friction coefficients. Under intermediate-high and high SLR scenarios, the migration to higher lands was apparent in areas that have the topographic profile to be flooded regularly when sea-level rises and are adjacent to previously productive salt marshes.

In the year 2100 (Figure 4.5d), the accretion and SLR rate associated with the low SLR scenario increased productivity near East Bay and produced a more uniform salt marsh. The productivity loss near Lake Wimico is likely due to the increase in flood depth and duration. For the intermediate-high and high SLR scenarios, large swaths of salt marsh were converted to open water and some of the salt marshes in the upper elevation range migrated to higher lands. The area available for this migration was restricted to a thin band around the extended bay that had a topographic profile within the new tidal frame. If resource managers in the area were intent on providing additional area for future salt marsh migration, targeted regrading of upland area projected to be located near the future shoreline is a possible measure for achieving this.

4.5 Conclusions

The Hydro-MEM model was used to simulate the wetland response to four SLR scenarios in Apalachicola, Florida. The model coupled a two dimensional depth integrated hydrodynamic model and a parametric marsh model to capture the dynamic effect of SLR on salt marsh productivity. The parametric marsh model used empirical constants derived from experimental bio-assays installed in the Apalachicola marsh system over a two year period. The marsh platform topography used in the simulation was adjusted to remove the high elevation bias in the lidar-derived DEM. The average annual Apalachicola River flow rate was imposed as a boundary condition in the hydrodynamic model. The results for biomass density in the current condition were validated using remotely sensed-derived biomass density. The water levels and biomass density distributions for the four SLR scenarios demonstrated a range of responses with respect to both SLR magnitude and rate. The low and intermediate-low scenarios resulted in generally higher water levels with more extreme gradients in the rivers and creeks. In the intermediate-high and high SLR scenarios, the water level gradients were less pronounced due to the large extent of inundation (45 and 68 percent increase in inundated area). The biomass density in the low SLR scenario was relatively uniform and showed a productivity increase in some regions and a decrease in the others. In contrast, the higher SLR cases resulted in massive salt marsh loss (conversion to open water), productivity decreased and migration to areas newly within the optimal tidal frame. The inundation path generally began in areas of no productivity, proceeded through low productivity areas, and stopped when the local topography prevented further progress.

4.6 Future Considerations

One of the main factors in sediment transport and marsh geomorphology is velocity variation within tidal creeks. These velocities are dependent on many factors including water level, creek bathymetry, bank elevation, and marsh platform topography (Wang et al., 1999). The maximum tidal velocities for four transects, two in the distributaries flowing into the Bay in the islands between Apalachicola River and East Bay (T1 and T2), one in the main river (T3), and the fourth one in the tributary of the main river far from main marsh platform (T4) (Figure 4.1) were calculated.

The magnitude of the maximum tidal velocity generally increased with increasing sea level (Figure 4.6). The rate of increase in the creeks closer to the bay was higher due to reductions in bottom roughness caused by loss of biomass density. The magnitude of maximum velocity also increased as the creeks expanded. However, these trends leveled off under the intermediate-high and high SLR scenarios when the boundaries between the creeks and inundated marsh platform were less distinguishable. This trend progressed further under the high SLR scenario, where there was also an apparent decrease due to the bay extension effect.

Under SLR scenarios, the maximum flow velocity generally, but not uniformly, increased within the creeks. Transect 1 was chosen to show the marsh productivity variation effects in the velocity change. Here, the velocity increased with increasing sea level. However, under the intermediate-low and intermediate-high SLR scenarios, there were some periods of velocity decrease due to creation of new creeks and flooded areas. This effect was also seen in transect 2 for the intermediate-high and high SLR scenarios. Under the low SLR scenario in transect 2, a velocity

reduction period was generated in 2050 as shown in Figure 4.6. This period of velocity reduction is explained by the increase in roughness coefficient related to the higher biomass density in that region at that time. Transect 3, because of its location in the main river channel, was less affected by SLR induced variations on the marsh platform but still contained some variability due to the creation of new distributaries under the intermediate-high and high SLR scenarios. All of the curves for transect 3 show a slow decrease at the beginning of the time series indicating that tidal flow dominated in that section of the main river at that time. This is also evident in transect 4 located in a tributary of the Apalachicola River. The variations under intermediate-high and high SLR scenarios in transect 4 are mainly due to the new distributaries and flooded area. One exception to this is the last period of velocity reduction occurring as a result of the bay extension.

The creek velocities generally increased in the low and intermediate-low scenarios due to increased water level gradients, however there were periods of velocity decrease due to higher bottom friction values corresponding with increased biomass productivity in some regions. Under the intermediate-high and high scenarios, velocities generally decreased due to the majority of marshes being converted to open water and the massive increase in flow cross-sectional area associated with that. These changes will be considered in the future work of the model related with geomorphologic changes in the marsh system.

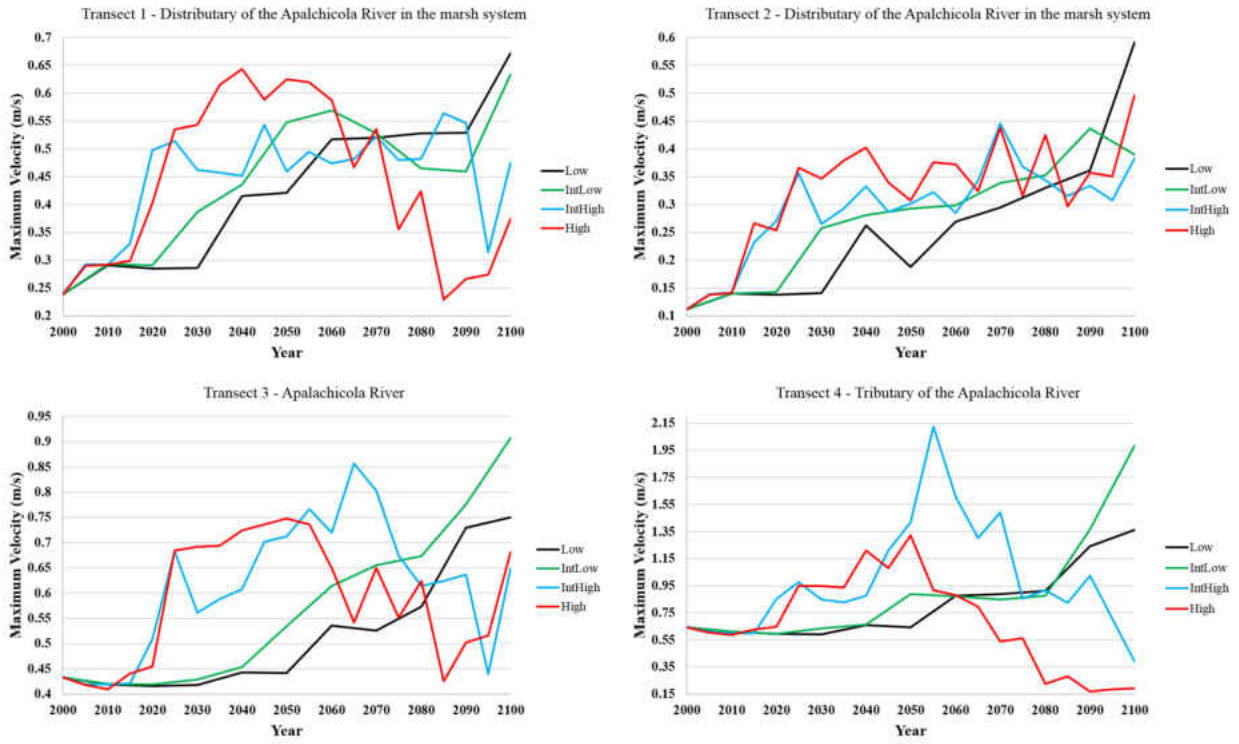

Figure 4.6: Maximum velocity variation with time under the low, intermediate-low, intermediate-high, and high SLR in four transects shown in Figure 4.1.

4.7 Acknowledgments

This research is partially funded under Award No. NA10NOS4780146 from the National Oceanic and Atmospheric Administration (NOAA) Center for Sponsored Coastal Ocean Research (CSCOR), and the Louisiana Sea Grant Laborde Chair. The computations for the hydrodynamic model simulations were performed using the STOKES Advanced Research Computing Center (ARCC) at University of Central Florida, the Extreme Science and Engineering Discovery Environment (XSEDE), and High Performance Computing at Louisiana State University (LSU)

and the Louisiana Optical Network Initiative (LONI). The authors would like to extend our thanks appreciation to ANERR staffs, especially Mrs. Jenna Harper for their continuous help and support. The statements and conclusions do not necessarily reflect the views of NOAA-CSCOR, Louisiana Sea Grant, STOKES ARCC, XSEDE, LSU, LONI, ANERR or their affiliates.

4.8 References

Alizad, K., Hagen, S. C., Morris, J. T., Bacopoulos, P., Bilskie, M. V., Weishampel, J. and Medeiros, S. C. (2016). "A coupled, two-dimensional hydrodynamic-marsh model with biological feedback." *Ecological Modeling* 327: 29-43.

Andersen, H.-E., Reutebuch, S. E. and McGaughey, R. J. (2005). "Accuracy of an IFSAR-derived digital terrain model under a conifer forest canopy." *Canadian Journal of Remote Sensing* 31(4): 283-288.

Arcement, G. J. and Schneider, V. R. (1989). Guide for selecting Manning's roughness coefficients for natural channels and flood plains, US Government Printing Office Washington, DC, USA.

Atkinson, J., McKee Smith, J. and Bender, C. (2013). "Sea-level rise effects on storm surge and nearshore waves on the Texas coast: Influence of landscape and storm characteristics." *Journal of Waterway, Port, Coastal, and Ocean Engineering* 139(2): 98-117.

Bakker, J. P., de Leeuw, J., Dijkema, K. S., Leendertse, P. C., Prins, H. H. T. and Rozema, J. (1993). "Salt marshes along the coast of The Netherlands." *Hydrobiologia* 265(1-3): 73-95.

Baustian, J. J., Mendelssohn, I. A. and Hester, M. W. (2012). "Vegetation's importance in regulating surface elevation in a coastal salt marsh facing elevated rates of sea level rise." *Global Change Biology* 18(11): 3377-3382.

Bilskie, M. V., Coggin, D., Hagen, S. C. and Medeiros, S. C. (2015). "Terrain-driven unstructured mesh development through semi-automatic vertical feature extraction." *Advances in Water Resources* 86, Part A: 102-118.

Bilskie, M. V. and Hagen, S. C. (2013). "Topographic accuracy assessment of bare earth lidar-derived unstructured meshes." *Advances in Water Resources* 52(0): 165-177.

Bilskie, M. V., Hagen, S. C., Alizad, K., Medeiros, S. C., Passeri, D. L., Needham, H. and Cox, A. (2016). "Dynamic simulation and numerical analysis of hurricane storm surge under sea level rise with geomorphologic changes along the northern Gulf of Mexico." *Earth's Future*: n/a-n/a.

Bilskie, M. V., Hagen, S. C., Medeiros, S. C., Cox, A. T., Salisbury, M. and Coggin, D. (2016). "Data and numerical analysis of astronomic tides, wind-waves, and hurricane storm surge across the northern Gulf of Mexico." *Geophysical Research*: In Revision.

Bilskie, M. V., Hagen, S. C., Medeiros, S. C. and Passeri, D. L. (2014). "Dynamics of sea level rise and coastal flooding on a changing landscape." *Geophysical Research Letters* 41(3): 927-934.

Carter, W., Shrestha, R., Tuell, G., Bloomquist, D. and Sartori, M. (2001). "Airborne laser swath mapping shines new light on Earth's topography." *Eos, Transactions American Geophysical Union* 82(46): 549-555.

Chassereau, J. E., Bell, J. M. and Torres, R. (2011). "A comparison of GPS and lidar salt marsh DEMs." *Earth Surface Processes and Landforms* 36(13): 1770-1775.

D' Alpaos, A., Lanzoni, S., Marani, M. and Rinaldo, A. (2007). "Landscape evolution in tidal embayments: Modeling the interplay of erosion, sedimentation, and vegetation dynamics." *Journal of Geophysical Research: Earth Surface* 112(F1): F01008.

Daiber, F. (1977). "Salt marsh animals: Distributions related to tidal flooding, salinity and vegetation." *Ecosystems of the world*.

Egbert, G. D., Bennett, A. F. and Foreman, M. G. G. (1994). "TOPEX/POSEIDON tides estimated using a global inverse model." *Journal of Geophysical Research: Oceans* 99(C12): 24821-24852.

Egbert, G. D. and Erofeeva, S. Y. (2002). "Efficient Inverse Modeling of Barotropic Ocean Tides." *Journal of Atmospheric and Oceanic Technology* 19(2): 183-204.

Elsey-Quirk, T., Seliskar, D., Sommerfield, C. and Gallagher, J. (2011). "Salt Marsh Carbon Pool Distribution in a Mid-Atlantic Lagoon, USA: Sea Level Rise Implications." *Wetlands* 31(1): 87-99.

Fagherazzi, S., Kirwan, M. L., Mudd, S. M., Guntenspergen, G. R., Temmerman, S., D'Alpaos, A., van de Koppel, J., Rybczyk, J. M., Reyes, E., Craft, C. and Clough, J. (2012). "Numerical models of salt marsh evolution: Ecological, geomorphic, and climatic factors." *Reviews of Geophysics* 50(1): RG1002.

FDEP (2013). "Apalachicola National Estuarine Research Reserve Management Plan, June 2013". Tallahassee, FL, Florida Department of Environmental Protection.

Florida Oceans and Coastal Council (2009). "The effects of climate change on Florida's ocean and coastal resources". A special report to the Florida Energy and Climate Commission and the people of Florida. Tallahassee, FL. **34**.

French, J. R. (2008). "Hydrodynamic Modelling of Estuarine Flood Defence Realignment as an Adaptive Management Response to Sea-Level Rise." *Journal of Coastal Research*: 1-12.

Hagen, S., Morris, J., Bacopoulos, P. and Weishampel, J. (2013). "Sea-Level Rise Impact on a Salt Marsh System of the Lower St. Johns River." *Journal of Waterway, Port, Coastal, and Ocean Engineering* 139(2): 118-125.

Hagen, S. C. and Bacopoulos, P. (2012). "Coastal Flooding in Florida's Big Bend Region with Application to Sea Level Rise Based on Synthetic Storms Analysis." *Terr. Atmos. Ocean. Sci.* 23: 481-500.

Hagen, S. C., Zundel, A. K. and Kojima, S. (2006). "Automatic, unstructured mesh generation for tidal calculations in a large domain." *International Journal of Computational Fluid Dynamics* 20(8): 593-608.

Halpin, P. M. (2000). "Habitat use by an intertidal salt-marsh fish: trade-offs between predation and growth." *Marine Ecology Progress Series* 198: 203-214.

Hearn, C. J. and Atkinson, M. J. (2001). "Effects of sea-level rise on the hydrodynamics of a coral reef lagoon: Kaneohe Bay, Hawaii." *Sea-level Changes and Their Effects*: 25.

Hicks, D. M., Duncan, M. J., Walsh, J. M., Westaway, R. M. and Lane, S. N. (2002). "New views of the morphodynamics of large braided rivers from high-resolution topographic surveys and time-lapse video." *IAHS PUBLICATION*: 373-380.

Hladik, C. and Alber, M. (2012). "Accuracy assessment and correction of a LIDAR-derived salt marsh digital elevation model." *Remote Sensing of Environment* 121(0): 224-235.

Homer, C., Huang, C., Yang, L., Wylie, B. and Coan, M. (2004). "Development of a 2001 national land-cover database for the United States." *Photogrammetric Engineering & Remote Sensing* 70(7): 829-840.

Hsing-Chung, C., Linlin, G., Rizos, C. and Milne, T. (2004). "Validation of DEMs derived from radar interferometry, airborne laser scanning and photogrammetry by using GPS-RTK." *Geoscience and Remote Sensing Symposium, 2004. IGARSS '04. Proceedings. 2004 IEEE International*.

Isphording, W. C. (1985). "Sedimentological Investigation of the Apalachicola Bay, Florida Estuarine System: prepared for the Mobile District, Corps of Engineers", University of Alabama.

James, T. D., Barr, S. L. and Lane, S. N. (2006). "Automated correction of surface obstruction errors in digital surface models using off-the-shelf image processing." *The Photogrammetric Record* 21(116): 373-397.

Kirwan, M. L. and Murray, A. B. (2007). "A coupled geomorphic and ecological model of tidal marsh evolution." *Proceedings of the National Academy of Sciences* 104(15): 6118-6122.

Kraus, K. and Pfeifer, N. (1998). "Determination of terrain models in wooded areas with airborne laser scanner data." *ISPRS Journal of Photogrammetry and Remote Sensing* 53(4): 193-203.

Lane, S. N. (2000). "The Measurement of River Channel Morphology Using Digital Photogrammetry." *The Photogrammetric Record* 16(96): 937-961.

Leorri, E., Mulligan, R., Mallinson, D. and Cearreta, A. (2011). "Sea-level rise and local tidal range changes in coastal embayments: An added complexity in developing reliable sea-level index points." *Journal of Integrated Coastal Zone Management* 11: 307-314.

Liu, S. K. (1997). "Using coastal models to estimate effects of sea level rise." *Ocean & Coastal Management* 37(1): 85-94.

Livingston, R. J. (1984). "The ecology of the Apalachicola Bay system: an estuarine profile", U.S. Fish and Wildlife Service.

Medeiros, S., Hagen, S., Weishampel, J. and Angelo, J. (2015). "Adjusting Lidar-Derived Digital Terrain Models in Coastal Marshes Based on Estimated Aboveground Biomass Density." *Remote Sensing* 7(4): 3507.

Medeiros, S. C. (2012). "Incorporating Remotely Sensed Data Into Coastal Hydrodynamic Models: Parameterization of Surface Roughness and Spatio-temporal Validation of Inundated Area", University of Central Florida Orlando, Florida.

Medeiros, S. C., Ali, T., Hagen, S. C. and Raiford, J. P. (2011). "Development of a Seamless Topographic / Bathymetric Digital Terrain Model for Tampa Bay, Florida." *Photogrammetric Engineering & Remote Sensing* 77(12): 1249-1256.

Medeiros, S. C. and Hagen, S. C. (2013). "Review of wetting and drying algorithms for numerical tidal flow models." *International Journal for Numerical Methods in Fluids* 71(4): 473-487.
Medeiros, S. C., Hagen, S. C. and Weishampel, J. F. (2012). "Comparison of floodplain surface roughness parameters derived from land cover data and field measurements." *Journal of Hydrology* 452–453: 139-149.
Moller, I., Kudella, M., Rupprecht, F., Spencer, T., Paul, M., van Wesenbeeck, B. K., Wolters, G., Jensen, K., Bouma, T. J., Miranda-Lange, M. and Schimmels, S. (2014). "Wave attenuation over coastal salt marshes under storm surge conditions." *Nature Geosci* 7(10): 727-731.
Montane, J. M. and Torres, R. (2006). "Accuracy assessment of LIDAR saltmarsh topographic data using RTK GPS." *Photogrammetric Engineering & Remote Sensing* 72(8): 961-967.
Morris, J. (2007). "Ecological engineering in intertidial saltmarshes." *Hydrobiologia* 577(1): 161-168.
Morris, J. T., Sundareshwar, P. V., Nietch, C. T., Kjerfve, B. and Cahoon, D. R. (2002). "Responses of coastal wetlands to rising sea level." *Ecology* 83(10): 2869-2877.
Morris, J. T., Sundberg, K. and Hopkinson, C. S. (2013). "Salt marsh primary production and its responses to relative sea level and nutrients in estuaries at Plum Island, Massachusetts, and North Inlet, South Carolina, USA." *Oceanography* 26(3): 78-84.
Mortazavi, B., Iverson, R. L., Huang, W., Lewis, F. G. and Caffrey, J. M. (2000). "Nitrogen budget of Apalachicola Bay, a bar-built estuary in the northeastern Gulf of Mexico." *Marine Ecology Progress Series* 195: 1-14.
Nicholls, R. J. (2004). "Coastal flooding and wetland loss in the 21st century: changes under the SRES climate and socio-economic scenarios." *Global Environmental Change* 14(1): 69-86.
Nicholls, R. J., Hoozemans, F. M. J. and Marchand, M. (1999). "Increasing flood risk and wetland losses due to global sea-level rise: regional and global analyses." *Global Environmental Change* 9, Supplement 1(0): S69-S87.
Nichols, M. M. (1989). "Sediment accumulation rates and relative sea-level rise in lagoons." *Marine Geology* 88(3–4): 201-219.
Nyman, J. A., Walters, R. J., Delaune, R. D. and Patrick Jr, W. H. (2006). "Marsh vertical accretion via vegetative growth." *Estuarine, Coastal and Shelf Science* 69(3–4): 370-380.
Parris, A., Bromirski, P., Burkett, V., Cayan, D., Culver, M., Hall, J., Horton, R., Knuuti, K., Moss, R., Obeysekera, J., Sallenger, A. and Weiss, J. (2012). "Global Sea Level Rise Scenarios for the US National Climate Assessment." *NOAA Tech Memo OAR CPO*: 1-37.
Passeri, D. L., Hagen, S. C., Medeiros, S. C., Bilskie, M. V., Alizad, K. and Wang, D. (2015). "The dynamic effects of sea level rise on low gradient coastal landscapes: a review." *Earth's Future*: n/a-n/a.
Passeri, D. L., Hagen, S. C., Plant, N., Bilskie, M. V., Medeiros, S. C. and Alizad, K. (2016). "Tidal Hydrodynamics under Future Sea Level Rise and Coastal Morphology in the Northern Gulf of Mexico." *Earth's Future*: n/a-n/a.
Pennings, S. C. and Bertness, M. D. (2001). "Salt marsh communities." *Marine community ecology*: 289-316.
Reed, D. J. (1995). "The response of coastal marshes to sea-level rise: Survival or submergence?" *Earth Surface Processes and Landforms* 20(1): 39-48.

Sithole, G. and Vosselman, G. (2004). "Experimental comparison of filter algorithms for bare-Earth extraction from airborne laser scanning point clouds." *ISPRS Journal of Photogrammetry and Remote Sensing* 59(1–2): 85-101.

Temmerman, S., Bouma, T. J., Van de Koppel, J., Van der Wal, D., De Vries, M. B. and Herman, P. M. J. (2007). "Vegetation causes channel erosion in a tidal landscape." *Geology* 35(7): 631-634.

Turner, R. E., Swenson, E. M. and Milan, C. S. (2000). Organic and inorganic contributions to vertical accretion in salt marsh sediments. Concepts and Controversies in Tidal Marsh Ecology. M. Weinstein and D. Kreeger, Springer Netherlands**:** 583-595.

Valentim, J. M., Vaz, L., Vaz, N., Silva, H., Duarte, B., Cacador, I. and Dias, J. (2013). "Sea level rise impact in residual circulation in Tagus estuary and Ria de Aveiro lagoon." *Journal of Coastal Research* Special Issue No. 65: 1981-1986.

Vosselman, G. (2000). "Slope based filtering of laser altimetry data." *International Archives of Photogrammetry and Remote Sensing* 33(B3/2; PART 3): 935-942.

Wang, C., Menenti, M., Stoll, M. P., Feola, A., Belluco, E. and Marani, M. (2009). "Separation of Ground and Low Vegetation Signatures in LiDAR Measurements of Salt-Marsh Environments." *Geoscience and Remote Sensing, IEEE Transactions on* 47(7): 2014-2023.

Wang, Y. P., Renshun, Z. and Shu, G. (1999). "Velocity Variations in Salt Marsh Creeks, Jiangsu, China." *Journal of Coastal Research* 15(2): 471-477.

Warren, R. S. and Niering, W. A. (1993). "Vegetation change on a northeast tidal marsh: Interaction of sea-level rise and marsh accretion." *Ecology* 74(1): 96-103.

Wolanski, E. and Chappell, J. (1996). "The response of tropical Australian estuaries to a sea level rise." *Journal of Marine Systems* 7(2–4): 267-279.

Yang, S. L., Li, H., Ysebaert, T., Bouma, T. J., Zhang, W. X., Wang, Y. Y., Li, P., Li, M. and Ding, P. X. (2008). "Spatial and temporal variations in sediment grain size in tidal wetlands, Yangtze Delta: On the role of physical and biotic controls." *Estuarine, Coastal and Shelf Science* 77(4): 657-671.

CHAPTER 5. APPLICATION OF THE MODEL IN MARINE AND MIXED ESTUARINE SYSTEMS

The content in this chapter is under preparation to submit as: Alizad, K., Hagen, S.C., Morris, J. T., Medeiros, S.C. 2016. Salt Marsh System Response to Seal Level Rise in a Marine and Mixed Estuarine Systems.

5.1 Introduction

Salt marshes in the Northern Gulf of Mexico (NGOM) are some of the most vulnerable to sea level rise (SLR) in the United States (Turner, 1997; Nicholls et al., 1999; Thieler and Hammer-Klose, 1999). These estuaries are dependent on hydrodynamic influences that are unique to each individual system (Townend and Pethick, 2002; Rilo et al., 2013). The vulnerability to SLR is mainly due to the microtidal nature of the NGOM and lack of sufficient sediment (Day et al., 1995). Since the estuarine systems respond to SLR by accumulating or releasing sediments according to local conditions (Friedrichs et al., 1990), it is critical to study the response of different estuarine systems, assessed by salt marsh productivity, accounting for their unique topography and hydrodynamic variations. These assessments can aid coastal managers to choose effective restoration planning pathways (Broome et al., 1988).

In order to assess salt marsh response to SLR, it is important to use marsh models that capture as many of the processes and interactions between the salt marsh and local hydrodynamics as possible. Several integrated models has been developed and applied in different regions to study SLR impact on wetlands (D' Alpaos et al., 2007; Kirwan and Murray, 2007; Hagen et al., 2013; Alizad et al., 2016). In addition, SLR can effectively change the hydrodynamics in estuaries (Wolanski and Chappell, 1996; Hearn and Atkinson, 2001; Leorri et al., 2011), which are

inherently dynamic due to the characteristics of the systems (Passeri et al., 2014) and need to be considered in the marsh model time progression. The Hydro-MEM model (Alizad et al., 2016) was developed to capture the dynamics of SLR (Passeri et al., 2015) by coupling hydrodynamic and parametric marsh models. Hydro-MEM incorporates the rate of SLR using a time stepping framework and also includes the complex interaction between the marsh and its hydrodynamics by adjusting the platform elevation and friction parameters in response to the conditions at each coupling time step (Alizad et al., 2016). The Hydro-MEM model requires an accurate topographic elevation map (Medeiros et al., 2015), Marsh Equilibrium Model (MEM) experimental parameters (Morris et al., 2002), SLR rate projection from National Oceanic and Atmospheric Administration (NOAA) (Parris et al., 2012), initial spatially distributed bottom friction parameters (Manning's *n*) from the National Land-Cover Database 2001 (NLCD 2001) (Homer et al., 2004), and a high resolution hydrodynamic model (Alizad et al., 2016). The objective of this study is to investigate the potential changes in wetland productivity and the response to SLR in two unique estuarine systems (one marine and one tributary) that are located in the same region (northern Gulf of Mexico).

Grand Bay, AL and Weeks Bay, MS estuaries are categorized as marine dominated and tributary estuaries, respectively. Grand Bay is one of the last remaining major coastal systems in Mississippi, located at the border with Alabama (Figure 5.1) and consisting of several shallow bays (0.5 m to 3 m deep in Point aux Chenes Bay) and barrier islands that are low in elevation but effective in damping wave energy (O'Sullivan and Criss, 1998; Peterson et al., 2007; Morton, 2008). The salt marsh system covers 49% of the estuary and is dominated by *Spartina alterniflora* and *Juncus romerianus*. The marsh serves as the nursery and habitat for commercial species such

as shrimp, crabs, and oysters (Eleuterius and Criss, 1991; Peterson et al., 2007). Historically, this marsh system has been prone to erosion and loss of productivity under SLR (Resources, 1999; Clough and Polaczyk, 2011). The main processes that facilitate the erosion are (1) the Escatawpa River diversion in 1848, which was the estuary's main sediment source and (2) the Dauphin Island breaching caused by a hurricane in the late 1700s that allowed the propagation of larger waves and tidal flows from the Gulf of Mexico (Otvos, 1979; Eleuterius and Criss, 1991; Morton, 2008). In addition, when the water level is low, the waves break along the marsh platform edge; this erodes the marsh platform and breaks off large chunks of the marsh edge. When the water level is high, the waves break on top of the marsh platform and can cause undermining of the marsh; this can open narrow channels that dissect the marsh (Eleuterius and Criss, 1991).

The Weeks Bay estuary, located along the eastern shore of Mobile Bay in Baldwin County, AL is categorized as a tributary estuary (Figure 5.1). Weeks Bay provides bottomland hardwood followed by intertidal salt marsh habitats for mobile animals and nurseries for commercially fished species such as shrimp, blue crab, shellfish, bay anchovy and others. Fishing and harvesting is restricted in Weeks Bay; however, adult species are allowed to be commercially harvested in Mobile Bay, after they emerge from Weeks Bay (Miller-Way et al., 1996). This estuary is mainly affected by the fresh water inflow from the Magnolia River (25%), the Fish River (73%), and some smaller channels (2%) with a combined annual average discharge of 5 cubic meters per second (Lu et al., 1992) , as well as Mobile Bay, which is the estuary's coastal ocean salt source. Sediment is transported to the bay by Fish River during winter and spring as a result of overland flow from rainfall events but this process is limited during summer and fall when the discharge is typically low (Miller-Way et al., 1996). Three dominant marsh species are *J. romerianus* and *S. alterniflora*

in the higher salinity regions near the mouth of the bay, and *Spartina cynosuroides* in the brackish region at the head of the bay. In the calm waters near the sheltered shorelines, submerged aquatic vegetation (SAV) is dominant. The future of the reserve is threatened by recent urbanization, which is the most significant change in the Weeks Bay watershed (Weeks Bay National Estuarine Research Reserve, 2007). Also, as a result of SLR already occurring, some marsh areas have converted to open water and others have been replaced by forest (Shirley and Battaglia, 2006).

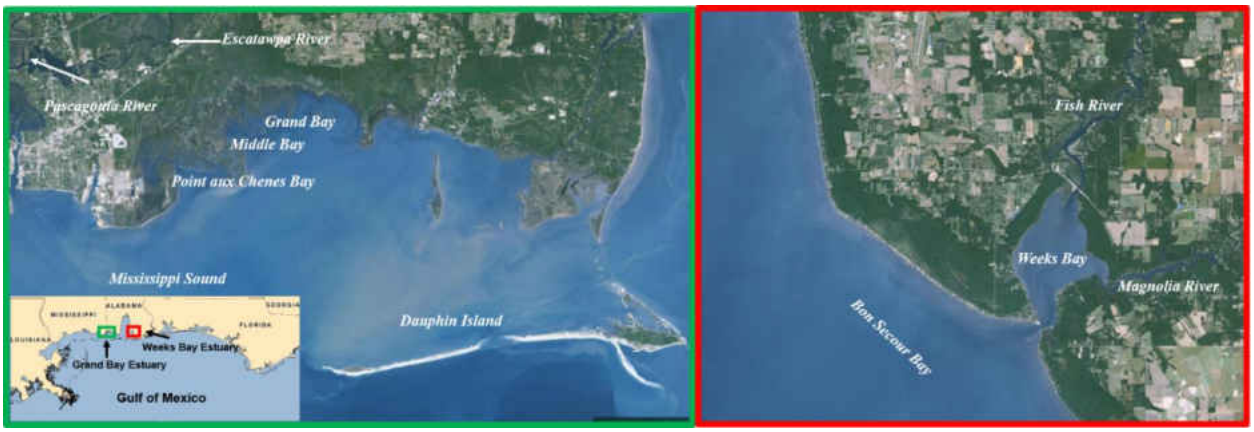

Figure 5.1: Study area and location of the Grand Bay estuary (left) and Weeks Bay estuary (right)

5.2 Methods

Wetland response to SLR was assessed using the integrated Hydro-MEM model comprised of coupled hydrodynamic and marsh models. This model was developed to include the interconnection between physics and biology in marsh systems by applying feedback processes in a time stepping framework. The time step approach helped to capture the rate of SLR by incorporating the two-way feedback between the salt marsh system (vegetation and topography)

and hydrodynamics after each time step. Additionally, the model implemented the dynamics of SLR by applying a hydrodynamic model that provided input for the parametric marsh model (MEM) in the form of tidal parameters. The elevation and Manning's *n* were updated using the biomass density and accretion results from the MEM and then input into the hydrodynamic model. Once the model reached the target time, the simulation stopped and generated results (Alizad et al., 2016).

The hydrodynamic model component of Hydro-MEM model was the two-dimensional, depth-integrated ADvanced CIRCulation (ADCIRC) model that solves the shallow water equations over an unstructured finite element mesh (Luettich and Westerink, 2004; Luettich and Westerink, 2006). The developed unstructured two-dimensional mesh consisted of 15 m elements, on average, in the marsh regions both in the Grand Bay and Weeks Bay estuaries and manually digitized rivers, creeks, and intertidal zones. This new high resolution mesh for Grand Bay and Weeks Bay estuaries was fused to an existing mesh developed by Hagen et al. (2006) in the Western North Atlantic Tidal (WNAT) model domain that spans from the 60 degree west meridian through the Atlantic Ocean, Gulf of Mexico, and Caribbean Sea and includes 1,095,214 nodes. This new combined mesh was developed with consideration of numerical stability in cyclical floodplain wetting (Medeiros and Hagen, 2013) and the techniques to capture tidal flow variations within the marsh system (Alizad et al., 2016).

The most important inputs to the model consisted of topography, Manning's *n*, and initial water level (with SLR) and the model was forced by tides and river inflow. The elevation was interpolated onto the mesh using an existing digital elevation model (DEM) developed by Bilskie

et al. (2015) incorporating the necessary adjustment to the marsh platform (Alizad et al., 2016) due to the high bias of the lidar derived elevations in salt marshes (Medeiros et al., 2015). Since this marsh is biologically similar to Apalachicola, FL (*J. romerianus* dominated, *Spartina* fringes, and similar above-ground biomass density), the adjustment for most of the marsh platform was 42 cm except for the high productivity regions where the adjustment was 65 cm as suggested by Medeiros et al. (2015). Additionally, the initial values for Manning's *n* were derived using the NLCD 2001 (Homer et al., 2004) along with *in situ* observations (Arcement and Schneider, 1989) and was updated based on the biomass density level of low, medium, and high or reclassified as open water (Medeiros et al., 2012; Alizad et al., 2016). The initial water level input, including SLR, to Hydro-MEM model input was derived from the NOAA report data that categorized them as low (0.2), intermediate-low (0.5 m), intermediate-high (1.2 m) and high (2.0 m) calculated using different climate change projections and observed data (Parris et al., 2012). Since the coupling time step for low and intermediate-low scenarios was 10 years and for the intermediate-high and high cases was 5 years (Alizad et al., 2016), the SLR at each time step varied based on the SLR projection data (Alizad et al., 2016). In addition, the hydrodynamic model was forced by seven principal harmonic tidal constituents (M_2, S_2, N_2, K_1, O_1, K_2, and Q_1) along the open ocean boundary at the 60 degree west meridian and river inflow at the Fish River and Magnolia River boundaries. No flow boundary conditions were applied along the coastline. The river discharge boundary conditions were calculated as the mean discharge from 44 years of record for the Fish River (http://waterdata.usgs.gov/usa/nwis/uv?site_no=02378500) and 15 years of record for Magnolia River (http://waterdata.usgs.gov/nwis/uv?site_no=02378300) and as of February 2016 were 3.18 and 1.11 cubic meters per second, respectively. The hydrodynamic model forcings were

ramped by two hyperbolic tangential functions: one for the tidal constituents and the other for river inflows. To capture the nonlinearities and dynamic effects induced by geometry and topography, the output of the model in the form of harmonic tidal constituents were resynthesized and analyzed to produce Mean High Water (MHW) in the rivers, creeks and marsh system. This model has been applied in previous studies and extensively validated (Bilskie et al., 2016; Passeri et al., 2016).

The MEM component of the model used MHW and topography as well as experimental parameters to derive a parabolic curve used to calculate biomass density at each computational node. The parabolic curve used a relative depth (D) defined by subtracting the topographic elevation of each point from the computed MHW elevation. The parabolic curve determined biomass density as a function of this relative depth (Morris et al., 2002) as follows:

$$B = aD + bD^2 + c \tag{5.1}$$

where a, b, and c were unique, experimentally derived parameters for each estuary. In this study, the parameters were obtained from field bio-assay experiments (Alizad et al., 2016) in both Grand Bay and Weeks Bay. These curves are typically divided into sub-optimal and super-optimal branches that meet at the parabola maximum point. The left and right parameters for Grand Bay were a_l = 32 g.m^{-3}.yr^{-1}, b_l = -3.2 g.m^{-4}.yr^{-1}, c_l =1920 g.m^{-2}.yr^{-1}, and a_r = 6.61 g.m^{-3}.yr^{-1}, b_r = -0.661 g.m^{-4}.yr^{-1}, c_r =1983 g.m^{-2}.yr^{-1}, respectively. The biomass density curve for Weeks Bay was defined using the parameters a = 73.8 g.m^{-3}.yr^{-1}, b = -1.14 g.m^{-4}.yr^{-1}, c =1587.1 g.m^{-2}.yr^{-1}. Additionally, the MEM element of the model calculated the organic and inorganic accretion rates on the marsh platform using an accretion rate formula incorporating the parameters for inorganic sediment load

(q) and organic and inorganic accumulation generated by decomposing vegetation (k) (Morris et al., 2002) as follows:

$$\frac{dY}{dt} = (q + kB)D \qquad \text{for} \qquad D>0 \tag{5.2}$$

Based on this equation, salt marsh platform accretion depended on the productivity of the marsh, the amount of sediment and the water level during the high tide. It also depended on the coupling time step (dt) that updated elevation and bottom friction inputs in the hydrodynamic model.

5.3 Results

The hydrodynamic results in both estuaries showed little variation in MHW within the bays and slight changes within the creeks (first row of Figure 5.2a) in the current condition. The MHW in the current condition has a 2 cm difference between Bon Secour Bay and Weeks Bay (first row of Figure 5.2b). Under the low SLR scenario for the year 2100, the maps implied higher MHW levels close to the SLR amount (0.2 m) with lower variation in the creeks in both Grand Bay and Weeks Bay (second row of Figure 5.2a and Figure 5.2b). The MHW in the intermediate-low SLR scenario also increased by an amount close to SLR (0.5 m) but with creation of new creeks and flooded marsh platform in Grand Bay (third row of Figure 5.2a). However, the amount of flooded area in Weeks Bay is much less (0.1 percent) than Grand Bay (1.3 percent). Under higher SLR scenarios, the bay extended over marsh platform in Grand Bay and under high SLR scenario, the bay connected to the Escatawpa River over highway 90 (fourth and fifth rows of Figure 5.2a) and the wetted area increased by 25 and 45 percent under intermediate high and high SLR (Table 5.1). The

flooded area in the Weeks Bay estuary was much less (5.8 and 14 percent for intermediate-high and high SLR) with some variation in the Fish River (fourth and fifth rows of Figure 5.2b).

Biomass density results showed a large marsh area in Grand Bay and small patches of marsh lands in Weeks Bay (first row of Figure 5.3a and Figure 5.3b). Under low SLR scenario for the year 2100, biomass density results demonstrated a higher productivity with an extension of the marsh platform in Grand Bay (second row of Figure 5.3a), but only a slight increase in marsh productivity in Weeks Bay with some marsh migration near Bon Secour Bay (second row of Figure 5.3b). Under the intermediate-low SLR, salt marshes in the Grand Bay estuary lost productivity and parts of them were drowned by the year 2100 (third row of Figure 5.3a). In contrast, Weeks Bay showed more productivity and the marsh lands both in the upper part of the Weeks Bay and close to Bon Secour Bay were extended (third row of Figure 5.3b). Under intermediate-high and high SLR, both estuaries demonstrated marsh migration to higher lands and a new marsh land was created near Bon Secour Bay under high SLR (fifth row of Figure 5.3b).

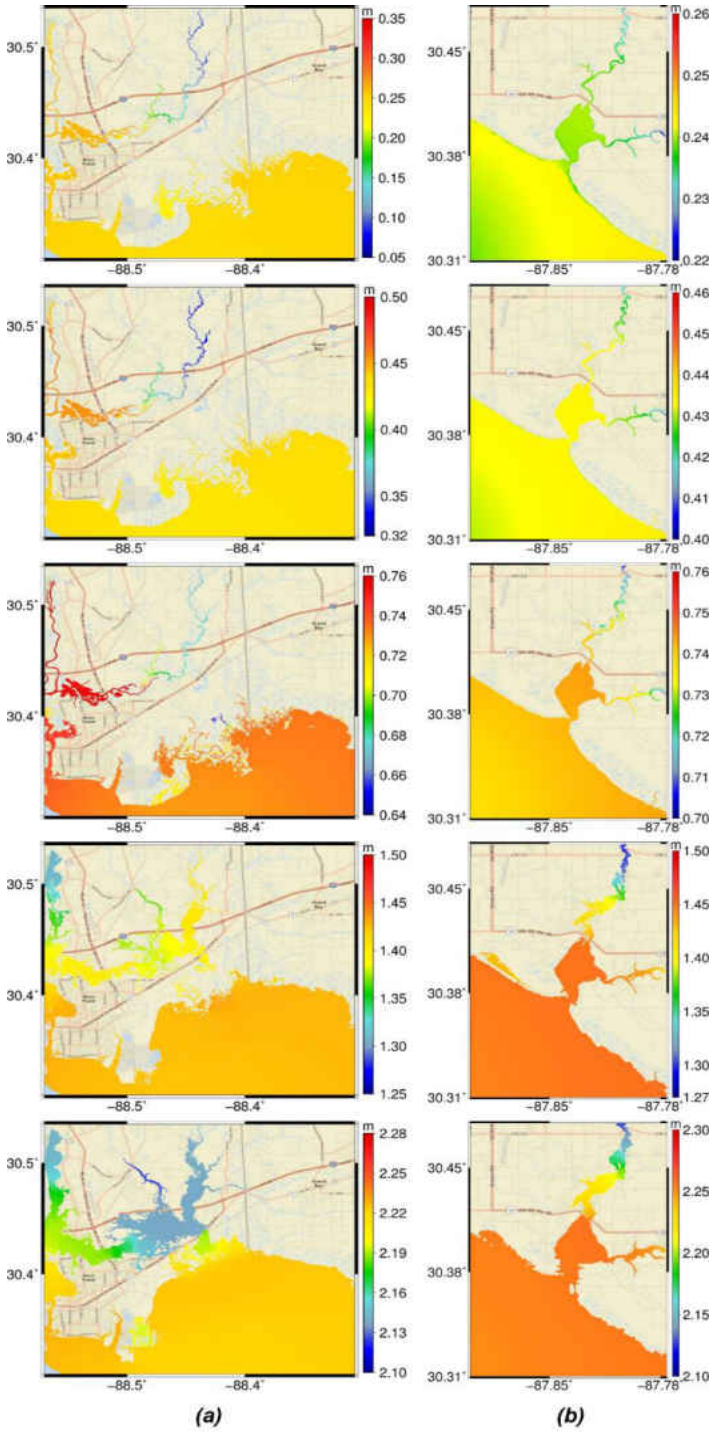

Figure 5.2: MHW results for (a) Grand Bay and (b) Weeks Bay. The rows from top to bottom are for the current sea level, and the Low (0.2 m), intermediate-low (0.5 m), intermediate-high (1.2 m), high (2 m) SLR for the year 2100.

Table 5.1: The wetted area in the Grand Bay and Weeks Bay estuaries under different SLR scenarios.

Grand Bay

Scenario	Inundated Area (km^2)	Percent Increase from Current Condition
Current	316	-
Low	316	0
Intermediate-Low	320	1.3
Intermediate-High	397	25.7
High	446	41.1

Weeks Bay

Scenario	Inundated Area (km^2)	Percent Increase from Current Condition
Current	133	-
Low	133	0
Intermediate-Low	133	0.1
Intermediate-High	141	5.8
High	152	14.0

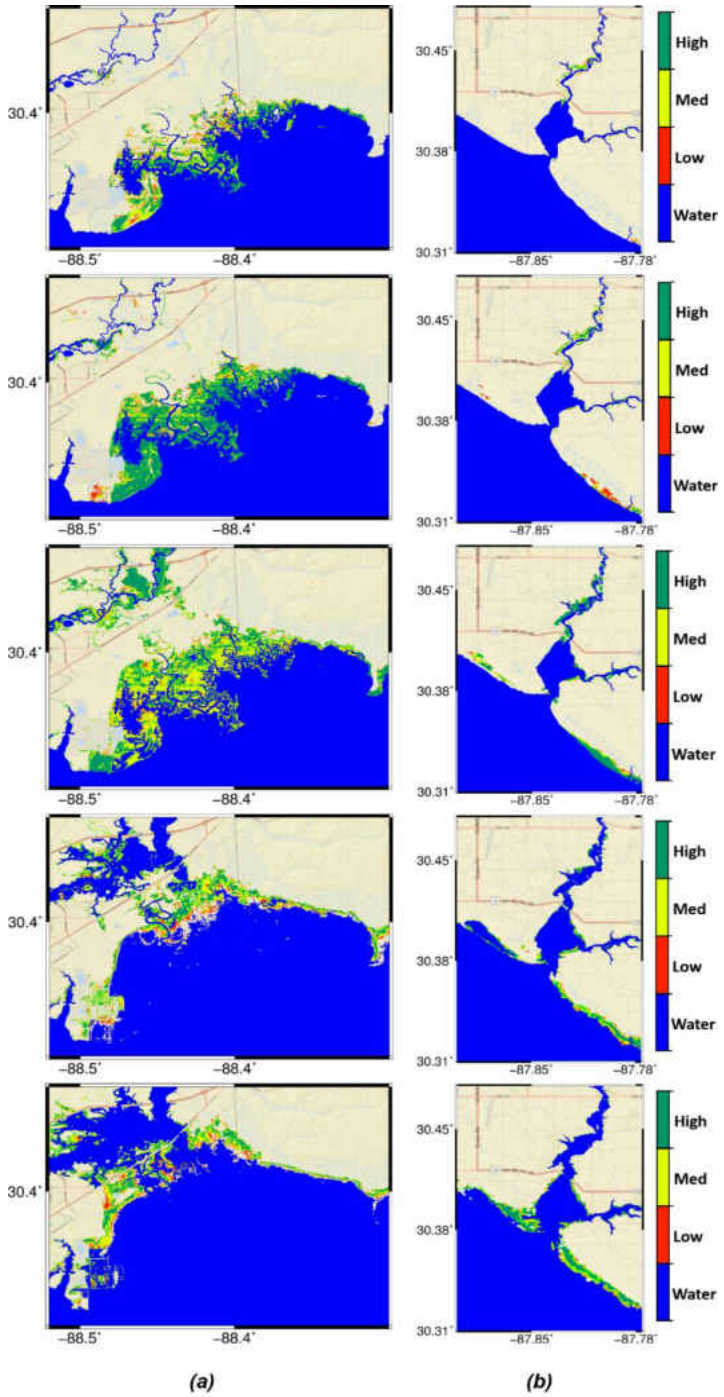

Figure 5.3: Biomass density results categorized into low, medium, and high productive regions represented by red, yellow, and green, respectively for (a) Grand Bay and (b) Weeks Bay. The rows from top to bottom are for the current sea level, and the Low (0.2 m), intermediate-low (0.5 m), intermediate-high (1.2 m), high (2 m) SLR for the year 2100.

5.4 Discussion

The current condition maps for MHW illustrates one of the primary differences between the Grand Bay and Weeks Bay in terms of their vulnerability to SLR. The MHW within Grand Bay, along with the minor changes in the creeks, demonstrated its exposure to tidal flows, whereas the more distinct MHW change between Bon Secour Bay and Weeks Bay illustrated how the narrow inlet of the bay can dampen currents, waves, and storm surge. The tidal flow in Weeks Bay dominates the river inflow while the bay receives sediments from the watershed during the extreme events. The amount of flooded area under high SLR scenarios demonstrates the role of the bay inlet and topography of the Weeks Bay estuary in protecting it from inundation.

MHW significantly impacts the biomass density results in both the Grand Bay and Weeks Bay estuaries. Under the low SLR scenario, the accretion on the marsh platform in Grand Bay established an equilibrium with the increased sea level and produced a higher productivity marsh. This scenario did not appreciably change the marsh productivity in Weeks Bay but did cause some marsh migration near Bon Secour Bay, where some inundation occurred.

Under the intermediate-low SLR scenario, higher water levels were able to inundate the higher lands in Weeks Bay and produce new marshes with high productivity there as well as in the regions close to Bon Secour Bay. Grand Bay began losing productivity under this scenario and some marshes, especially those directly exposed to the bay, were drowned.

In Grand Bay, salt marshes migrated to higher lands under the intermediate-high and high SLR scenarios and all of the current marsh platform became open water and created an extended bay

that connected to the Escatawpa River under the high SLR scenario. The Weeks Bay inlet became wider and allowed more inundation under these scenarios and created new marsh lands between Weeks Bay and Bon Secour Bay.

5.5 Conclusions

Weeks Bay inlet offers some protection from SLR, enhanced by the higher topo that allows for marsh migration and new marsh creation.

Grand Bay is much more exposed to SLR and therefore less resilient. Historic events have combined to both remove its sediment supply and expose it to tide and wave forces. It's generally low topography facilitates conversion to open water, rather than marsh migration, at higher SLR rates.

5.6 References

Alizad, K., Hagen, S. C., Morris, J. T., Bacopoulos, P., Bilskie, M. V., Weishampel, J. and Medeiros, S. C. (2016). "A coupled, two-dimensional hydrodynamic-marsh model with biological feedback." *Ecological Modeling* 327: 29-43.

Alizad, K., Hagen, S. C., Morris, J. T., Medeiros, S. C. and Bilskie, M. V. (2016). "Coastal wetland response to sea level rise in a fluvial estuarine system." *Earth's Future*.

Arcement, G. J. and Schneider, V. R. (1989). Guide for selecting Manning's roughness coefficients for natural channels and flood plains, US Government Printing Office Washington, DC, USA.

Bilskie, M. V., Coggin, D., Hagen, S. C. and Medeiros, S. C. (2015). "Terrain-driven unstructured mesh development through semi-automatic vertical feature extraction." *Advances in Water Resources* 86, Part A: 102-118.

Bilskie, M. V., Hagen, S. C., Medeiros, S. C., Cox, A. T., Salisbury, M. and Coggin, D. (2016). "Data and numerical analysis of astronomic tides, wind-waves, and hurricane storm surge across the northern Gulf of Mexico." *Geophysical Research*: In Revision.

Broome, S. W., Seneca, E. D. and Woodhouse Jr, W. W. (1988). "Tidal salt marsh restoration." *Aquatic Botany* 32(1–2): 1-22.

Clough, J. S. and Polaczyk, A. (2011). "SLAMM Analysis of Grand Bay NERR and Environs. A report prepared for The Nature Conservancy". Waitsfield, VT.

D' Alpaos, A., Lanzoni, S., Marani, M. and Rinaldo, A. (2007). "Landscape evolution in tidal embayments: Modeling the interplay of erosion, sedimentation, and vegetation dynamics." *Journal of Geophysical Research: Earth Surface* 112(F1): F01008.

Day, J., Pont, D., Hensel, P. and Ibañez, C. (1995). "Impacts of sea-level rise on deltas in the Gulf of Mexico and the Mediterranean: The importance of pulsing events to sustainability." *Estuaries* 18(4): 636-647.

Eleuterius, C. K. and Criss, G. A. (1991). "Point aux Chenes: Past, Present, and Future Persepctive of Erosion". Ocean Springs, Mississippi, Physical Oceanography Section Gulf Coast Research Laboratory

Friedrichs, C., Aubrey, D. and Speer, P. (1990). Impacts of Relative Sea-level Rise on Evolution of Shallow Estuaries. Residual Currents and Long-term Transport. R. T. Cheng, Springer New York. **38:** 105-122.

Hagen, S., Morris, J., Bacopoulos, P. and Weishampel, J. (2013). "Sea-Level Rise Impact on a Salt Marsh System of the Lower St. Johns River." *Journal of Waterway, Port, Coastal, and Ocean Engineering* 139(2): 118-125.

Hagen, S. C., Zundel, A. K. and Kojima, S. (2006). "Automatic, unstructured mesh generation for tidal calculations in a large domain." *International Journal of Computational Fluid Dynamics* 20(8): 593-608.

Hearn, C. J. and Atkinson, M. J. (2001). "Effects of sea-level rise on the hydrodynamics of a coral reef lagoon: Kaneohe Bay, Hawaii." *Sea-level Changes and Their Effects*: 25.

Homer, C., Huang, C., Yang, L., Wylie, B. and Coan, M. (2004). "Development of a 2001 national land-cover database for the United States." *Photogrammetric Engineering & Remote Sensing* 70(7): 829-840.

Kirwan, M. L. and Murray, A. B. (2007). "A coupled geomorphic and ecological model of tidal marsh evolution." *Proceedings of the National Academy of Sciences* 104(15): 6118-6122.

Leorri, E., Mulligan, R., Mallinson, D. and Cearreta, A. (2011). "Sea-level rise and local tidal range changes in coastal embayments: An added complexity in developing reliable sea-level index points." *Journal of Integrated Coastal Zone Management* 11: 307-314.

Lu, Z., McCormick, B. C., Faison, C., April, G. C., Raney, D. C. and Schroeder, W. W. (1992). "Numerical Simulation of a Shallow Estuary -- Weeks Bay, Alabama". Estuarine and Coastal Modeling**:** 418-429.

Luettich, R. and Westerink, J. (2006). "ADCIRC: A parallel advanced circulation model for oceanic, coastal and estuarine waters; users manual for version 45.08".

Luettich, R. A. and Westerink, J. J. (2004). Formulation and numerical implementation of the 2D/3D ADCIRC finite element model version 44. XX, R. Luettich.

Medeiros, S., Hagen, S., Weishampel, J. and Angelo, J. (2015). "Adjusting Lidar-Derived Digital Terrain Models in Coastal Marshes Based on Estimated Aboveground Biomass Density." *Remote Sensing* 7(4): 3507.

Medeiros, S. C. and Hagen, S. C. (2013). "Review of wetting and drying algorithms for numerical tidal flow models." *International Journal for Numerical Methods in Fluids* 71(4): 473-487.

Medeiros, S. C., Hagen, S. C. and Weishampel, J. F. (2012). "Comparison of floodplain surface roughness parameters derived from land cover data and field measurements." *Journal of Hydrology* 452–453: 139-149.

Miller-Way, T. L., Dardeau, M. and Crozier, G. (1996). "Weeks Bay National Estuarine Research Reserve: An Estuarine Profile and Bibliography", Dauphin Island Sea Lab.

Morris, J. T., Sundareshwar, P. V., Nietch, C. T., Kjerfve, B. and Cahoon, D. R. (2002). "Responses of coastal wetlands to rising sea level." *Ecology* 83(10): 2869-2877.

Morton, R. A. (2008). "Historical Changes in the Mississippi-Alabama Barrier-Island Chain and the Roles of Extreme Storms, Sea Level, and Human Activities." *Journal of Coastal Research* 24(6): 1587-1600.

Nicholls, R. J., Hoozemans, F. M. J. and Marchand, M. (1999). "Increasing flood risk and wetland losses due to global sea-level rise: regional and global analyses." *Global Environmental Change* 9, Supplement 1(0): S69-S87.

O'Sullivan, W. T. and Criss, G. A. (1998). "Continuing Erosion in Southeastern Coastal Mississippi-Point aux Chenes Bay, West Grand Bay, Middle Bay, Grande Batture Islands: 1995-1997". Sixty-Second Annual Meeting of the Mississippi Academy of Sciences. Biloxi Mississippi.

Otvos, E. G. (1979). "Barrier island evolution and history of migration, north central Gulf Coast." *Barrier Islands from the Gulf of St. Lawrence to the Gulf of Mexico*: 291-319.

Parris, A., Bromirski, P., Burkett, V., Cayan, D., Culver, M., Hall, J., Horton, R., Knuuti, K., Moss, R., Obeysekera, J., Sallenger, A. and Weiss, J. (2012). "Global Sea Level Rise Scenarios for the US National Climate Assessment." *NOAA Tech Memo OAR CPO*: 1-37.

Passeri, D., Hagen, S., Bilskie, M. and Medeiros, S. (2014). "On the significance of incorporating shoreline changes for evaluating coastal hydrodynamics under sea level rise scenarios." *Natural Hazards*: 1-19.

Passeri, D. L., Hagen, S. C., Medeiros, S. C., Bilskie, M. V., Alizad, K. and Wang, D. (2015). "The dynamic effects of sea level rise on low gradient coastal landscapes: a review." *Earth's Future*: n/a-n/a.

Passeri, D. L., Hagen, S. C., Plant, N. G., Bilskie, M. V., Medeiros, S. C. and Alizad, K. (2016). "Tidal Hydrodynamics under Future Sea Level Rise and Coastal Morphology in the Northern Gulf of Mexico." *Earth's Future*: n/a-n/a.

Peterson, M. S., Waggy, G. L. and Woodrey, M. S. (2007). "Grand Bay National Estuarine Research Reserve: An Ecological Characterization", Grand Bay National Estuarine Research Reserve, Moss Point, MS**:** 268.

Resources, M. D. o. M. (1999). "Mississippi's Coastal Wetlands". Biloxi, MS, Coastal Preserves Program.

Rilo, A., Freire, P., Guerreiro, M., Fortunato, A. B. and Taborda, R. (2013). "Estuarine margins vulnerability to floods for different sea level rise and human occupation scenarios." *Journal of Coastal Research* Special Issue No. 65: 820-825.

Shirley, L. and Battaglia, L. (2006). "Assessing vegetation change in coastal landscapes of the northern Gulf of Mexico." *Wetlands* 26(4): 1057-1070.

Thieler, E. R. and Hammer-Klose, E. S. (1999). "National Assessment of Coastal Vulnerability to Sea Level rise: Preliminary Results for the U.S. Atlantic Coast". Woods Hole, Massachusetts, US Geological Survey.

Townend, I. and Pethick, J. (2002). "Estuarine flooding and managed retreat." *Philosophical Transactions of the Royal Society of London A: Mathematical, Physical and Engineering Sciences* 360(1796): 1477-1495.

Turner, R. E. (1997). "Wetland loss in the Northern Gulf of Mexico: Multiple working hypotheses." *Estuaries* 20(1): 1-13.

Weeks Bay National Estuarine Research Reserve (2007). "Weeks Bay National Estuarine Research Reserve Management Plan", Weeks Bay National Estuarine Research Reserve**:** 86.

Wolanski, E. and Chappell, J. (1996). "The response of tropical Australian estuaries to a sea level rise." *Journal of Marine Systems* 7(2–4): 267-279.

CHAPTER 6. CONCLUSION

This research aimed to develop an integrated model to assess SLR effects on salt marsh productivity in coastal wetland systems with a special focus on three NERRs in the NGOM. The study started with a comprehensive literature review about SLR and hydrodynamic modeling of SLR and its dynamic effects on coastal systems, different models of salt marsh systems based on their modeling scales including coupled models and the interconnection between hydrodynamics and biological processes. Most of the models that consist of a coupling between hydrodynamics and marsh processes are small scale models that apply SLR all at once. Moreover, they generally capture neither the dynamics of SLR (e.g., the nonlinearity in hydrodynamic response to SLR) nor the rate of SLR (e.g., applying time step approach to capture feedbacks and responses in a time frame). The model presented herein (HYDRO-MEM) consists of a two-dimensional hydrodynamic model and a time stepping framework was developed to include both dynamic effects of SLR and rate of SLR in coastal wetland systems.

The coupled HYDRO-MEM model is a spatial model that interconnects a two-dimensional depth-integrated finite element hydrodynamic model (ADCIRC) and a parametric marsh model (MEM) to assess SLR effects on coastal marsh productivity. The hydrodynamic component of the model was forced at the open ocean boundary by the dominant harmonic tidal constituents and provided tidal datum parameters to the marsh model, which subsequently produces biomass density distributions and accretion rate. The model used the marsh model outputs to update elevations on the marsh platform, bottom friction, and SLR within a time stepping feedback loop. When the

model reached the target time, the simulation terminated and results in the form of spatial maps of projected biomass density, MLW, MHW, accretion, or bottom friction were generated.

The model was validated in the Timucuan marsh in northeast Florida, where rivers and creeks have changed very little in the last 80 years. Low and high SLR scenarios for the year 2050 were used for the simulation. The hydrodynamic results showed higher water levels with more variation under the low SLR scenario. The water level change along a transect also implied that changes in water level appeared to be a function of distance from creeks as well as topographic gradients. The results also indicated that the effect of topography is more pronounced under low SLR in comparison to the high SLR scenario. Biomass density maps demonstrated an increase in overall productivity under the low SLR and a contrasting decrease under the high SLR scenario. That was a combined result of nonlinear salt marsh platform accretion and the dynamic effects of SLR on the local hydrodynamics. The calculation using different coupling time steps for the low and high SLR scenarios indicated that the optimum time steps for a linear (low) and nonlinear (high) SLR cases are 10 and 5 years, respectively. The HYDRO-MEM model results for biomass density were categorized into low, medium, and high productivity compared with MEM only and demonstrated better performance in capturing the spatial variability in biomass density distribution. Additionally, the comparison between the categorized results and a similar product derived from satellite imagery demonstrated the model performance in capturing the sub-optimal, optimal and super-optimal regions of the biomass productivity curve.

The HYDRO-MEM model was applied in a fluvial estuary in Apalachicola, FL using NOAA projected SLR scenarios. The experimental parameters for the model were derived from a two-

year experiment using bio-assays in Apalachicola, FL. The marsh topography was adjusted to eliminate the bias in lidar-derived elevations. The Apalachicola river inflow boundary was applied in the hydrodynamic model. The results using four future SLR projections indicated higher water levels with more variations in rivers and creeks under the low and intermediate-low SLR scenarios with some inundated areas under intermediate-low case. Under higher SLR scenarios, the water level gradients are low and the bay extended over the marsh and even some forested upland area. As a result of the changes in hydrodynamics, biomass density results showed a uniform marsh productivity with some increase in some regions under the low SLR scenario, whereas under the intermediate-low SLR scenario, salt marsh productivity declined in most of the marsh system. Under higher SLR scenarios, the results demonstrated a massive salt marsh inundation and some migration to higher lands.

Additionally, a marine dominated and mixed estuarine system in Grand Bay, MS and Weeks Bay, AL under four SLR scenarios were assessed using the HYDRO-MEM model. Their unique topography and geometry and individual hydrodynamic characteristics demonstrated different responses to SLR. Grand Bay showed more vulnerability to SLR due to more exposure to open water and less sediment supply. Its lower topography facilitate the conversion of marsh lands to open water. However, Weeks Bay topography and the Bay's inlet protect the marsh lands from SLR and provide lands to create new marsh lands and marsh migration under higher SLR scenarios.

The future development of the HYDRO-MEM model is expected to include more complex geomorphologic changes in the marsh system, sediment transport, and salinity change. The model

also can be improved by including a more complicated model for groundwater change in the marsh platform. Climate change effects will be considered by implementing the extreme events and their role in sediment transport into the marsh system.

6.1 Implications

This dissertation enhanced the understanding of the marsh system response to SLR by integrating physical and biological processes. This study was an interdisciplinary research endeavor that connected engineers and biologists each with their unique skill sets. This model is beneficial to scientists, coastal managers, and the natural resource policy community. It has the potential to significantly improve restoration and planning efforts as well as provide guidance to decision makers as they plan to mitigate the risks of SLR.

The findings can also support other coastal studies including biological, engineering, and social science. The hydrodynamic results can help other biological studies such as oyster and SAV productivity assessments. The biomass productivity maps can project reasonable future habitat and nursery conditions for birds, fish, shrimp, and crabs, all of which drive the seafood industry. It can also show the effect of SLR on the nesting patterns of coastal salt marsh species. From an engineering standpoint, biomass density maps can serve as inputs to estimate bottom friction parameter changes under different SLR scenarios both spatially and temporally. These data are used in storm surge assessments that guide development restrictions and flood control infrastructure projects. Additionally, projected biomass density maps indicate both vulnerable regions and possible marsh migration lands that can guide monitoring and restoration activities in the NERRs.

The developed HYDRO-MEM model is a comprehensive tool that can be used in different coastal environments by various organizations, both in the United States and internationally, to assess SLR effects on coastal systems to make informed decisions for different restoration projects. Each estuary is likely to have a unique response to SLR and this tool can provide useful maps that illustrate these responses. Finally, the outcomes of this study are maps and tools that will aid policy makers and coastal managers in the NGOM, NERRs, and different estuaries in other parts of the world as they plan to monitor, protect and restore vulnerable coastal wetland systems.